

# Role of Y-Box Binding Protein-1 mediated cell signaling in proliferation and radiotherapy resistance of breast cancer cells

## **Dissertation**

der Mathematisch-Naturwissenschaftlichen Fakultät  
der Eberhard-Karls-Universität Tübingen  
zur Erlangung des Grades eines  
Doktors der Naturwissenschaften  
(Dr. rer. nat.)

vorgelegt von

Ms. Aadhya Tiwari,  
Lucknow, India

Tübingen

2019

Gedruckt mit Genehmigung der Mathematisch-Naturwissenschaftlichen Fakultät  
der Eberhard Karls Universität Tübingen.

Tag der mündlichen Qualifikation: 09.09.2019

Dekan: Prof. Dr. Wolfgang Rosenstiel

1. Berichterstatter: Prof. Dr. Mahmoud Toulany

2. Berichterstatter: Prof. Dr. Ulrich Rothbauer

Dedicated to my beloved mother

## **ACKNOWLEDGEMENT**

No journey could be completed without the support of the nice people. The least I can do is to thank the people who helped me keep moving this far. To begin with, I would like to extend my deepest gratitude to my PhD advisor Prof. Mahmoud Toulany for supervising my PhD project. I thank him immensely for giving me the freedom to think on my own and design my own experiments and guiding me. I would also like to thank Prof Ulrich Rothbauer for his continuous monitoring of my research through annual meetings as well as a project collaborator. His suggestions and advices were extremely valuable for my research. I am very grateful to Prof Hans P Rodemann for providing me the lab space and the useful scientific discussions during weekly lab meetings. I cannot forget the countless chocolates we received from him especially on Nicholas day. I am deeply indebted to his support and guidance for my further career in science. I am beholden to the Director of Radiooncology Prof Daniel Zips for his very constructive suggestions for my project during my departmental presentation. His encouraging words inspired me to keep believing on myself and strive for the best. I also want to thank him for the research collaboration and providing us the tumor samples from cancer patients for my PhD project. I cannot thank him in words for his support and guidance in my further career in cancer biology. I want to immensely thank Prof. Klaus Dittman for all the funny scientific discussions we had, for his guidance and continuous motivation. He has taught me how to stay happy and funny in science irrespective of all the hardships. My deepest thanks to a very special person Dr Petra Ohneseit for all the amazing scientific and non-scientific discussions and the great time we spend together doing the funny stuffs. She is a great inspiration for me. I will never forget your guidance and teaching in science and life. Thanks Petra for all your time and the amazing book you have gifted me.

My sincere thanks to Prof Stefan Huber for his kind and motivational words. He taught me how to be a good teacher and maintain a positive attitude towards science in any circumstances. I would also like to thank Prof Birget Schitteck for her research collaboration with us. Because of her collaboration it was possible to perform the knockout experiments. This brings me to extend my sincere gratitude to Dr Corinna Kosnopfel for helping me in preparing the knockout cell lines. Her extremely friendly nature and always ready to helping attitude has made a huge impact on me. I cannot mention the number of knockout or permanent knockdown cell lines we tried to make together, it was a great fun to work with her. I wish her great success in life. I would also like to thank Apostolos and Pierlugi for their help in providing the tumor tissues from cancer patients and helping me with the

immunofluorescence experiments. I am grateful to Ciara as well for providing us the patient information of the tumor samples for the study.

I would also like to thank Ms Fehrenbacher for helping me with the immunofluorescence staining and microscopy. She is extremely polite, friendly and dedicated person who has taught me important scientific and interpersonal skills. I am grateful to Mirita and Silke for helping in proteomic study which is one of the critical parts of the study. I also want to thank Ms Eva Bartelt for taking care of the paper works and making all the administrative work so easy for me. I also want to acknowledge the former PhD students of the lab, Rena and Katherina for nice talks and discussions. Although the interaction was for short duration but it was very fruitful. I would like to thank my colleagues Mozghan and Tahereh for all the scientific or non scientific discussions and fun activities we did together. Thanks a lot for Hafiz readings and cake parties and also for supporting me during my hard time. It was a great time working with you girls. I also want to thank Larissa and Koni for keeping the lab atmosphere quite funny and light. I also want to thank the tech staff Klaus, Felix and Simone.

My most important and sincere thanks goes to my family, without their support and constant motivation I could have never finished my PhD. My mother and father always encouraged me to be a good scientist and supported me during all the phases of life. My sister Dr Deepshikha was always there for me and constantly motivated and supported me during my setbacks and hard times. She has taught me how to keep smiling at the face of adversity and emerge out stronger. My big brother Amit has guided and supported me during the hard phase of PhD duration. He has taught me to always aim high and have extreme levels of self faith. I would also like to thank our labrador Dazzy for giving me the positivity and laugh during the difficult time of thesis writing. I cannot mention in words and could never thank enough for the amount of support and encouragement I received from my family. I wish them all the happiness in life.

Last but in no way least, I would like to thank all my friends Rahul, Jon, Vesa, Lisa, Rama, Ferdi, Ahishek, Daniel, Pierre, David and the list is huge, for their endless support and motivation. Thanks for being in my life and making it easier to stay strong and positive during the course of my PhD.

Aadhya Tiwari

# SUMMARY

Cancer is one of the major causes of death after cardiovascular disorders. The key property of cancer cells is to evade the cell cycle checkpoints and proliferate in an uncontrollable fashion. The major therapeutic interventions available to treat cancer are mostly surgery, radiotherapy and chemotherapy alone or in combination. Despite being one of the oldest and most researched diseases, treatment rate in cancer remains extremely low.

Y-Box binding protein-1 (YB-1) is a multifunctional protein; which regulates the transcription and translation of many essential genes and proteins involved in cell proliferation, growth and DNA repair. It is a vital protein required for embryonic growth and postnatal development. YB-1 slowly declines with adolescent and disappears virtually from all the organs of body with age. According to clinical reports, YB-1 is overexpressed in almost all kinds of cancers. This overexpression is associated with poor prognosis and therapy resistance. Also *KRAS* mutation is associated with aggressive and therapy resistance in various types of tumors. It is known that YB-1 is constitutively activated in *KRAS(G12V)*-mutated breast cancer cells (BCC). In the present study the role of YB-1 in *KRAS(G13D)*-mutated BCC was investigated and following novel findings were obtained:

- 1) YB-1 is constitutively activated by phosphorylation at Ser-102 in *KRAS(G13D)* BCC, and this phosphorylation cannot be further stimulated by epidermal growth factor (EGF) or ionizing radiation (IR) as checked until 24 hours post stimulation.
- 2) Mitogen-activated protein kinase (MAPK) pathway is the predominating pathway responsible for the constitutive phosphorylation of YB-1 in *KRAS(G13D)*-mutated BCC. However, in the presence of an additional PTEN mutation along with *KRAS(G13D)* mutation, phosphoinositide 3-kinase (PI3K) becomes the predominant pathway responsible for the constitutive YB-1 phosphorylation in these BCC.
- 3) A dynamic crosstalk exists between MAPK and PI3K signaling pathways, which is responsible for the regulation of constitutive phosphorylation of YB-1 in *KRAS(G13D)*-mutated BCC. Therefore dual targeting of both the pathways inhibits YB-1 phosphorylation significantly more than the additive effect of both the pathways.
- 4) YB-1 strongly regulates proliferation of *KRAS(G13D)*-mutated BCC and stimulates repair of IR-induced DNA double strand breaks (DSB) leading to radioresistance .

- 5) YB-1 regulates DSB repair through homologous recombination (HR) and alternate non-homologous end joining (A-NHEJ) DSB repair pathways. YB-1 plays no significant role in regulating classical non-homologous end joining (C-NHEJ) repair pathway.
- 6) Phosphorylation of YB-1 at Ser-102 is essential for its role in DSB repair and post-irradiation cell survival.
- 7) Proteomic studies revealed that knocking out YB-1 results into down regulation and up regulation of several important proteins involved in DNA repair. KAP1 is one of the important protein involved in DNA end resection that was found to be down regulated in YB-1 knockout cells.
- 8) YB-1 regulates HR and A-NHEJ DSB repair pathways through KAP-1 mediated end resection.

Thus, based on the described findings, YB-1 is proposed to be a potential therapeutic target to treat *KRAS*-mutated cancers in combination with radiotherapy.

## TABLE OF CONTENTS

<b>ACKNOWLEDGEMENT</b>	<b>IV</b>
<b>SUMMARY</b>	<b>VI</b>
<b>TABLE OF CONTENTS</b>	<b>VIII</b>
<b>LIST OF ABBREVIATION</b>	<b>XI</b>
<b>1.MATERIAL AND METHODS</b>	<b>1</b>
<b>1.1 Materials</b>	<b>1</b>
<b>1.1.1 Equipments</b>	<b>1</b>
<b>1.1.2 Consumables</b>	<b>2</b>
<b>1.1.3 Laboratory chemicals and compounds</b>	<b>2</b>
<b>1.1.4 Composition of used buffers and solutions</b>	<b>4</b>
<b>1.1.5 Antibodies</b>	<b>6</b>
<b>1.1.6 Secondary Antibody</b>	<b>7</b>
<b>1.1.7 Molecular targeted inhibitors</b>	<b>7</b>
<b>1.1.8 Cell lines</b>	<b>8</b>
<b>1.1.9 Cell culture media</b>	<b>9</b>
<b>1.2 Methods</b>	<b>10</b>
<b>1.2.1 Cell culture</b>	<b>10</b>
<b>1.2.2 Treatment of cells with the inhibitors</b>	<b>10</b>
<b>1.2.3 Transfection of cells with specific siRNAs</b>	<b>10</b>
<b>i) Lipofectamine based transfection</b>	<b>10</b>
<b>ii) Reverse Transfection</b>	<b>11</b>
<b>1.2.4 Exposure to ionizing radiation (IR)</b>	<b>11</b>
<b>1.2.5 Proliferation assay</b>	<b>11</b>
<b>1.2.6 Colony formation assay</b>	<b>12</b>
<b>1.2.7 <math>\gamma</math>-H2AX foci assay</b>	<b>12</b>
<b>1.2.8 Immunofluorescence staining in tissue samples from patients</b>	<b>13</b>
<b>1.2.9 Western Blotting</b>	<b>14</b>
<b>1.2.9.1 Preparation of the total cell lysate</b>	<b>14</b>
<b>1.2.9.2 Protein determination</b>	<b>14</b>
<b>1.2.9.3 SDS PAGE</b>	<b>15</b>
<b>1.2.9.4 Sample preparation</b>	<b>15</b>
<b>1.2.9.5 Transfer of proteins to the nitrocellulose membrane</b>	<b>16</b>
<b>1.2.9.6 Ponceau S staining</b>	<b>16</b>
<b>1.2.9.7 Blocking</b>	<b>16</b>
<b>1.2.9.8 Immunodetection</b>	<b>16</b>
<b>1.2.9.9 Stripping of Western blot membranes</b>	<b>17</b>
<b>1.2.10 YBX1 knockout using CRISPR/Cas9</b>	<b>17</b>
<b>1.2.11 DNA repair reporter assay</b>	<b>17</b>
<b>1.2.12 Flowcytometry</b>	<b>18</b>
<b>1.2.13 Proteomic study</b>	<b>18</b>
<b>1.2.14 Statistics</b>	<b>19</b>



<b>2 INTRODUCTION</b>	<b>20</b>
<b>2.1 RAS</b>	<b>21</b>
<b>2.2 MAPK signaling pathway</b>	<b>22</b>
<b>2.3 PI3K/Akt/mTOR signaling pathway</b>	<b>24</b>
<b>2.4 Y-Box Binding Protein-1 (YB-1)</b>	<b>26</b>
<b>2.5 YB-1 in cancer</b>	<b>28</b>
<b>2.6 Activation/Phosphorylation of YB-1</b>	<b>30</b>
<b>2.7 YB-1 in DNA repair</b>	<b>30</b>
<b>3 RESULTS</b>	<b>36</b>
<b>3.1 Underlying signaling pathways involved in phosphorylation of YB-1</b>	<b>36</b>
<b>3.1.1 YB-1 is highly phosphorylated at S102 in BCC compared to normal breast epithelial cells</b>	<b>36</b>
<b>3.1.2 External stimuli lead to long-term phosphorylation of YB-1 in KRAS wild-type but not in KRAS(G13D)-mutated cells.</b>	<b>37</b>
<b>3.1.3 KRAS(G13D)-MAPK-RSK is the major pathway regulating constitutive YB-1 phosphorylation in KRAS-mutated cells</b>	<b>39</b>
<b>3.1.4 Mutation in KRAS induces constitutive phosphorylation of YB-1 through MEK/ERK and PI3K signaling pathways</b>	<b>40</b>
<b>3.1.5 Mutated KRAS induces constitutive phosphorylation of YB-1 predominantly through MEK/ERK pathway in cytoplasmic and nuclear fractions.</b>	<b>43</b>
<b>3.1.6 PTEN mutation dominates mutated KRAS for a constitutive phosphorylation of YB-1 through PI3K signaling pathway</b>	<b>44</b>
<b>3.1.7 Dual targeting of MAPK and PI3K is an efficient approach to block YB-1 S102 phosphorylation in KRAS(G13D)-mutated BCC expressing PTEN wild-type or PTEN-mutation</b>	<b>46</b>
<b>3.1.8 Constitutive YB-1 phosphorylation in KRAS(G13D)-mutated cells is independent of Akt</b>	<b>48</b>
<b>3.1.9 A positive correlation exists between P-YB-1 and P-ERK as well as expression of EGFR in the tissue samples from breast cancer patients</b>	<b>52</b>
<b>3.2 Role of YB-1 in proliferation of KRAS(G13D)-mutated BCC</b>	<b>56</b>
<b>3.2.1 Dual targeting of PI3K and MEK is an efficient approach to block proliferation of KRAS(G13D)-mutated BCCs in a YB-1 dependent manner</b>	<b>57</b>

<b>3.2.2 Reactivation of PI3K or MEK/ERK pathways after long-term treatment with LY and PD</b>	<b>59</b>
<b>3.2.3 Dual targeting of PI3K and MEK is also an efficient approach to block proliferation of BRAF(V600E) mutated melanoma cells in a YB-1-dependent manner</b>	<b>60</b>
<b>3.2.4 YB-1 knockdown by siRNA strongly inhibits the cell proliferation in KRAS mutated BCC</b>	<b>61</b>
<b>3.2.5 YB-1 knockout in MDA-MB-231 and NM2C5 cells by CRISPR/Cas9</b>	<b>62</b>
<b>3.2.6 Dual targeting of MEK/ERK and PI3K pathways strongly inhibits proliferation through YB-1</b>	<b>63</b>
<b>3.2.7 Dual targeting of MEK/ERK and PI3K pathways does not regulates proliferation entirely through YB-1 in BRAF(V600E) melanoma cells</b>	<b>64</b>
<b>3.2.8 Dual targeting of MEK/ERK and PI3K pathways has no effect on cell proliferation in KRAS wild-type BCC</b>	<b>65</b>
<b>3.2.9 P-YB-1 strongly regulates cell proliferation of KRAS(G13D)-mutated BCCs</b>	<b>66</b>
<b>3.3 Role of YB-1 in DNA DSB repair and radioresistance</b>	<b>67</b>
<b>3.3.1 YB-1 stimulates repair of ionizing radiation induced DNA DSB</b>	<b>68</b>
<b>3.3.2 YB-1 induces radioresistance in KRAS(G13D)-mutated BCC</b>	<b>69</b>
<b>3.3.3 YB-1 stimulates DNA DSB repair through HR and A-NHEJ repair pathways</b>	<b>70</b>
<b>3.3.4 YB-1 regulates DNA DSB repair through HR</b>	<b>71</b>
<b>3.3.5 YB-1 knockout further inhibits repair of DSB through C-NHEJ</b>	<b>73</b>
<b>3.3.6 YB-1 regulates DSB repair through A-NHEJ repair pathway</b>	<b>73</b>
<b>3.3.7 Phosphorylation of YB-1 at Ser-102 is essential for regulating DSB repair and radioresistance</b>	<b>74</b>
<b>3.3.8 Proteomic Study</b>	<b>78</b>
<b>3.3.9 YB-1 knockout results in significant reduction in end resection</b>	<b>80</b>
<b>4 DISCUSSION</b>	<b>81</b>
<b>4.1 Signaling pathways regulating phosphorylation of YB-1 in KRAS (G13D)- mutated BCC</b>	<b>81</b>
<b>4.2 Crosstalk between MAPK and PI3K pathways regulate YB-1 Phosphorylation</b>	<b>85</b>
<b>4.3 YB-1 regulates proliferation of KRAS(G13D)-mutated BCC</b>	<b>87</b>
<b>4.4 YB-1 regulates DNA DSB repair by HR and A-NHEJ pathways through Kap-1 mediated end resection</b>	<b>89</b>
<b>CONCLUSION</b>	<b>92</b>
<b>REFERENCES</b>	<b>93</b>
<b>CURRICULUM VITAE</b>	<b>104</b>

## List of abbreviations:

A-NHEJ	Alternative Non-Homologous End Joining
APS	Ammonium Persulfate
BCC	Breast Cancer Cells
BSA	Bovine Serum Albumin
C-NHEJ	Classical Non-Homologous End Joining
DMEM	Dulbecco's Modified Eagle's Medium
DMSO	Dimethyl Sulfoxide
DSB	Double Strand Breaks
EGF	Epidermal Growth Factor
EGFR	Epidermal Growth Factor Receptor
ERK	Extracellular-Signal Regulated Kinase
FBS	Fetal Bovine Serum
HR	Homologous Recombination
IGF	Insulin Growth Factor
IR	Ionizing Radiation
KRAS	Kirsten rat Sarcoma Viral Oncogene Homolog
LY	LY294002
MAPK	Mitogen Activated Protein Kinases
MEK	MAPK/ERK Kinase
MK	MK2206
Mtor	Mammalian Target of Rapamycin
Nu	Nu-7441

PBS	Phosphate-Buffered Saline
PBST	Phosphate-Buffered Saline/Tween20
PD	PD98059
PDT	Population Doubling Time
PI3K	Phosphoinositide 3-Kinase
PTEN	Phosphatase and Tensin Homolog
RPMI	Roswell Park Memorial Institute medium
RSK	p90 Ribosomal S6 Kinase
SDS-PAGE	Sodium Dodecyl Sulfate Polyacrylamide Gel Electrophoresis
TNBC	Triple Negative Breast Cancer
S473	Serine 473
T308	Threonine 308

# 1 Material and Methods

## 1.1 Materials

### 1.1.1 Equipments

<b>Device</b>	<b>Manufacturer</b>
Analytical balance	Kern & Sohn
Binocular	Carl Zeiss
Centrifuges	Andreas Hettich, Eppendorf
ELISA reader	Anthos Labtec
Fluorescence microscope	Zeiss
Flowcytometer	BD Biosciences
Fuchs-Rosenthal counting chamber	Witeg laboratory technology
Gel electrophoresis chamber	Hofer
Incubator	Binder
Light microscope	Leitz
Magnetic stirrer	Heidolph Instruments
pH meter	WTW
Pipettes	Eppendorf
Pipetting aid, Pipetboy	Integra Biosciences
Power supply for electrophoresis	Pharmacia
Precision balance	Sartorius
Semi-dry blot system	Hofer
Shaker (shaking)	Edmund Bühler
Sonifier B-12	Branson Ultrasonics Corporation
Sterile bench for cell culture	BDK Luft- u. Reinraumtechnik
Steriler	Heidolph Instruments
Vortexer	UniEquip
Water bath GFL	GFL
X-ray unit (RS-225)	Gulmay Medical

### 1.1.2 Consumables:

<b>Product</b>	<b>Manufacturer</b>
Culture flasks, slides	BD Falcon
Cell scraper	Costar
Filter pipette tips (10 µl, 100 µl, 1000 µl)	Sarstedt
Filtropur filtration units	Sarstedt
Multi-well plates (96-well)	Greiner Bio-One
Nitrile gloves Hartmann	Kimberly-Clark
Nitrocellulose membrane (0.2 µm)	Carl Roth
Pasteur pipettes	Wu Mainz
Pipette tips (10 µl, 100 µl, 1000 µl)	Eppendorf, Greiner Bio-One
Centrifuge tubes (0.5 ml, 1.5 ml, 2.0 ml)	Eppendorf
Reaction tubes (15 ml)	Sarstedt
Reaction vessels (50 ml)	Greiner Bio-One
Whatman Chromatography Paper (3mm)	Whatman, GE Healthcare

### 1.1.3 Laboratory chemicals and compounds:

Acrylamide	Roth
Agarose	Sigma
APS	AppliChem
Bicarbonate	Biochrom AG
β-Mercaptoethanol	Sigma-Aldrich
Boric acid	Sigma-Aldrich

Bromophenol blue	Pharmacia Biotech
BSA	Roth
Complete protease inhibitor tablets	Roche
Cresyl violet stain	Applichem
DC protein assay reagent A	BioRad
DC protein assay reagent B	BioRad
DMSO	Applichem
Di-Na hydrogen phosphate	Applichem
DTT	Sigma
ECL Plus Western blot detection reagent	VWR
EDTA	Applichem
Ethanol	Merck
Formaldehyde	Merck
Glycin	Roth
Glycerol	Applichem
G418	InvivoGen
HCl	Roth
HEPES	Sigma
KCl	Merk
Lipofectamine	ThermoFisher Scientific
Lipofectamine RNAi MAX transfection reagent	ThermoFisher Scientific
Methanol	VWR
Dry Milk	Roth
NaCl	Applichem

Penicilin-Streptomycin	Gibco
Phosphatase inhibitor cocktail 2 (for tyrosine protein phosphatases, acid and alkaline phosphatases)	Sigma
Phosphatase inhibitor cocktail 3 (for serine/threonine protein phosphatases and L-isozymes of alkaline phosphatase)	Sigma
Ponceau S	Sigma
Precision plus protein standard	BioRad
Protease inhibitor	Roche
Protein assay kit	Bio-Rad
SDS pellets	Serva
Sodium bicarbonate	Biochrom AG
TEMED	Sigma
Tris-Base	Sigma
Tris-HCl	Applichem
Trypsin	Sigma
Tween 20	Roth
Vectashield mounting medium with DAPI	Vector Laboratories

#### 1.1.4 Composition of used buffers and solutions

Blotting buffer (Anode) pH 9,0

3,1 g Boric acid  
4 ml 10 % SDS (v/v)  
200 ml Methanol  
ad 1 l H<sub>2</sub>O

Blotting buffer (Cathode) pH 9,0

3,1 g Boric acid  
4 ml 10 % SDS (v/v)  
50 ml Methanol  
ad 1 l H<sub>2</sub>O

Cresyl violet stain

0,5 g Cresyl violet



	27 ml Formaldehyde, 37 % ad 1 l PBS
Loading buffer	2.5 ml Stacking gel buffer (4x) 2.0 ml 10 % SDS (v/v) 2.0 ml Glycerin 0.25 mg Bromphenol blue ad 10 ml H <sub>2</sub> O <i>5 % β-Mercaptoethanol added during sample preparation</i>
Lysis buffer, pH 7, 5	50 mM Tris HCl 50 mM Glycerol-2-phosphate 150 mM NaCl 1 mM Na <sub>3</sub> VO <sub>4</sub> 10 % Glycerin 1 % Tween-20 1 mM NaF <i>0,1 % 1 M DTT, 1 % Protease inhibitor und 1 % Phosphatase inhibitor-cocktail 2 and 3 added fresh before use</i>
PBS, pH 7.4	13,7 mM NaCl 2,7 mM KCl 80,9 mM Na <sub>2</sub> HPO <sub>4</sub> 1,5 mM KH <sub>2</sub> PO <sub>4</sub>
Stacking gel buffer (4x), pH 6,8	30,3 g Tris Base 20 ml 10 % SDS (v/v) ad 500 ml H <sub>2</sub> O
Running buffer	144,1 g Glycin 30 g Tris Base 5 g SDS ad 5 l H <sub>2</sub> Odest
Stripping buffer, pH 2,2	7,5 g Glycin 0.5 g SDS 5 ml Tween-20 ad 500 ml H <sub>2</sub> O
TBST, pH 7,5	3,152 g Tris HCl 11,688 g NaCl 2 ml Tween-20 ad 2 l H <sub>2</sub> O

Separating gel buffer, pH 8,8

18.17 g Tris Base  
4 ml 10 % SDS (v/v)  
ad 100 ml H<sub>2</sub>O

FACS buffer

1% 0.5mM EDTA  
5% FCS  
500 PBS

### 1.1.5 Antibodies

S. No.	Antibody	Dilution	Source	Company	Catalogue No.
1	YB-1	1:1000 in 3% milk	Anti-Rabbit	Cell Signaling	4202
2	P-YB-1 (S102)	1:1000 in 3% BSA	Anti-Rabbit	Cell Signaling	2900
3	ERK1/2	1:1000 in 3% BSA	Anti-Rabbit	Cell Signaling	4695
4	P-ERK1/2 (T185/Y187)	1:1000 in 3% BSA	Anti-Rabbit	Cell Signaling	4377S
5	Akt 1	1:1000 in 3% milk	Anti-Mouse	Cell Signaling	2967
6	Akt 2	1:1000 in 3% milk	Anti-Rabbit	Cell Signaling	2962
7	Akt 3	1:1000 in 3% milk	Anti-Mouse	Cell Signaling	3788
8	P-Akt (S473)	1:1000 in 3% BSA	Anti-Rabbit	Cell Signaling	4060
9	Ki67	1:100 in 3% BSA	Anti-Rabbit	eBioscience	14-5698-82
10	KRAS	1:1000 in 3% milk	Anti-Mouse	Calbiochem	OP24
11	EGFR	1:1000 in 3% milk	Anti-Rabbit	Abcam	Ab52894
13	RSK	1:1000 in 3% milk	Anti-Rabbit	Cell Signaling	9355
14	P-RSK (T359/S363)	1:1000 in 3% BSA	Anti-Rabbit	Cell Signaling	9344
15	PRAS40	1:1000 in 3% milk	Anti-Rabbit	Cell Signaling	2691

16	P-PRAS40 (T246)	1:1000 in 3% BSA	Anti-Rabbit	Cell Signaling	2997
17	Tubulin	1:1000 in 3% milk	Anti-Mouse	Calbiochem	CP06
18	Lamin A/C	1:1000 in 3% BSA	Anti-Mouse	Abcam	Ab40567
19	Actin	1:1000 in 3% milk	Anti-Rabbit	Sigma	A2066
20	GAPDH	1:1000 in 3% milk	Anti-Rabbit	Cell Signaling	5174
21	Kap1	1:1000 in 3% BSA	Anti-Mouse	Cell Signaling	4123S
22	RPA	1:300 in 1% TBST	Anti-Rabbit	Cell Signaling	2267S
23	$\gamma$ H2AX (S139)	1:300 in 1% TBST	Anti-Mouse	Merck Millipore	05-636
24	YO-PRO-1	1:2000 in 1% PBS	Anti-Mouse	Invitrogen	Y3603

### 1.1.6 Secondary Antibody

Anti-Rabbit IgG HRP	1:2000 GE Healthcare
Anti-Mouse IgG HRP	1:2000 GE Healthcare
Anti-Mouse IgG Alexa-Fluor 488	1:300 Invitrogen

### 1.1.7 Molecular targeted inhibitors

To access the specific activities of KRAS dependent signaling pathways involved in regulation of YB-1 phosphorylation and radioresistance, stimulating ligand and inhibitors were used at concentrations indicated:

Inhibitor	Concentration	Specificity	Manufacturer	Catalogue No.
B02	5 $\mu$ M	Rad51	Selleckchem	S8434
LY294002	10 $\mu$ M	PI3K	Calbiochem	440202
MK2206	10 $\mu$ M	Akt	Selleckchem	S1078
Nu7441	5 $\mu$ M	DNAPKcs	Selleckchem	S2638

PD98059	20 $\mu$ M	MEK	Selleckchem	S1177
Talazoparib	25 nM	PARP	Selleckchem	S7048
U0126	5 $\mu$ M	MEK	Calbiochem	662005

### 1.1.8 Cell lines

The following established human cell lines of different tumor entities and normal cells as well as transformed breast epithelial cell lines were used in the present study.

#### Cell line description, origin and reference

Cell line	Entity, culture media
MDA-MB-231 (Parental)	Breast epithelial cancer cell line (ATCC <sup>®</sup> HTB-26 <sup>™</sup> ) DMEM + 10% FCS + 1%P/S
MDA-MB-231 shSCR ,shAkt1, shAkt2, shAkt3	Breast epithelial cancer cell line, transduced with-shRNA for scramble and Akt1, Akt2 and Akt3 DMEM + 10% FCS + 1%P/S + 2 $\mu$ g/ml Puramycin
MDA-MB-231 YB-1 knockout	DMEM + 10% FCS + 1%P/S + 2 $\mu$ g/ml Puramycin
MDA-MB-231 - Wild-type – YB-1 overexpression	DMEM + 10% FCS + 1%P/S + 2 $\mu$ g/ml Puramycin + 1 mg/ml G418
MDA-MB-231 – Mutant-YB-1 S102A overexpression	DMEM + 10% FCS + 1%P/S + 2 $\mu$ g/ml Puramycin + 1 mg/ml G418
MDA-MB-453	Breast epithelial cancer cell line (ATCC <sup>®</sup> HTB-131 <sup>™</sup> ) DMEM + 10% FCS + 1% P/S
SKBr3	Breast epithelial cancer cell line (ATCC <sup>®</sup> HTB-30 <sup>™</sup> ) RPMI + 10% FCS + 1%P/S
HBL-100	Transformed breast epithelial cell line derived from milk of healthy lactating woman RPMI + 10% FCS + 1%P/S

NM2C5	Melanoma epithelial cell line RPMI + 10% FCS + 1%P/S
MCF10A	Normal breast epithelial cells (ATCC <sup>®</sup> CRL-10317 <sup>™</sup> )
U2OS	Osteosarcoma cells McCoy's Media
U2OS-DRGFP	U2OS cells with the reporter construct for Homologous Recombination (HR) McCoy's Media + 2µg/ml Puramycin
U2OS-NJ5GFP	Osteosarcoma with the reporter construct for DNA-PKcs dependent Non Homologous End Joining (D-NHEJ) McCoy's Media + 2µg/ml Puramycin
U2OS-NJ2GFP	Osteosarcoma with the reporter construct for Alternate Non-Homologous End Joining (A-NHEJ) McCoy's Media + 2µg/ml Puramycin

MDA-MB-231 cells stably expressing scramble-shRNA, Akt1-shRNA, Akt2-shRNA and Akt3-shRNA were received from Prof. Dr. Manfred Jücker (Institute of Biochemistry and Signal Transduction, University Medical Center Hamburg-Eppendorf, Hamburg, Germany.)

### 1.1.9 Cell culture media

**Dulbecco's Modified Eagle Medium (DMEM)** containing 4.5 mg/ml glucose from Gibco supplemented with 44.04 mM NaHCO<sub>3</sub> and 10% FCS + 1%P/S.

**RPMI-1640** containing L-glutamine from Gibco, supplemented with 26.8 mM NaHCO<sub>3</sub> and 10% FCS + 1%P/S.

**McCoy's Media** – McCoys media (Sigma-M-4892) 11.9g/L supplemented with 2.2 g/L NaHCO<sub>3</sub> and 10%FCS + 1%P/S.

For cryo-protection of cells DMEM, MEM or RPMI-1640 supplemented with 20% FCS containing 5% DMSO as cryo-conservative was used.

## **1.2 Methods**

### **1.2.1 Cell Culture**

All cell culture work was performed under a sterile laminar flow hood with aseptic condition and using sterile working materials. All the necessary solutions required for cell culture work were stored at 4 ° C. The culture media was always heated in water bath at 37 ° C before use. The cell cultures were maintained in incubators with humidified atmosphere of 93% air and 7% CO<sub>2</sub> at 37°C. The cells were routinely checked for mycoplasma contamination by using 4', 6-diamidin-2-phenylindole (Dapi) staining.

### **1.2.2 Treatment of cells with the inhibitors**

All inhibitors were dissolved in DMSO. The stock solutions (10 mM) were stored at -20 ° C. According to the required concentrations, the stock solution of the inhibitors was diluted with cell culture medium. Control cells received same concentration of DMSO as vehicle. The final concentrations used and the duration of treatment varied depending on experimental protocol. This has been addressed in every experiment in the results section.

### **1.2.3 Transfection of cells with specific siRNAs**

siRNA based transfection methods were used to transiently knock down the protein expression of various proteins mentioned in the result part. Two different types of transfection methods were used based on the experimental protocol.

#### **i) Lipofectamine based transfection:**

Cell were plated in 6-well plates (450,000 for MDA-MB-231 cells and 800,000 for MDA-MB-453 cells) Transfection procedure was performed 24 h later when the cells were in a 75% confluent. 50nM concentration of siRNA was used in all the transfection methods. The siRNA solution was prepared in the desired concentration with opti-MEM in a total volume of 50 µl. Two microliter µl of Lipofectamine <sup>TM</sup>2000 per one ml of medium was used per transfection. Two microliter µl of Lipofectamine diluted in 48 µl Opti-MEM and incubated for 5 minutes at room temperature (transfection reagent). Thereafter, the siRNA solution (50 µl) was added to

the transfection solution (50 µl), mixed gently and incubated for 20 minutes at room temperature. Finally, the siRNA-Lipofectamine™ 2000 mixture was used to treat the cells. The medium was changed with the fresh medium 24 h after transfection. Protein isolation for Western blotting was performed 72 h after transfection.

## **ii) Reverse Transfection:**

Cells were splitted and centrifuged at 750 g for 5 minutes. Cell pellet was dissolved in required media and siRNA solution was added. The siRNA solution was prepared in the desired concentration. Opti-MEM in a total volume of 200 µl was dissolved in 2 µl of RNAmix solution and 2.5 µl of siRNA per one millilitre media. The siRNA solution was allowed to incubate for 30 minutes at room temperature and thereafter was mixed with cells. The cells were then plated into 6-well plate. Medium was changed after 48 hours after transfection

### **1.2.4 Exposure to ionizing radiation (IR)**

Irradiation (4 Gy) was performed at 37°C using a Gulmay RS225 X-ray machine (Gulmay limited, Chertsey, UK) with a dose rate of 1 Gy/minute with the following exposure parameters: 200 kVp, 15 mA and 0.5 mm Copper additional filtering

### **1.2.5 Proliferation assay**

Proliferation assays were performed to monitor the antiproliferative effect of YB-1, PI3K inhibitor LY and MEK inhibitor PD in single or combination treatment. For this purpose, 30,000 cells (MDA-MB-231), 300,000 cells (MDA-MB-453) per, 60,000 cells (SKBR, HBL-100) were seeded in 6-cm culture dishes. Twenty-four hours later, medium was changed with fresh medium and the cells were treated with the inhibitors or siRNA indicated in the result part of the respective experiment. Control cells received DMSO at the appropriate concentration. Cells were counted at day 1, 2, 3 and 5 after treatment using a Fuchs-Rosenthal counting chamber under light microscope. The mean number of cells ± standard deviation (SD) was calculated from indicated numbers of biologically independent experiments and graphed.

### 1.2.6 Colony formation assay

The colony-forming test was developed in 1956 by Puck and Marcus (Puck et al., 1956) and is now regarded as the golden standard for the determination of cellular radiosensitivity. After exposure to ionizing radiation, tumor cells undergo massive cell death. However, some cells still have the potential to undergo at least 5 to 6 cell divisions and form colony of at least 50 daughter cells. Such cells are called clonogenic cells. To study the cellular radiosensitivity after treatment with different inhibitors or in YB-1 knockout clones, depending on cell line and treatments, 250 or 500 cells were seeded per well in 6-well plates (6 parallel cultures per experimental condition) or 1000 cells in 10-cm cell culture dishes (3 parallel cultures per experimental condition). Cell culture medium containing 20% FCS was used. After a 24-hour incubation, cells were treated with the inhibitors or DMSO for 2 h and irradiated. The inhibitor concentrations and treatment times varied depending on the experiment and indicated while describing the respective experiment in the result section. Ten to twelve days after treatment the colonies were stained for 20 minutes with cresyl violet staining solution. All the colonies consisting 50 cells or more were counted under light microscope. The colony forming efficiency (plating efficiency, PE), was determined by the following formula:

$$\text{PE (xGy)} = \text{No. of colonies with 50 cells or more} / \text{number of cells seeded}$$

Using a linear-quadratic model, the survival fractions (SF) of irradiated cells was calculated based on PE as below:

$$\text{SF (x Gy)} = \text{PE (x Gy)} / \text{PE (0 Gy)}$$

Survival curves were prepared in Sigmablot, in which SF was shown in a logarithmic scale.

### 1.2.7 $\gamma$ -H2AX foci assay

Ionizing radiation exposure produces massive DNA double strand breaks (DSBs) in cells. Intrinsic repair mechanisms determine the biological effect of the ionizing radiation. Most of the DSBs are repaired within 24 hours after radiation. The radiation-induced DSB, which are not repaired after 24 hours are determined by  $\gamma$ -H2AX focus assay. This test is based on the detection of phosphorylation of the histone H2AX at Ser-139 known as  $\gamma$ -H2X (Rogakou et al., 1998). Since the number of  $\gamma$ -H2AX foci correlate with the amount of residual DNA DSB, it is possible to determine the efficiency of DNA repair by counting the



number of residual  $\gamma$ -H2AX foci, 24 h after irradiation. For these experiments, indicated number of cells were seeded in 4-chamber culture slides. Confluent or sub-confluent cells (depending on the experiment and end-point) were treated with the appropriate inhibitors, as indicated in the result section. Thereafter, cells were mock irradiated or irradiated with single dose 4 Gy and  $\gamma$ -H2AX staining was performed after 24 hours. For that, media were removed and the cells were fixed with PBS / 2% formaldehyde solution (37%) for 15 minutes and then washed three times with PBS for a total of 10 minutes. Subsequently, the cells were incubated with PBS / 1% BSA / 0.2% Triton X-100 at 4 ° C for 5 minutes to permeabilize the cell membrane. After a 5 minutes wash with PBS / 1% BSA, the non-specific binding sites were blocked with PBS / 3% BSA for 1 hour, followed by the incubation with P-H2AX-specific antibody (Ser-139) for 2 hours in PBS / 1% BSA / 0.5% Tween-20. Thereafter, the cells were washed three times in PBS / 1% BSA / 0.5% Tween-20 for 5 minutes. Fluorescent conjugated secondary antibody (AlexaFluor@488) diluted in PBS / 1% BSA / 0.5% Tween-20 was added and cells were incubated for 1 hour. The cells were again washed thrice with PBS / 1% BSA / 0.5% Tween-20 for 5 minutes each and mounted with vectashield containing DAPI (nuclear marker). The evaluation of the foci was carried out by fluorescence microscopy at a magnification of 40X. The foci were counted in 100 cell nuclei per experiment and the graph was plotted with the mean of foci per cells  $\pm$  standard error (SEM) from indicated number of biologically independent experiments.

### **1.2.8 Immunofluorescence staining in tissue samples from patients**

Breast cancer patients undergoing surgery as a primary treatment were included in the study. Previous neo-adjuvant treatment and chemoradiotherapy were considered as exclusion criteria. The study was approved by the Ethics Committee of the Medical Faculty of the University of Tuebingen (confirmation # 426/2013BO1). All patients provided signed informed consent. Freshly excised material from the six tumors and one corresponding normal tissue were retrieved from the operation theatre and embedded into paraffin as described before (Menegakis et al., 2015a, Menegakis et al., 2015b). Cross-sections of the paraffin-embedded material were used for staining. Paraffin sections were deparaffinised and rehydrated. Slides were incubated in citrate buffer pH 6.0 (Thermo Scientific) using a pressure cooker. Sections were blocked with 10% donkey serum in PBS at room temperature for 30 minutes followed by incubation with rabbit antiserum to phospho-YB-1 (Cell

Signaling, 1:150), p-ERK1/2 (Cell Signaling, 1:300), EGFR (Abcam, 1:100) and rat antiserum to Ki67 (eBioscience, 1:100). Nuclei were stained with YO-PRO-1 (Invitrogen, 1:2000). All washing steps were performed with TBS/Tween (TBST) and antibody incubations were done in TBST with 3% BSA or TBST with 5% dry milk. The sections were analysed with a confocal laser scanning microscope (Leica TCS SP; Leica Microsystems) at 250x or 400x magnification.

## **1.2.9 Western Blotting**

### **1.2.9.1 Preparation of the total cell lysate**

All steps of the protein isolation were performed on ice. The confluent cells seeded on 6-cm cell culture dishes were washed twice with ice-cold PBS and an adequate amount of the lysis buffer was added. 0.1% 1 M DTT, 1% protease inhibitor and 1% each phosphatase inhibitor Cocktail 2 or 3 were added in the lysis buffer before use. With the help of a cell scraper, the cells were scratched from the surface of the cell culture dish and placed in a 1.5 ml centrifuge tube. The cell membrane was disrupted by sonication. Subsequently, the total cell lysate was separated by centrifugation (14000 g, 4 ° C, 15 minutes) from the cell pellet.

### **1.2.9.2 Protein determination**

The determination of the protein content of the total cell extracts was carried out by the DC protein Assay kits (modified Lowry assay). A calibration graph with known BSA concentrations was prepared and protein concentration corresponding to the total cell lysate calculated. The test was carried out in a 96-well plate. Five microliter of the standards and the cell extracts were pipetted into 3 wells (triplet) and mixed with 25 µl of reagent A (alkaline copper tartrate solution). The proteins form a complex with Cu<sup>2+</sup> ions. Then, 200 µl of reagent B (diluted Folin solution) was added. Within a 6 minute of incubation, the Cu<sup>+</sup> ions form an unstable blue complex with the folin reagent, which serves as a measure of protein concentration. The absorption was measured at 620 nm in the ELISA reader. The mean values were calculated based on optical density as a readout of absorption values. A graph was prepared with respect to the standards, which gives the protein concentration in the respective condition.

### 1.2.9.3 SDS PAGE

The gel electrophoretic separation of the proteins was carried out by means of SDS-PAGE (Sodium dodecyl sulphate-polyacrylamide gel electrophoresis) in which an SDS-containing, discontinuous Tris-glycine buffer system was used. The proteins pass first through a stacking gel, where they get concentrated at the bottom before entering the separating gel. Different percentage of acrylamide/bisacrylamide solutions were used depending on the molecular weight of the proteins, which needed to be detected by separating gels (Table 2.1).

**Tab.. 2.1: Composition of stacking and separating gel for the SDS-PAGE.**

	Stacking gel	Separating gel 8%	Separating gel 12%
Deionized water	3 ml	9.5 ml	7 ml
Stacking gel buffer	1.25 ml	-	-
Separating gel buffer	-	5 ml	5 ml
Acrylamide solution 30%	0.75 ml	5.5 ml	8 ml
TEMED	5 $\mu$ l	10 $\mu$ l	10 $\mu$ l
10% APS v/v	100 $\mu$ l	100 $\mu$ l	100 $\mu$ l

### 1.2.9.4 Sample preparation:

Equal amount of protein (50 to 100  $\mu$ g) samples were taken from each condition and mixed with the equal volume of loading buffer. Subsequently, the samples were denatured at 95 ° C for 5 minutes and loaded on the gel. The maximum capacity of the gel was 100  $\mu$ l. The samples were loaded on the gel along with the molecular weight marker. Electrophoresis was performed with 1x SDS running buffer in the electrophoretic device under cooling condition (6 ° C). The samples were run at an electric voltage of 35 volt

### **1.2.9.5 Transfer of proteins to the nitrocellulose membrane**

The proteins on SDS-PAGE were transferred non-covalently to a nitrocellulose membrane. using semi-dry blotting method. In this method, a nitrocellulose membrane soaked for 5 minutes in anode buffer was applied on the gel, followed by 3 piles of the whatman paper also pre-soaked in anode buffer. It is then kept on the transfer device with the other side of the gel upright. Another 3 piles of whatman paper pre-soaked with cathode buffer were kept on the exposed side of the gel. The bubbles were carefully removed by gently rolling the glass pipette on the surface of whatman paper. The protein transfer was performed for 2 hours 30 minutes at 270 V (0.8 mA/cm<sup>2</sup>).

### **1.2.9.6 Ponceau S staining**

To check the protein transfer on the nitrocellulose membrane, the membrane was stained by red dye known as Ponceau stain. The membrane was kept in Ponceau S solution for 1 minute at room temperature and then washed off with distilled water. The dye stains the proteins on the membrane non-specifically and reversibly. With the help of the bands of the molecular weight markers the areas of interested proteins were marked on the membrane.

### **1.2.9.7 Blocking**

To saturate non-specific binding sites, the membrane was incubated in 3% BSA or 5% dry-milk in TBST for 1 hour at room temperature on a shaking device.

### **1.2.9.8 Immunodetection**

After blocking, protein detection was performed by antibody labelling. For this purpose, the membrane was first incubated with protein specific primary antibody diluted in 3% BSA or 3% milk in TBST overnight at 4 ° C on a shaking device. Unbound primary antibody was removed by washing the membrane three times with TBST each 10 minutes at room temperature with shaking. After that, the membrane was incubated in secondary antibody diluted in 3% BSA or 3% milk in TBST for 1 hour at room temperature. Secondary antibody that was not attached to the constant Fc portion of the primary antibody was removed by washing the membrane three times with TBST, 10 minutes each, room temperature. The secondary antibodies used are tagged with horseradish peroxidase (HRP), through which the specific antibody-protein

binding was visualized. For this purpose, the ECL Western blotting detection Kit was used. This peroxidase substrate system contains luminol; which is oxidized by the secondary antibody-coupled HRP and forms a chemiluminescent product, which can be detected in the LI-COR detection system. The signal strength correlates with the activation/expression of protein of interest.

#### **1.2.9.9 Stripping of Western blot membranes**

Wherever a second protein was required to detect from one blot, specifically bound primary and secondary antibodies from the membrane are removed by the method known as stripping. This was done at room temperature. For this purpose, the membrane was briefly washed with TBST and put in stripping buffer thrice for 10 minutes (15 minutes for strong stripping) on a shaking device. Thereafter, the membrane was washed with TBST thrice for 10 minutes and blocked again with the required blocking solution and entire procedure of primary antibody and secondary antibody incubation was performed followed by the detection. The densitometry of the protein bands was obtained by using the analysis feature of the LI-COR software.

#### **1.2.10 *YBX1* knockout using CRISPR/Cas9**

*YBX1* gene knockout by CRISPR/Cas9-mediated genome engineering was performed by Dr Corinna Kosnofel in the lab of Prof. Birgit Schitteck, Department of Dermatology, University of Tuebingen as described previously (Kosnofel et al., 2017) using the lentiCRISPRv2 one vector system harbouring *YBX1* specific sgRNA sequences (YB-1 sgRNA1 (forward): 5'-cac cgg gac cat acc tgc gga atc g-3', YB-1 sgRNA1 (reverse): 5'-aaa ccg att ccg cag gta tgg tcc c-3'; YB-1 sgRNA2 (forward): 5'- cac cgc gta gtg ccg ggc ttg gtg tcg g-3', YB-1 sgRNA2 (reverse): 5'-aaa ccc gac acc aag ccc ggc act acg c -3'; Sigma-Aldrich, Taufkirchen, Germany). Following lentiviral transduction and selection with 2 µg/ml puromycin for 14 days, single cell clones were generated and selected based on the loss of YB-1 expression.

#### **1.2.11 DNA repair reporter assay**

Human osteosarcoma cell line U2OS harbouring a chromosomally integrated copy of an individual reporter for specific repair pathway was generated in the lab of Prof. Dr. Jeremy Stark and gifted for the present study by Prof. George Illiakis. Each reporter construct

contains an inactive expression cassette for green fluorescent protein (GFP) that is interrupted by one or more recognition sites for the rare-cutting endonuclease I-SceI (Gunn and Stark, 2012). The individual reporters were designed in a way that a defined DSB repair outcome leads to restoration of a *GFP* expression cassette. The cells were cultured in McCoy's media with 2 µg/ml of selection marker puromycin. For the experiment, the osteosarcoma cells with the reporter construct for specific repair pathways were split and transfected with YB-1-siRNA and seeded in McCoy's media. Seventy-two hours after transfection, cell were transfected with the plasmid expressing I-sceI endonuclease which transport into the nucleus independent of external stimulation and produce DNA DSB on the reporter construct. After 24 hours, the percentage of *GFP* positive cells was determined by flow cytometry analysis.

### **1.2.12 Flowcytometry**

After splitting, the cells were passed through 50 µm filter and collected in 10 ml media in a falcon tube and centrifuged at 750 g for 5 minutes. After removing the supernatant cells, were washed with PBS and again centrifuged at 750 g for 5 minutes. After removing the PBS cell pellet was dissolved in FACS buffer. Flowcytometry analysis was performed using a plot of forward scatter versus side scatter to gate for events that are consistent with individual cells. The gated cells were analysed in a plot for green fluorescence on the y-axis, and orange or red fluorescence on the x-axis. This plot allows a distinction between cells with high autofluorescence versus green fluorescent cells. Cells expressing GFP were used as the outcome of reporter assay experiments

### **1.2.13 Proteomic study**

Proteomic analysis was performed by stable isotope labelling by amino acids in cell culture (SILAC). It is a simple, robust, yet powerful approach in mass spectrometry (MS)-based quantitative proteomics. The SILAC tags cellular proteomes through typical metabolic processes, which include incorporation of non-radioactive, stable isotope-containing amino acids into newly synthesized proteins. Growth medium is prepared in which natural or "light" amino acids are substituted by "medium" or "heavy" SILAC amino acids. Cells grown in such medium integrate the medium or heavy isotope tagged amino acids completely in about five cell doubling and the labelled or SILAC amino acids have no effect on alteration

of cell morphology or growth rates. In this way when light, medium and heavy cell populations are mixed, they remain discrete by MS, and protein levels are determined from the relative MS signal intensities. SILAC delivers precise relative quantification without any chemical manipulation and permits the development of elegant functional assays in proteomics. MDA-MB-231 parental and two YB-1 knockout clones 5 and 10 that were prepared by CRISPR-Cas9 technology, were used for the study. Three differently labelled media was used to culture the cells. Light Media for parental cell and medium and heavy labelled media for clone 5 and clone 10, respectively. Cells were grown for four passages to ensure the complete incorporation of the labelled amino-acids. After fourth passages the protein was isolated for mass spectrometry (MS) which was performed by Dr. Mirita Franz-Wachtel, Proteome Center Tuebingen, University of Tuebingen.

#### **1.2.14 Statistics**

Student's t-test was used to compare the difference between two groups.  $P < 0.05$  was considered statistically significant (\* $P < 0.05$ ; \*\* $P < 0.01$ ; \*\*\* $P < 0.001$ ). Densitometry of the immunoblots was performed in LI-COR Odyssey<sup>®</sup> Fc using the Image Studio Lite Software Version 5.2. Pearson correlation test was performed to analysis the correlation between different proteins analyzed in immunofluorescence staining of patient tumor samples.

## **2 Introduction**

Cancer is the second main cause of death and poses major health hazard after cardiovascular diseases worldwide. Using the Global Burden of Disease methodology, it is estimated that there were 17.5 million cancer cases, 8.7 million deaths, and 208 million disability-adjusted life-years worldwide in 2015 (Global Burden of Disease Cancer et al., 2017). The global cancer liability has risen to 18.1 million new cases and 9.6 million deaths in 2018. One out of five men and one out of 6 women develop cancer worldwide during their lifetime, and one in eight men and one in eleven women die from the disease. The latest World Health Organization (WHO) statistics predicted 13.2 million cancer related deaths worldwide by 2030 (Biemar and Foti, 2013) . Hence, cancer is one of the major global diseases which demands special attention from oncologist around the world to find a proper cure. The major therapeutic paradigms prevalent in cancer treatment comprised of single or combination of surgery, radiotherapy and chemotherapy. The advancement in medical technology and high throughput sequencing based personalized therapy increased the sophistication of cancer management but, unfortunately, could only contribute slightly in extending the duration of survival but not the complete cure of cancer. Therefore, it is urgent requirement to search for novel therapeutic strategies to target cancer.

Among various kinds of cancer, breast cancer is the most commonly diagnosed cancer in women (24.2%) (Ghoncheh et al., 2016). Around one out of four, all new cancer cases diagnosed in women worldwide are breast cancer. It is also the leading cause of cancer death in women (15.0%) as per the International Agency for Research on Cancer by WHO. Breast is the part of the body, which is not critical for the survival and hence could be removed to treat primary tumors. However, most of the breast cancer tumors are highly aggressive and invasive. Thus, metastasis to other organs makes the management of breast cancers very complicated. Breast tissue is largely dependent on hormones secreted by ovaries like estrogen and progesterone for its proliferation and growth. Besides that, epithelial growth factor receptor 2, known as Her2 is also highly expressed in most of the breast cancers. Hence, high number of the breast cancers are estrogen receptor(ER), progesterone receptor(PR) and/or Her2 positive/over-expressing and targeted by specific inhibitors of these receptors (Tamoxifen, Fulvestrant etc) or monoclonal antibody, e.g. Trastuzumab in the case of Her2 positive cancer. Approximately, 15-20% of breast cancer are known as triple negative breast cancer (TNBC) (Diana et al., 2018). TNBC by definition means that these tumors are negative for ER, PR and Her2. TNBC are highly aggressive and drug resistant tumors, which shows epithelial to



mesenchymal transformation and distant metastasis (Yao et al., 2017). Although representing only 15–20% of breast cancer, distant recurrence and mortality in the TNBC is significantly higher than the other breast cancer subtypes (Goncalves et al., 2018). Due to the lack of the three receptors in TNBC, hormonal therapies and anti-Her2 therapies remains ineffective and chemotherapy is the primary option for these patients. Despite initial responses to chemotherapy, resistance develops quickly and makes the treatment non-effective (Shao et al., 2017). Therefore, it is the biggest challenge in modern oncology to develop effective targeted therapy to treat TNBC. Several studies have shown that there is an increased rate of activating mutation in the RAS/MAPK pathway in TNBC (Giltneane and Balko, 2014, Bianchini et al., 2016) as opposed to other subtypes of breast cancer. Thus targeting RAS/MAPK pathway might provide a therapeutic approach to treat TNBC.

## 2.1 RAS

RAS is a small membrane bound GTPase, which acts as molecular switches regulating the transfer of the extracellular signals inside the cell. The three human *RAS* genes [i.e. Kirsten rat sarcoma viral oncogene homolog (*KRAS*), neuroblastoma RAS viral (v-ras) oncogene homolog (*NRAS*) and Harvey rat sarcoma viral oncogene homolog (*HRAS*)] encode four RAS proteins, with two *KRAS* isoforms that arise from alternative RNA splicing. *KRAS* is the most frequently mutated oncogene in human cancers (85%), followed by *NRAS* (11%) and least percentage of mutation about 4% are reported in *HRAS* (Hobbs et al., 2016). Synthesized in cytosol, RAS is transferred to the inner part of the plasma membrane, where it interacts with diverse membrane receptors like epidermal growth factor receptor (EGFR), insulin-like growth factor 1 receptor (IGF-1R), and platelet-derived growth factor receptor (PDGFR). Thus, RAS regulates major signaling pathways including the RAF/mitogen-activated protein kinase (MAPK) / extracellular-signal regulated kinase (ERK1/2) (Vikis and Guan, 2002, Smith et al., 2004) and phosphoinositide 3-kinase (PI3K)/Akt/mammalian target of rapamycin (mTOR) (Castellano and Downward, 2011, Manning and Toker, 2017). These pathways control important cellular functions, including cell proliferation, differentiation, migration and apoptosis (McCubrey et al., 2007, Peng et al., 2018, Yang et al., 2017). RAS proteins acts as binary switch, which cycles between *on* and *off* states depending upon the kind of bound guanine (di or tri) phosphate molecule. Guanine nucleotide exchange factor (GEF) regulates the conversion of inactive GDP bounded state to the active GTP bounded state. GTPase

activating protein (GAP) regulates the conversion of GTP bounded state back into the more stable GDP bounded inactive state of RAS protein. Hence, RAS activation is strictly regulated under normal cellular condition. Due to mutation in *RAS* or in its activating protein the on and off switching goes aberrant, which results into the permanent binding of GTP with RAS and constitutive activation of the signaling pathways regulated by RAS. This is the most common phenomenon seen in many kinds of KRAS driven cancers. The most common signaling pathway, which is regulated by RAS, is MEK-ERK pathway. Strategies to target KRAS will be highly beneficial to the patients having KRAS driven cancer. Unfortunately, there are no direct KRAS inhibitors available. As an alternative approach, targeting the downstream effectors of KRAS like MAPK or PI3K pathways could be an effective strategy in managing such tumors.

## **2.2 MAPK signaling pathway**

Mitogen-activated protein kinase (MAPK) is a serine/threonine protein kinase, which is found in eukaryotic cells. The MAPK signaling comprises of conservative three-step kinase cascade of RAF/MEK/ERK (Li et al., 2016a, McCain, 2013). The initiation of this cascade is activated by ligands (growth factors) that bind to a variety of membrane receptors, such as receptor tyrosine kinases (RTKs), G protein coupled receptors (GPCRs), toll-like receptors and cytokine receptors (Katz et al., 2007, Volinsky and Kholodenko, 2013). After the initial activation, the membrane bound RAS becomes activated by GTP binding and then recruits and activates the RAF kinase in the MAPK kinase cascade. RAF a serine/threonine protein kinase comprises of three main family members RAF-1, B-RAF, and A-RAF. RAF is a RAS effector and upstream activator of the ERK pathway. It can phosphorylate proteins directly or can promote the phosphorylation of protein via activation of downstream substrates like MEK/ERK. In most cases RAF phosphorylates downstream MEK, which makes the cascade fully activated (Dhillon et al., 2007) (Fig. 2.1) . MEK1/2 in turn activates ERK1/2 (T202/Y204) by dual phosphorylation on a threonine and a tyrosine residue located in the activation loop of the protein. Recent studies have shown that activated ERK1/2 can phosphorylate about two hundred downstream substrates, which in turn regulates gene expression, cell proliferation, differentiation and migration (Lefloch et al., 2009, Chen et al., 2009).

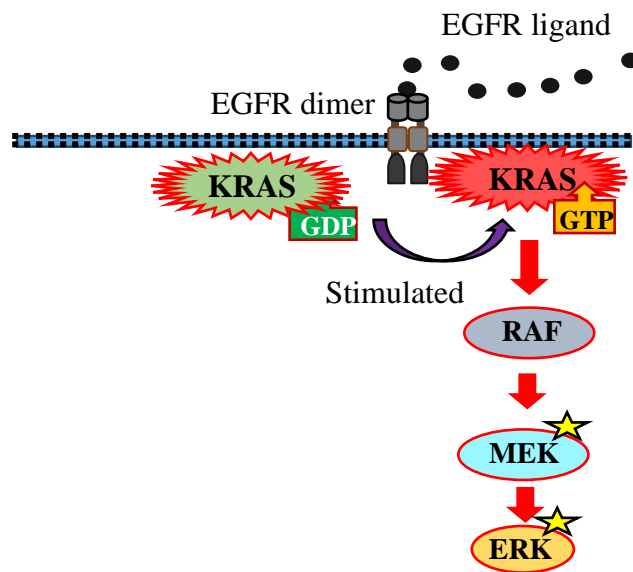


**Fig. 2.1 Schematic representation of MAPK signaling pathway.** Ligand stimulation induces dimerization of EGFR, which induces autophosphorylation of EGFR and conversion of inactivated GDP coupled KRAS to activated GTP bound KRAS. The activated KRAS phosphorylates downstream kinases RAF and stimulates the subsequent activation of MEK and ERK (own compilation).

Many studies have shown that genetic mutations or aberrations in any of the component of RAS-RAF-MEK-ERK cascade plays an important role in development and progression of various human cancers (Shao et al., 2018, Nandan and Yang, 2011, Burotto et al., 2014, Leung et al., 2019). In various malignant tumors including thyroid, colorectal, breast and melanoma cancer, RAF-MEK-ERK pathway is reported to be constitutively hyperactivated (Levidou et al., 2012, Wellbrock and Arozarena, 2016, Yang et al., 2017, Steelman et al., 2010, Vicent et al., 2004). Extensive statistical studies have demonstrated that activation of RAF-MEK-ERK pathway is associated with the oncogenesis of malignant cancers, making it an attractive target for efficient anticancer therapeutics (Montagut and Settleman, 2009, Yu et al., 2015). Based on this, a number of molecular agents targeting BRAF or MEK have entered clinical trials (de Langen and Smit, 2017, Welsh and Corrie, 2015). Unfortunately, they failed to sustain results due to the emergence of acquired resistance. Consequently, there is an urgent need to develop potential therapeutic targets to prevent the onset of the acquired resistance. The most common mechanism of the acquired resistance against RAF or MEK inhibitors is through reactivation of the ERK1/2 by some other pathway or activation of

another parallel pathway responsible for activation of similar processes. One of the prominent parallel pathway, which is also regulated by KRAS is PI3K/Akt/mTOR pathway.

### **2.3 PI3K/Akt/mTOR signaling pathway**

Phosphatidylinositol 3-kinase (PI3K) , Akt and the mechanistic target of rapamycin (mTOR) signaling pathway regulates many essential cellular functions like cell cycle progression, survival, metabolism, motility, and genomic instability (Hanahan and Weinberg, 2011). There are eight mammalian PI3K enzymes which are grouped into three classes known as Class I, II and III (Vanhaesebroeck et al., 2010). Class I is further divided into Class IA and IB out of which Class IA PI3K plays the predominant role in cancer. These PI3Ks are formed by a catalytic subunit p110 and a regulatory subunit p85. The p110 subunit generates phosphatidylinositol 3,4,5-triphosphate (PIP3) and p85 subunit is responsible for the interaction of PI3K with the upstream effectors. Both Class IA and IB PI3Ks phosphorylate phosphatidylinositol 4,5-bisphosphate to generate PIP3. Following activation of receptor tyrosine kinases by ligand, Class I PI3K generates PIP3 at the plasma membrane, which induces the recruitment of the phosphoinositide-dependent kinase-1 (PDK1) and Akt (Fig. 2.2) (Franke et al., 1995).

Tumor suppressor protein phosphatase and tensin homolog (PTEN), tightly regulates the levels of PIP3 by converting PIP3 back to phosphatidylinositol 4,5-bisphosphate and therefore exerts an opposing effect to PI3K (Maehama and Dixon, 1998) Recruitment of PDK1 and Akt to the plasma membrane leads to the direct interaction of both kinases. PDK1 phosphorylates Akt on a T308 residue and activates it partially (Alessi et al., 1997) (Stokoe et al., 1997). Complete activation of Akt is mediated by mTORC2 (mechanistic target of rapamycin complex 2) by an additional phosphorylation at S473 (Sarbasov et al., 2005). Activation of Akt leads to the phosphorylation of a large number of downstream targets for example Caspase-9 mouse double minute 2 homolog (MDM2), p27, glycogen synthase kinase 3 beta (GSK3 $\beta$ ), Forkhead box O transcription factor (FOXO), proline-rich Akt substrate of 40 kDa (PRAS40), Bcl-2-associated death promoter (BAD) and tuberous sclerosis complex (TSC2) which regulates cell growth, survival and proliferation (Manning and Cantley, 2007).

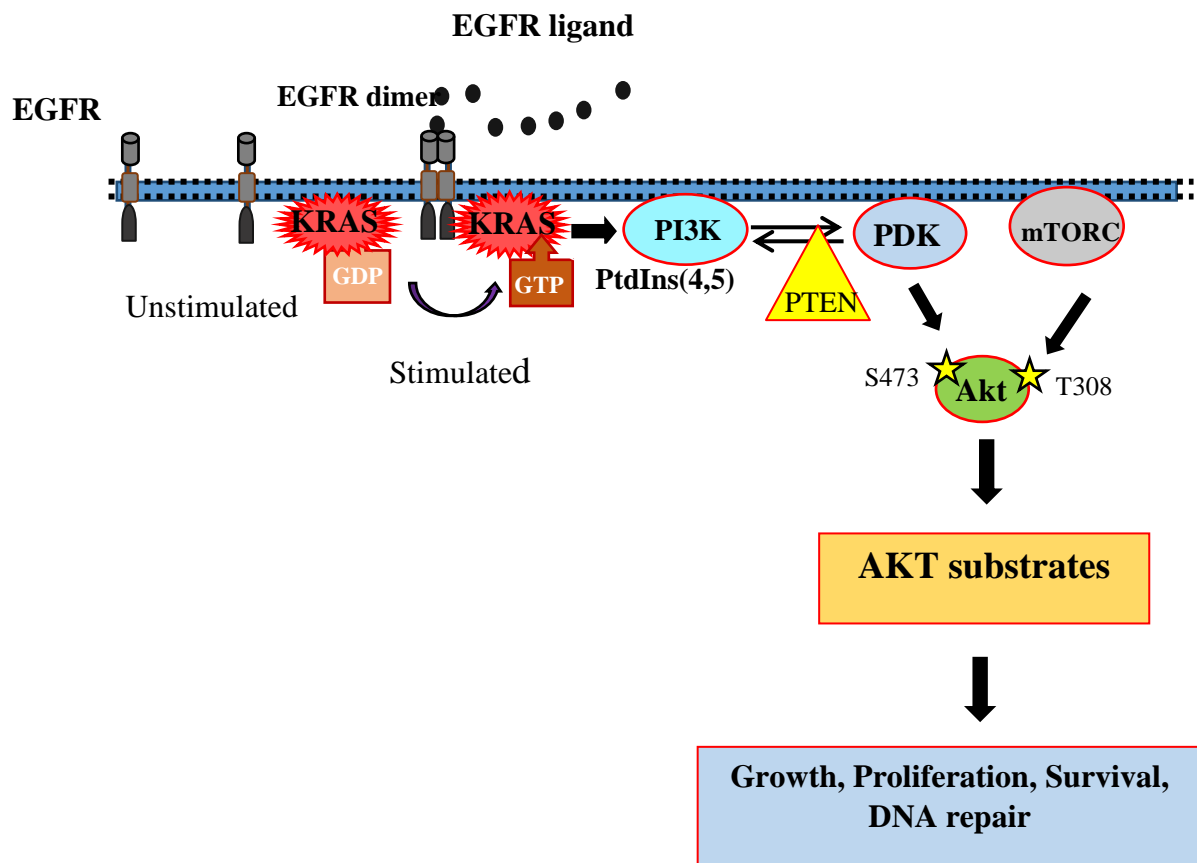


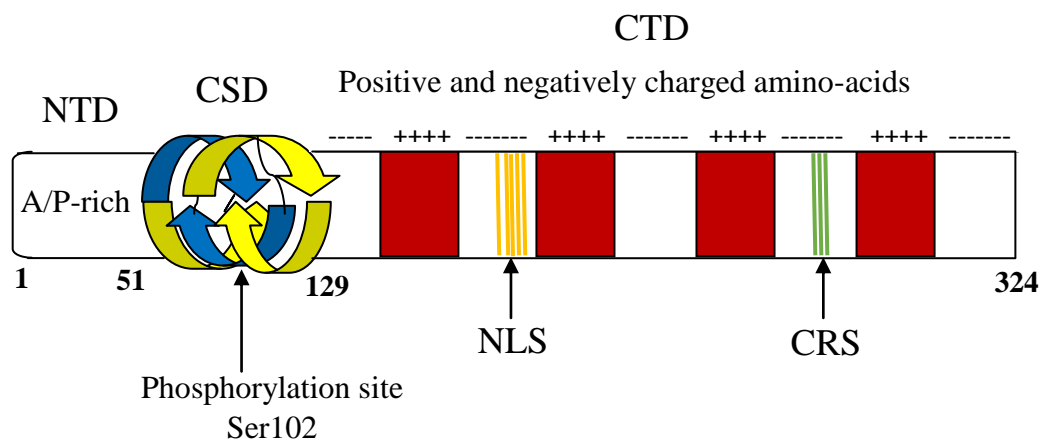
**Fig. 2.2 Schematic representation of PI3K/Akt signaling pathway under unstimulated and ligand induced stimulated conditions.** Ligand stimulation induces homo or hetero dimerization of EGFR which induces its autophosphorylation and conversion of inactivated GDP coupled KRAS to activated GTP bound KRAS. The activated KRAS phosphorylates PI3K that could further phosphorylate PDK1 under regulation of a phosphatase PTEN. mTORC2 and activated PDK1 phosphorylates Akt, which further phosphorylate several downstream substrate and regulate cell growth, survival, proliferation and DNA repair (own compilation).

PI3K/Akt pathway regulates cell growth and proliferation and therefore plays an important role in cancer. The pathway is frequently hyperactivated in human malignancies and associated with cancer progression. The pathway is also shown to be involved in cancer-promoting microenvironment such as angiogenesis and inflammatory cell recruitment (Beagle and Fruman, 2011) (Hirsch et al., 2014). Therefore, the inhibition of PI3K/Akt signaling pathway has become a promising approach in cancer therapy. However, the development of resistances due to abrogation of negative feedback mechanisms or the activation of other proliferative signaling pathways has substantially restricted the anticancer efficacy of PI3K/Akt inhibitors.

There are three different Akt isoforms known which are Akt1, Akt2 and Akt3. Akt1 promotes growth and survival, Akt2 controls cellular invasiveness and mesenchymal characteristics and Akt3 regulates synthesis of new protein and cell division (Irie et al., 2005) (Maroulakou et al., 2007). Although many studies have shown that Akt is the major downstream effector of PI3K but in many cases PI3K and Akt can operate independent of each other in cancer, which adds to another level of complexity in this signaling pathway. Therefore, targeted therapies used alone will not be efficient and combined therapies are needed to produce stronger anticancer effects.

#### **2.4 Y-Box Binding Protein-1 (YB-1)**

Y-box binding protein-1 (YB-1), encoded by the *YBX1* gene, is a member of the cold-shock domain protein superfamily (Eliseeva et al., 2011, Lindquist and Mertens, 2018). It is one of the unique multifunctional protein, which can bind with DNA, RNA and several proteins (Kuwano et al., 2004). Due to high flexibility in selecting binding partners, YB-1 is reported to regulate transcription and translation of a wide range of important genes and proteins involved in cell proliferation and progression (Wu et al., 2007, Schitteck et al., 2007), DNA replication (Wu et al., 2015) and repair (Pagano et al., 2017), multi-drug resistance (MDR) (Murugesan et al., 2018) and epithelial to mesenchymal transition (EMT) (Khan et al., 2014, Evdokimova et al., 2009) (Gopal et al., 2015). YB-1 is reported to present in cytoplasm, nucleus and mitochondria of the cell. As a nucleic acid binding protein, multimers of YB-1 combines with mRNAs to form ribonuclear particles (RNP) in cytoplasm and hence regulate the translation of many essential proteins. It is also involved in chromatin remodelling, pre-mRNA splicing (Wei et al., 2012) and stress related cellular response (Lyons et al., 2016, Guarino et al., 2018). YB-1 acquired its name from its first identification as a protein binding to the Y-box sequence (5'-CTGATTGG-3') in the promoter region of class II MHC genes (Lasham et al., 2013). Later it was reported that YB-1 can also bind with other promoters as well along with the Y-box sequence. YB-1 is a small protein comprise of 324 amino acids (Fig. 3). The predictable molecular mass based on the number of amino acids is 35.9 kDa. However, YB-1 protein runs at an anomalous size of about 50 kDa in SDS PAGE gel.



**NTD - N-Terminal Domain** (Alanine/Proline rich - transactivation domain)

**CSD - Cold Shock Domian** (DNA/RNA binding domain)

**CTD - C-Terminal Domain** (Protein binding domain)

**NLS - Nuclear Localization Sequence** (Nuclear translocation of YB-1)

**CRS - Cytoplasmic Retention Sequence (CRS):** Cytoplasmic accumulation of YB-1

**Fig. 2.3 Diagrammatic representation of YB-1 protein structure (own compilation).**

Y-box binding proteins can be classified into three subfamilies; YB-1, YB-2 and YB-3. The subfamily YB-1 is most studied and includes the human YB-1 protein, which is reported to present in almost all somatic cells. The members of the second subfamily YB-2 are expressed only in germ cells. While the members of the third subfamily YB-3 are expressed only during embryonic development and disappear after birth. The basic structural peculiarities of all members of the three subfamilies of vertebrate Y-box binding proteins are as follows: high content of alanine and proline in the highly variable N-terminal domain (A/P domain); presence of a highly conserved nucleic acid binding cold shock domain (CSD); presence of an elongated highly disordered C-terminal domain (CTD) containing alternating clusters of positively and negatively charged amino acid residues (Fig. 2.3) (Lasham et al., 2013) The cold shock domain (CSD) is highly conserved and comprises of tertiary structure containing a five-stranded  $\beta$ -barrel with consensus sequences (Maurya et al., 2017) . It is associated with both specific and non-specific binding with nucleic acid and has binding sites for Akt kinase, PDK-1, and RSK. The CTD also contains nuclear localization sequence (NLS), the

cytoplasmic retention sequence (CRS), and the 20S proteasome cleavage site (Eliseeva et al., 2011) . It binds with number of proteins and non-specifically with nucleic acids. The A/P domain of YB-1 has a disordered structure which contains binding sites for actin (Ruzanov et al., 1999) , cyclin D1 (Khandelwal et al., 2009) and transcription factor p53 (Okamoto et al., 2000) . The CTD is involved in the protein homo-multimerization (Tafari and Wolffe, 1992) (Murray, 1994) and has binding sites for several important regulatory proteins. Due to highly disordered structure there is no definite three-dimensional structure of YB-1 reported so far. There is a hypothesis according to which the conformation of these domains is fixed only upon binding to ligands and may vary in complexes with different ligands.

## **2.5 YB-1 in cancer**

YB-1 is a multifunctional protein, which is reported to regulate all the ten hallmarks of cancer as described by Hanahan and Weinberg (Fig. 2.4) and Lasham et al (Fig 2.5) (Hanahan and Weinberg, 2011, Lasham et al., 2013) YB-1 is reported to be over-expressed in almost all kind of cancers such as breast, lung, colorectal, melanocytic, prostate, ovary and bone cancer (Lasham et al., 2013, Lee et al., 2016, Jiang et al., 2017, Sinnberg et al., 2012, Kosnopfel et al., 2018). In many kinds of human cancers, the enhanced expression of YB-1 is correlated with multidrug resistance and poor therapy outcomes. In breast carcinomas, expression of cytoplasmic YB-1 has been shown to be associated with tumor aggressiveness while nuclear localization was shown as a predictive marker of recurrence after chemo- and radiotherapy (Mylona et al., 2014), also associated with increased tumor grading and tumor stage in breast cancer (Dahl et al., 2009). YB-1 is therefore regarded as a prognostic marker of disease aggressiveness and tumor resistance to chemotherapy (Bargou et al., 1997). Thus, YB-1 is a significant oncoprotein that stimulates cell proliferation, enhances multidrug resistance and promotes metastasis. The reduction in the expression levels of YB-1 is reported to be associated with growth repression and apoptosis in a large number of cancer cells such as breast, colon, lung and prostate cancer.



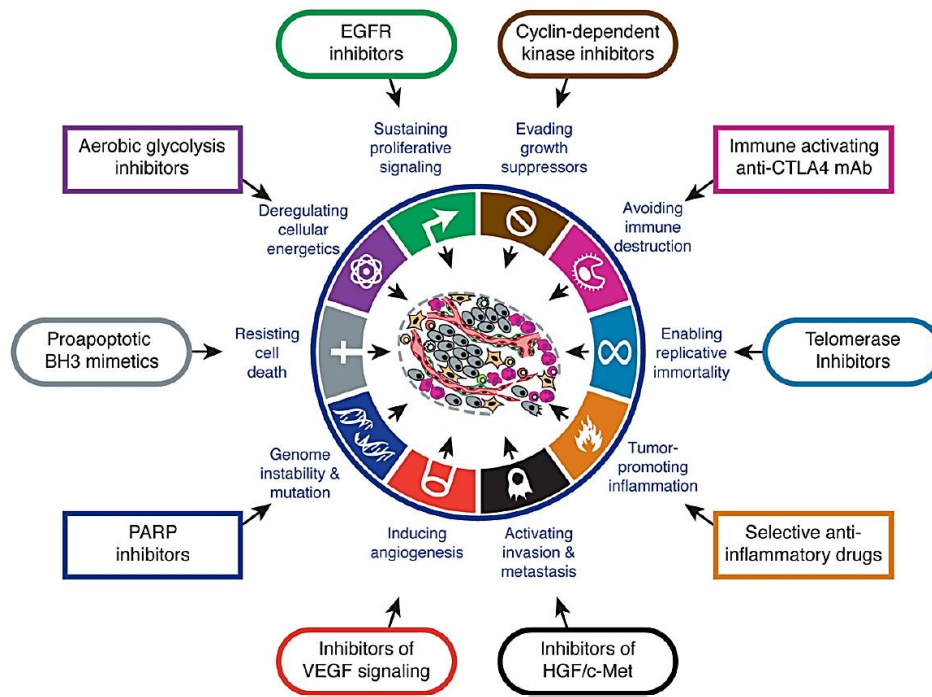


Fig. 2.4 Ten hallmarks of cancer; adapted from Cell Review 2011 (Hanahan and Weinberg, 2011)

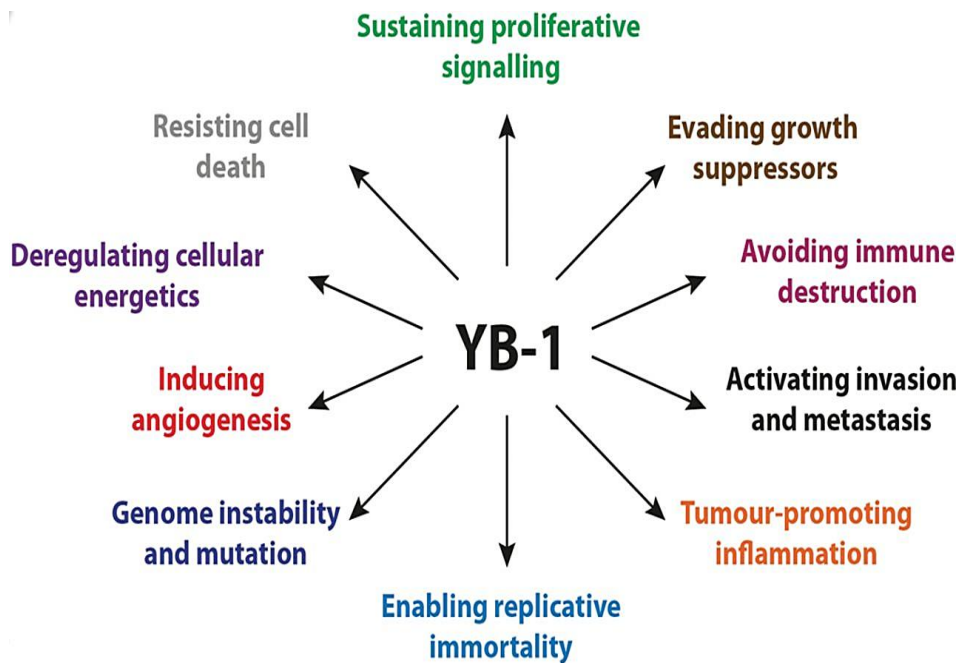


Fig. 2.5 Schematic diagram showing that YB-1 regulates all the ten cancer hallmarks; adapted from Biochemical Journal (Lasham et al., 2013)

YB-1 activates E2F pathways to promote uncontrolled cancer cell proliferation, which is a prevalent event in almost all types of cancers (Lasham et al., 2012). YB-1 inhibits the expression of tumor suppressor p53 gene in cancer cells and promotes uncontrolled proliferation (Zhao and Xu, 1999) (Tong et al., 2019). Hence, YB-1 overexpression results in hyperplasia (Krohn et al., 2007). Furthermore, cancer cells lose their ability for anchorage-independent growth on suppression of the YB-1 expression (Gopal et al., 2015). Studies involving transgenic mice showed that YB-1 over-expression resulted in malignant transformation of breast tissues (Davies et al., 2014). It is reported that overexpression of YB-1 is associated with an increase in the expression of EGFR, MET signaling, and HER-2 levels (Stratford et al., 2007, Guo et al., 2017, Wang et al., 2015). YB-1 is reported to enhance the cell resistance to different types of drugs used in treating cancer (Inoue et al., 2012). The mechanism of YB-1 induced chemoresistance is not completely clear but the most prevalent explanation is that YB-1 regulates the proteins ensuring multidrug resistance or it can be directly involved in DNA repair. Therefore, YB-1 is proposed as a potential target in therapy of various types of breast cancer.

## **2.6 Activation/Phosphorylation of YB-1**

YB-1 is reported to be phosphorylated at various sites. The most studied phosphorylating site is Serine 102 (S102). It is reported that YB-1 is activated to perform its function in transcriptional regulation after phosphorylation at S102.

## **2.7 YB-1 in DNA repair**

The human genome is being constantly attacked by various DNA damaging agents. According to the source of the toxic agents, DNA damage can be categorized into endogenous (spontaneous) and exogenous (environmental) damages (Rodriguez-Rocha et al., 2011, Chatterjee and Walker, 2017). Endogenous DNA damage occurs at a high frequency within normal cells, mainly caused by by-products of metabolic and biochemical reactions, such as reactive oxygen species (ROS) and reactive chemicals. In most cases, the endogenous toxic agents result in the modification or hydrolysis of the base components of DNA, such as through oxidation, alkylation, deamination, depurination and depyrimidination. Mismatch is another kind of endogenous DNA damage occasionally introduced during DNA replication (Tubbs and Nussenzweig, 2017, Li et al., 2016b). DNA damage caused by exogenous agents, such as ionizing radiation (IR), ultraviolet (UV), and radiomimetic drugs is much more catastrophic than that caused by endogenous agents. Gamma and x-rays as well as

radiomimetic drugs are the most dangerous types of DNA damaging agents, which can cause lethal lesions, such as DNA double-strand breaks (DSBs). Cell may incur tens of thousands of DNA lesions daily. Fortunately, mammalian cells have developed evolutionarily conserved mechanisms to cope with genotoxic threats, which have been termed as the DNA damage response (DDR). Upon DNA damage, cells detect the damaged DNA and relay the signal downstream to activate the cell cycle checkpoints to halt the cell cycle progression, allowing time for repairing the damage, or they bear the damage and continue replication, which may eventually cause mutations, or lead to apoptosis if the damage is too severe to be repaired (Nowsheen and Yang, 2012, De Zio et al., 2013) . Several conserved repair pathways responsible for eliminating specific types of lesions have been identified in mammalian cells. The repair pathways, which are involved in single strand repair include direct repair, base excision repair (BER), nucleotide excision repair (NER), and mismatch repair (MMR) (Fig. 2.6). The repair pathways actively involved in DNA DSB include homologous recombination (HR) repair and non-homologous end joining (NHEJ) repair. There is also considerable redundancy among these different pathways (Fig. 2.6)

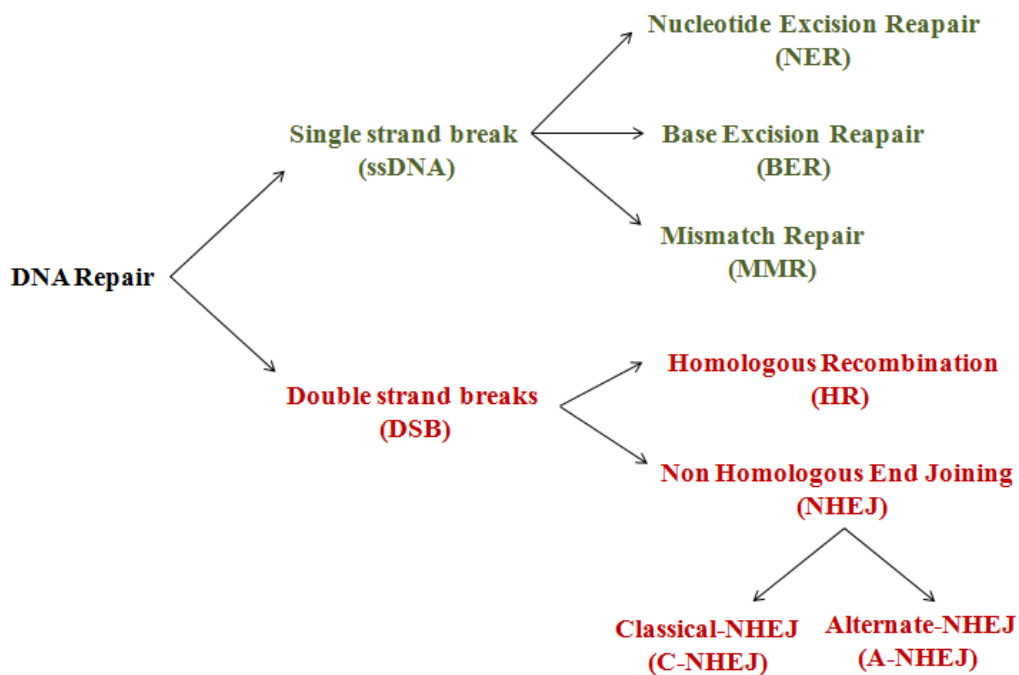


**Fig. 2.6 Schematic diagram showing different DNA repair pathways.** Single strand and double strand DNA breaks are repaired by specific repair pathways (Own compilation)

In 1991, Lenz and Hasegawa *et al.* proposed the involvement of YB-1 in DNA repair when YB-1 was identified as a protein possessing high affinity to DNA containing abasic sites (Hasegawa *et al.*, 1991). This assumption was further strengthened by the studies showing that YB-1 possess increased affinity towards damaged DNA or DNA containing mismatches (Gaudreault *et al.*, 2004, Izumi *et al.*, 2001, Kretov *et al.*, 2015). YB-1 is not only capable of separating the strands, but it can also cleave double-stranded DNA molecules. The hypothesis on the involvement of YB-1 in repair is also compatible with its exhibiting weak 3'-5' exonuclease activity on single stranded DNA and weak endonuclease activity on double stranded DNA. YB-1 is overexpressed in human cancer cell lines resistant to cisplatin, a platinum-containing anticancer drug that has been shown to damage cell DNA (Ise *et al.*, 1999). Several DNA repair proteins like PCNA (Yoshimatsu *et al.*, 2005), APE1 (Chattopadhyay *et al.*, 2008), MYC (Bommert *et al.*, 2013) and p53 (Okamoto *et al.*, 2000) can interact with YB-1, which further strengthens the concept that this multifunctional protein is involved in the repair of DNA damage. YB-1 has been also shown to regulate the expression of a number of other genes involved directly or indirectly in DNA repair. These genes include thymidine kinase (Fukada and Tonks, 2003), DNA polymerase  $\alpha$  (En-Nia *et al.*, 2005), Fas antigen (Lasham *et al.*, 2000), collagen  $\alpha 1(I)$  gene (Norman *et al.*, 2001), gelatinase A (Mertens *et al.*, 1999) and the multidrug resistance (*MDR1*) gene (Vaiman *et al.*, 2006). In addition, YB-1 interacts with wide variety of proteins involved in various DNA repair pathways such as NEIL2 (Das *et al.*, 2007), WRN (Maurya *et al.*, 2017), and MSH2 (Wu *et al.*, 2007) suggesting that YB-1 might assist in DNA repair complex assembly, making it a protein, which can play significant role in repair of all kinds of DNA damage. Furthermore, embryonic stem cells from YB-1 heterozygous mice exhibit increased sensitivity to DNA damaging agents including cisplatin and mitomycin C. Upon UV irradiation, YB-1 translocates from the cytoplasm to the nucleus (Koike *et al.*, 1997) and is known to bind to damaged nucleic acid (Wu *et al.*, 2007). All these reports suggest that YB-1 is indeed vital in DNA repair and drug resistance to tumor cells.

The nucleotide excision repair system (NER) is one of the main mechanisms protecting cellular DNA from lesions caused by genotoxic agents. One of the key factors during the damage recognition step of NER components is XPC-HR23B. YB-1 and XPC-HR23B stimulate each other's binding to the DNA having a bulky or clustered lesion, which points towards the possible role of YB-1 in the regulation of DNA repair by the NER mechanism. YB-1 as a component of the oxidative stress-induced NEIL2-initiated base excision repair

(BER) complex physically interacts with NEIL2, Lig3 $\alpha$  and Pol $\beta$ . On the other hand, Pestryakov et. al reported that YB-1, like RPA, suppresses NEIL's AP lyase activity on single stranded DNA substrates with AP sites while moderately stimulating the same with duplex DNA longer than 48 nts (Pestryakov et al., 2012). These could implicate role of YB-1 in transcription/replication-associated repair, where it simultaneously prevents induction of breaks at single stranded DNA and enhances repair of oxidized bases in double strand DNA. Interestingly, it has been shown that DNA damage-induced proteasome mediated cleavage of YB-1 results in loss of its cytoplasmic retention sequence and thus increases its nuclear accumulation in primary cancer cells. This may contribute to multidrug resistance phenotype of cancer cells (Maurya et al., 2017). Truncated YB-1 retains its interaction with DNA damage response proteins  $\gamma$ H2AX, MRE11, Rad50, Ku80 and WRN and in multiprotein repair complexes. Interaction of YB-1 with PCNA further suggests its role in NER and replication-associated repair. These studies demonstrate that YB-1 plays significant role in the repair of single strand breaks in DNA. However, the most fatal DNA damages are the DNA double strands breaks (DSB). Previous study showed that YB-1 stimulates repair of ionizing radiation-induced DSB (Toulany et al., 2011). DSB are among the most toxic lesions that is sufficient to promote genomic instability and cell death if left unrepaired (Schipler and Iliakis, 2013). These DSB may arise during meiosis or can result from exogenous stress by cytotoxic agents and ionizing radiation or endogenous insults such as reactive oxygen species (ROS) and replication errors. To repair DSB, cell employs primarily two standard DSB repair pathways: non-homologous end joining (NHEJ) and homologous recombination (HR) (Rothkamm et al., 2003) (Pfeiffer et al., 2000).

HR is highly conserved and error-free mechanism of DNA DSB repair. HR uses a sister chromatid as a template to repair the damaged sequence. Therefore, it is carried out during the S and G<sub>2</sub> phases of the cell cycle (Vignard et al., 2013). The initiation of HR relies heavily upon DNA end resection and formation of single-stranded 3' DNA overhangs (Symington, 2014). The formation of single stranded overhangs requires the recruitment of CtIP to the DSB break site, the stimulation of the endonuclease activity of MRE11 in complex with RAD50 and NSB1 (MRN complex), and the action of the nucleases EXO1 and BLM/DNA2. After end resection, replication protein A (RPA) loads onto the single strand DNA (ssDNA) and protects it from breakage (Ruff et al., 2016). Subsequently, other HR proteins like BRCA1, PALB2, and BRCA2, in complex with DSS1, promotes the replacement of RPA and the loading of RAD51 onto the ssDNA. RAD51 is the recombinase protein responsible

for homology search on the sister chromatid (Sonoda et al., 1999). Once the identical DNA is found on the sister chromatid, Rad51 is removed and the DNA is used as the template to synthesise the damaged DNA by polymerases.

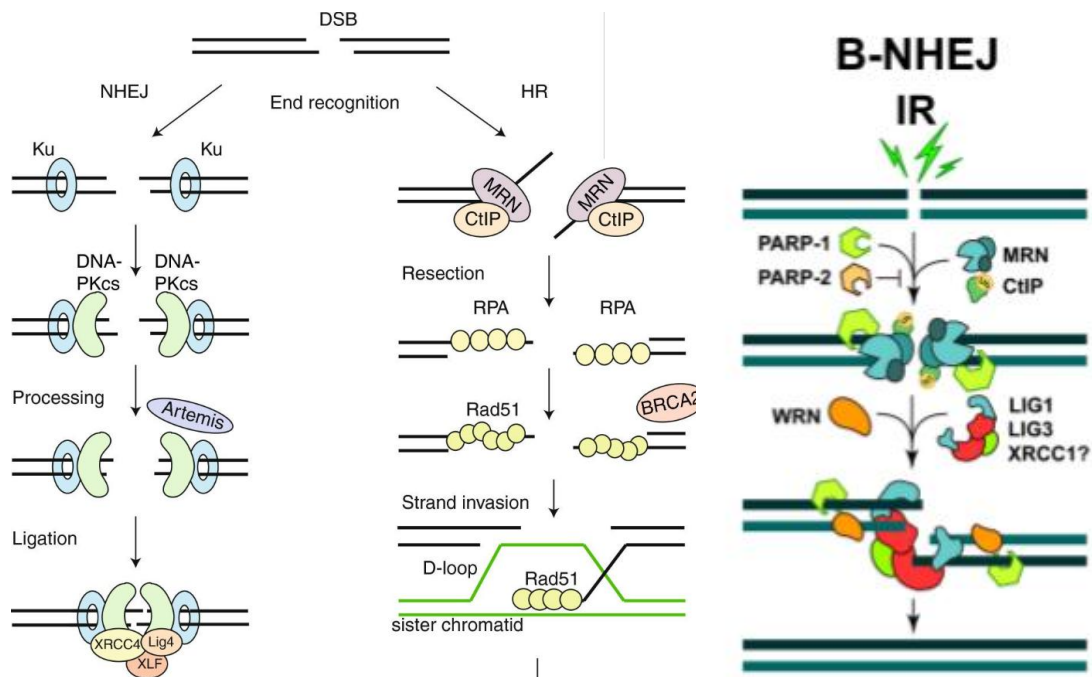


**Fig 2.7. Schematic representation of DNA DSB repair by homologous recombination (HR) and non-homologous end joining (NHEJ) pathways (Brandsma and Gent, 2012, Mladenov et al., 2013)**

Non Homologous End Joining (NHEJ) repair pathway is divided into pathways depending on the end resection and the regulatory proteins involved. 1) Classical NHEJ (C-NHEJ) is the predominant mechanism of DNA DSB repair; which operates in all phases of the cell cycle. It is a relatively simple and direct mechanism of DSB repair (Fig. 2.7). In C-NHEJ repair pathway as soon as the DNA DSB are formed, Ku70/Ku80 heterodimer immediately bound to both the ends of the DSB and protect the ssDNA from end resection. It is followed by recruitment of the catalytic subunit of the DNA dependent protein kinase (DNA-PKcs) (Davis and Chen, 2013, Hartlerode and Scully, 2009). DNA ends can either be directly ligated or processed slightly by nucleases such as Artemis or filled in by DNA polymerases until a ligatable configuration is attained. Processing of DNA ends results in nucleotide loss or addition, which results into mutation. Thus, C-NHEJ is an error prone DSB repair mechanism

(Fig. 2.7). 2) Alternate NHEJ (A-NHEJ) also known as backup NHEJ (B-NHEJ) is not very well defined pathway. This repair pathway has been shown recently to process DSBs when other two major DSB repair (HR and C-NHEJ) pathways are compromised. A-NHEJ starts with end resection by MRN complex similar to that of HR and PARP1/2 recruitment followed by RPA to protect ssDNA. The ssDNA ends are processed heavily and religated by ligase 1 and 2 (Fig. 2.7). This pathway is about 20-fold less efficient and slower than C-NHEJ.

There is no information in the literature regarding the specific DNA DSB repair pathways regulated by YB-1 and the underlying mechanism.

## 3 Results

### 3.1 Underlying signaling pathways involved in phosphorylation of YB-1

Phosphorylation of YB-1 is stimulated by ligands such as EGF, IGF-1 and exposure to IR (Toulany et al., 2011). It is reported that YB-1 is constitutively activated in *KRAS(G12V)*-mutated tumor cells and this phosphorylation cannot be stimulated further by treatment with ligands or exposure to IR (Toulany et al., 2011). Therefore, in the present study the signaling pathways responsible for the constitutive high level of P-YB-1 was evaluated in *KRAS(G13D)*-mutated breast cancer cells (BCC). YB-1 needs to be phosphorylated at serine 102 (S102) to carry out majority of its cellular functions. It is known that *KRAS* mutated BCC present high level of basal phosphorylation of YB-1 at S102 (Toulany et al., 2011). Mutation in *KRAS(G12V)* is one of the underlying mechanism by which YB-1 is constitutively phosphorylated in BCC (Toulany et al., 2011, Tiwari et al., 2018) . Thus, it is important to uncover the signaling pathways involved in constitutive high level of YB-1 phosphorylation.

#### 3.1.1 YB-1 is highly phosphorylated at S102 in BCC compared to normal breast epithelial cells

YB-1 expression level and its phosphorylation at S102 under non-stimulated condition was investigated in *KRAS* wild-type and *KRAS(G13D)*-mutated BCC as well as in normal breast epithelial cells. To this aim *KRAS(G13D)*-mutated MDA-MB-231 and MDA-MB-453 as well as *KRAS* wild-type SKBr3 and transformed breast epithelial cell line HBL-100 were compared with the normal breast epithelial MCF-10A cells. As shown in Fig 3.1, YB-1 was highly phosphorylated at S102 in all breast cancer cell lines compared to the normal breast epithelial cells. Interestingly the level of phosphorylation of the components of the MAPK pathway, i.e., ERK1/2 (T202/Y204) and RSK (T359/S363) was also elevated in all cancer cell lines except of P-RSK in MDA-MB-453 cells. Likewise, the PI3K pathway was also found to be highly activated in all breast cancer cell lines tested as indicated by enhanced Akt phosphorylation at S473. MCF-10A cells presented low levels of phosphorylation of YB-1 in association with the lack of phosphorylation at RSK1/2/3, Akt and ERK1/2. (Fig. 3.1). Data obtained from this experiment confirms that BCC present high level of phosphorylation of YB-1 and activation of the MAPK as well as PI3K pathway.



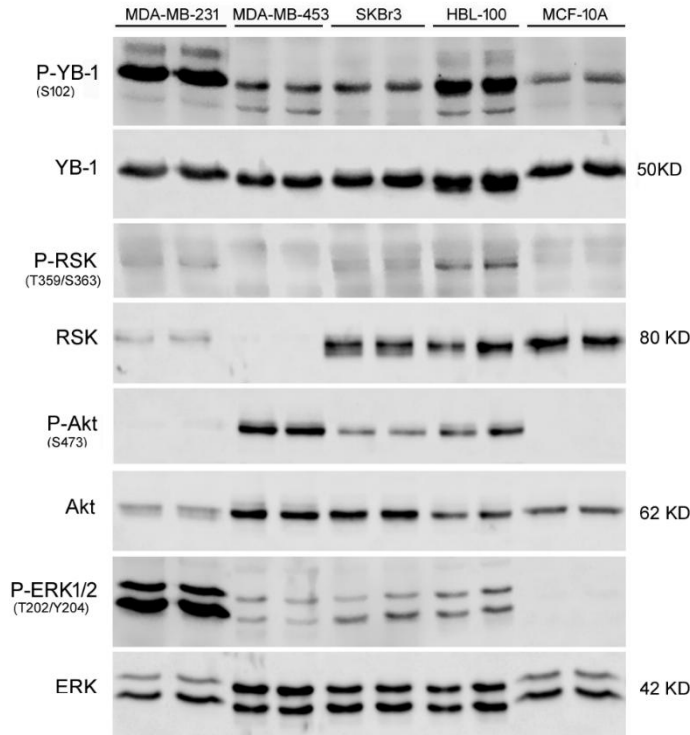


**Fig. 3.1 YB-1 is highly phosphorylated at S102 in BCC compared to normal breast epithelial cells.** Protein samples were isolated from indicated cell lines in a confluent status and subjected to SDS-PAGE. Phosphorylation level of indicated proteins was analysed by Western blotting using phospho-specific antibodies. Blots were stripped and incubated with antibodies detecting total protein. The protein samples were isolated from two parallel cultures.

### 3.1.2 External stimuli lead to long-term phosphorylation of YB-1 in *KRAS* wild-type but not in *KRAS*(G13D)-mutated cells.

Next, it was investigated if cellular stress differentially stimulates phosphorylation of YB-1 in cancer cell lines tested. To this end, effect of stimulation with EGF and exposure to clinically relevant dose of IR on YB-1 phosphorylation was tested within 24 h after treatment in cells, which were serum deprived for 24 hours. Data shown in Fig. 3.2 indicates that neither EGF treatment (Fig.3.2) nor exposure to IR (Fig.3.3) stimulated YB-1 phosphorylation in *KRAS*(G13D)-mutated MDA-MB-231 and MDA-MB-453 cells. In contrast, YB-1 phosphorylation was stimulated by both stimuli in *KRAS* wild-type SKBr3 and HBL-100 cells, as early as 30 minutes after stimulation and remained phosphorylated until 24 hours after EGF treatment in both cell lines and after irradiation in HBL-100 cells. In SKBr3 cells, IR induced YB-1 phosphorylation at 30 minutes' time-point and level of phosphorylation returned to the control level at longer time-points, i.e. 16 h and 24 h post-irradiation.

This data indicates that *KRAS*(G13D)-mutated MDA-MB-231 and MDA-MB-453 cells present constitutive high level of YB-1 phosphorylation that is not further inducible by external stimuli.

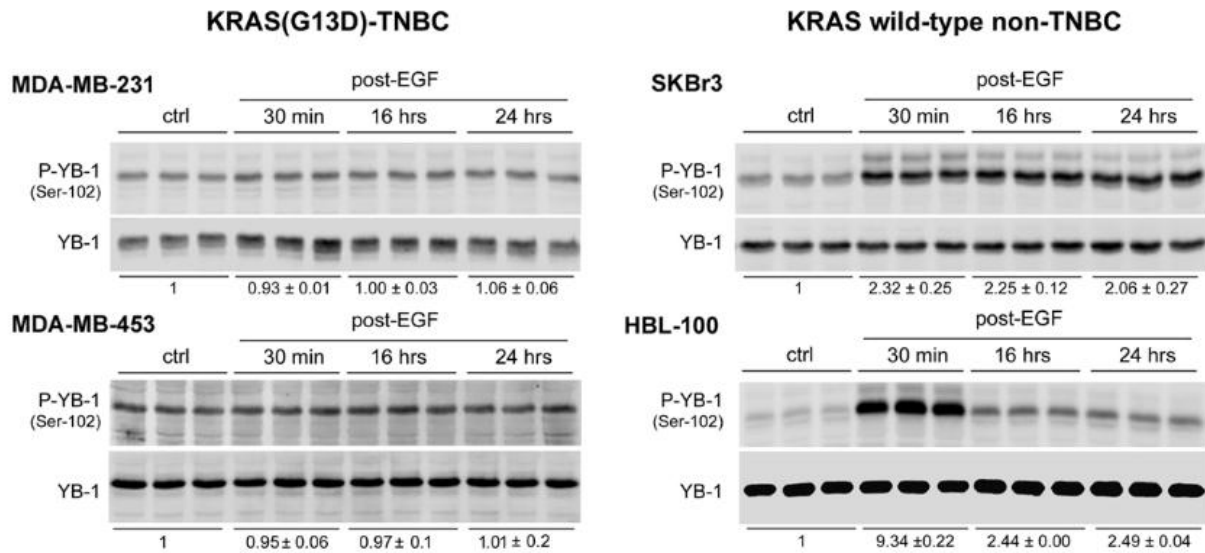


**Fig. 3.2 EGF treatment leads to long-term phosphorylation of YB-1 in *KRAS* wild-type but not in *KRAS*(G13D)-mutated cells.** Confluent cells were starved for 24 hours and treated with EGF (100ng/ml). Protein samples were isolated at indicated time points after stimulation and subjected to SDS-PAGE. Levels of P-YB-1 (S102) and YB-1 were analysed by Western blotting. Protein samples were isolated from three parallel cultures. Densitometry values represents the mean of P-YB-1/YB-1 ± standard deviation (SD) normalized to 1 in the control (ctrl) condition. The experiments were repeated twice. Data shown above is representation of one experiment.

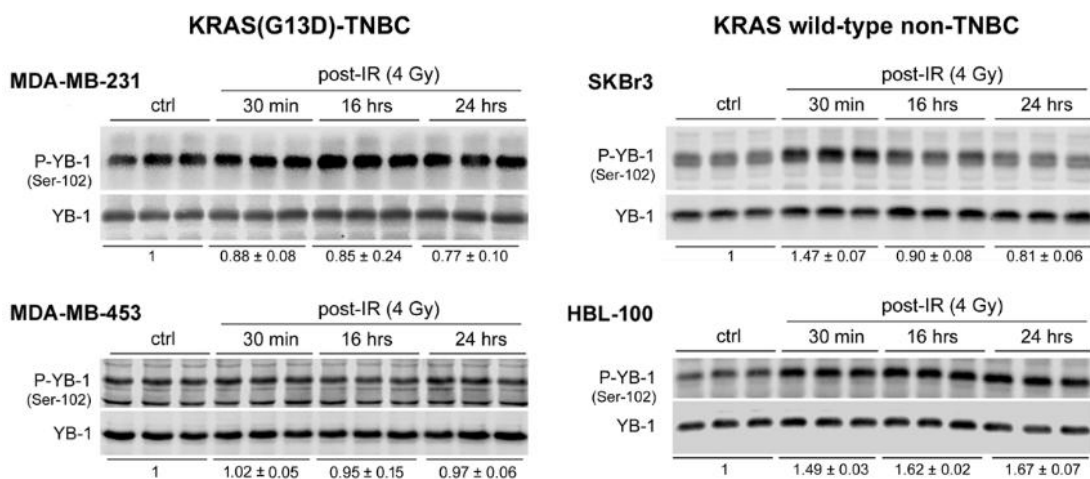


**Fig. 3.3 IR stimulates YB-1 phosphorylation in *KRAS* wild-type but not in *KRAS*(G13D)-mutated cells.** Confluent cells were starved for 24 hours and irradiated with 4 Gy. Protein samples were isolated at indicated time points after stimulation and subjected to SDS-PAGE. Levels of P-YB-1 (S102) and YB-1 were analysed by

Western blotting. Protein samples were isolated from three parallel cultures. Densitometry values represent the mean of P-YB-1/YB-1  $\pm$  standard deviation (SD) normalized to 1 in the control (ctrl) condition. The experiments were repeated twice. Figure shown above is representation of one experiment

### 3.1.3 *KRAS*(G13D)-MAPK-RSK is the major pathway regulating constitutive YB-1 phosphorylation in *KRAS*-mutated cells

*KRAS*-siRNA was applied to verify the role of *KRAS*(G13D) expression in constitutive YB-1 phosphorylation. Knockdown of *KRAS* resulted in a strong reduction in the level of downstream effector kinase P-ERK1/2, which subsequently leads to the strong reduction in downstream target P-YB-1 (Fig. 3.4). As shown in the previous experiments (Fig. 3.2 & 3.3) both IR exposure and EGF treatment could not stimulate further the high levels of basal phosphorylation of YB-1 in *KRAS* mutated cells, therefore in the next experiments knockdown of *KRAS* was performed to check the effect on P-YB-1 levels. Thereafter, the *KRAS* knockdown cells were treated with EGF or exposed to IR. Knockdown of *KRAS* resulted into strong reduction in the level of phosphorylation of YB-1 (Fig. 3.4) Interestingly, now when the cells were treated with IR (Fig. 3.5 A) or EGF (Fig. 3.5 B), both stimuli could enhance phosphorylation of YB-1 in *KRAS* knockdown group. The induction of phosphorylation of YB-1 was seen within 15 minutes of IR exposure or EGF treatment. This clearly demonstrates that mutation in *KRAS*(G13D) is indeed responsible for the high levels of constitutive phosphorylation of YB-1 in *KRAS*(G13D)-mutated BCC.

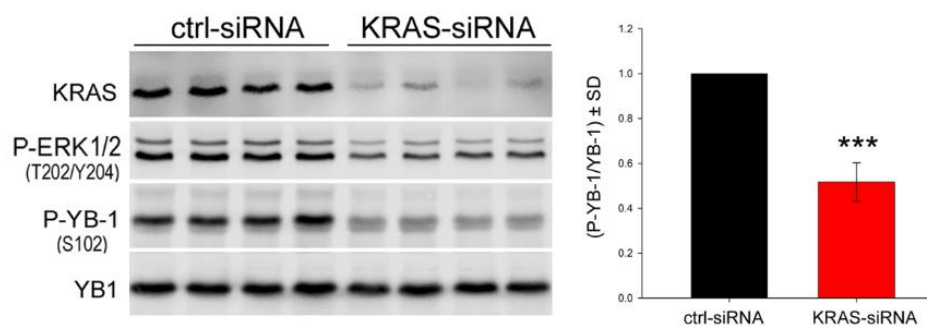


**Fig. 3.4 Constitutive phosphorylation of YB-1 in MDA-MB-231 cells depends on expression of *KRAS*(G13D).** MDA-MB-231 cells were transfected with control-siRNA (ctrl-siRNA) and the *KRAS*-siRNA. Protein samples were isolated 72 hours after transfection and subjected to SDS-PAGE. Levels of *KRAS*, P-ERK1/2, P-YB-1 (S102) and YB-1 were analysed by Western blotting. Protein samples were isolated from four parallel cultures. n=8 data from 3 independent experiments.

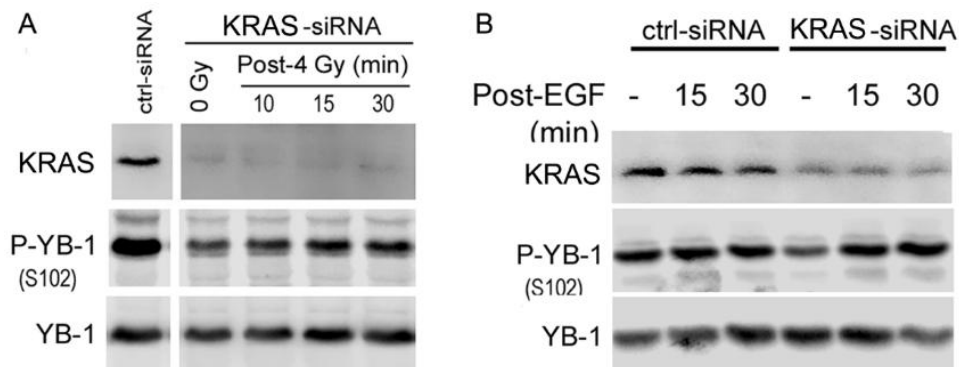


**Fig. 3.5 *KRAS*(G13D) mutation induces constitutive phosphorylation of YB-1.** MDA-MB-231 cells were transfected with control-siRNA (ctrl-siRNA) and the *KRAS*-siRNA and exposed to (A) 0 Gy and 4 Gy IR or (B) treated with EGF (100ng/ml). Protein samples were isolated at indicated time points after stimulation and subjected to SDS-PAGE. Levels of *KRAS*, P-YB-1 (S102) and YB-1 were analysed by Western blotting. Protein samples were isolated from indicated parallel cultures.

### 3.1.4 Mutation in *KRAS* induces constitutive phosphorylation of YB-1 through MEK/ERK and PI3K signaling pathways

The MAPK/ERK and PI3K/Akt pathways are the major signaling pathways downstream of EGFR and *KRAS*. Next, it was investigated if mutation in *KRAS* is responsible for over-activation of these two pathways. To evaluate the role of these two pathways in the phosphorylation of YB-1, LY294002 (LY) as PI3K inhibitor and PD98059 (PD) as MEK inhibitor were used in 10 $\mu$ M and 20 $\mu$ M concentrations for 2h. Both the concentrations of LY inhibited PI3K strongly as seen by complete inhibition of phosphorylation of Akt, which is the downstream substrate of PI3K. Phosphorylation of YB-1 was slightly inhibited by LY by about 10%, which was not further inhibited by increasing the concentration of LY from 10  $\mu$ M to 20  $\mu$ M (Fig. 3.6). Interestingly, PD strongly inhibited phosphorylation of YB-1 by about 35% at the concentration of 10  $\mu$ M and significantly higher inhibition of 53% was observed at the concentration of 20  $\mu$ M. The efficiency of PD can be seen by strong inhibition of P-ERK1/2 and P-RSK which are the downstream targets of MEK1/2 and ERK1/2, respectively.

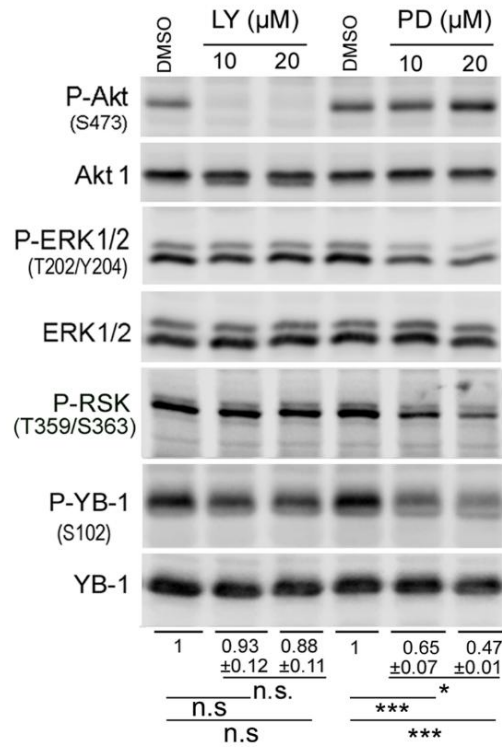


**Fig. 3.6 Mutation in *KRAS* induces constitutive phosphorylation of YB-1 through MEK/ERK and PI3K signaling pathways.** MDA-MB-231 cells were treated with DMSO (vehicle), the MEK inhibitor PD98059 (PD) and the PI3K inhibitor LY294002 (LY). Two hours after treatment with the indicated inhibitors, protein samples were isolated. The phosphorylation and expression of the indicated proteins were analysed by Western blotting. The densitometry analysis shows the mean ratio of P-YB-1/YB-1  $\pm$  SD normalized to 1 under DMSO treatment conditions. The asterisks indicate a significant difference compared with the related control (\* $p < 0.05$ , and \*\*\*  $p < 0.001$ , Student's *t*-test) LY, 5 data from 2 independent experiments; PD, 3 data from 2 independent experiments.

To further assess the role of MEK/ERK pathway, siRNA against *KRAS*, ERK2 and combination of both *KRAS* and ERK2 were used. Knockdown of *KRAS* inhibited phosphorylation of its downstream effectors ERK1/2 as well as RSK and consequently inhibited phosphorylation of YB-1 about 40% which was similar to the inhibition of P-YB-1 about 33% by the knockdown of ERK2 as shown in the densitometry values in Fig. 3.7. Combination of *KRAS* and ERK2 siRNA showed slight increase in the inhibition of P-YB-1 (about 50%). Therefore, it can be concluded that the major effect of *KRAS* mutation is predominantly through MEK/ERK pathway.

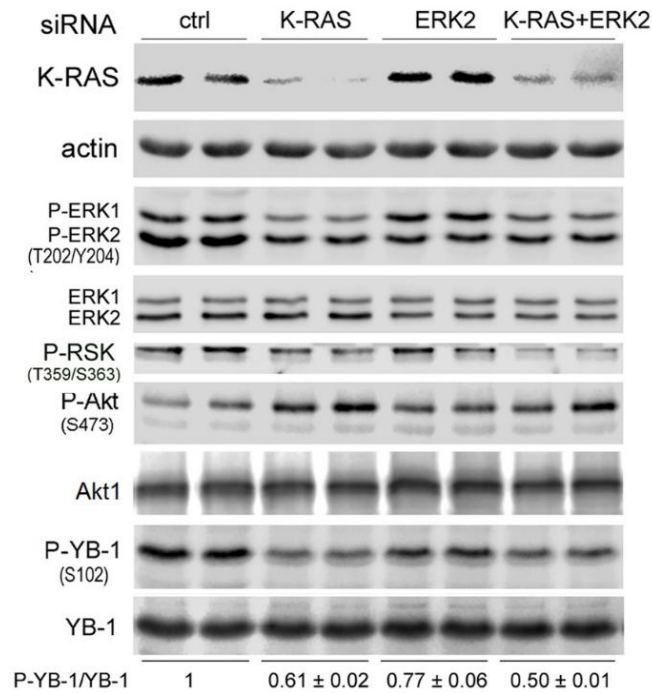


**Fig. 3.7 Mutation in *KRAS* induces constitutive phosphorylation of YB-1 predominantly through MEK/ERK signaling pathways.** MDA-MB-231 cells were transfected with control-siRNA (ctrl-siRNA) and the indicated specific siRNAs. Seventy-two hours after transfection, protein samples were isolated. The phosphorylation and expression of the indicated proteins were analysed by Western blotting. The densitometry analysis shows the mean ratio of P-YB-1/YB-1  $\pm$  SD normalized to 1 under the ctrl-siRNA conditions. n=4 from two independent experiments for the KRAS and ERK knockdown cells and n=2 for the ERK2+KRAS conditions.

Furthermore, knockdown of KRAS resulted in the increase in the phosphorylation of Akt, which is the major downstream substrate of PI3K pathway. This observation made it rational to investigate whether the inhibition of MEK/ERK pathway is actually responsible for activating PI3K/Akt pathway or activation of Akt is through some other pathway. LY, which is a PI3K inhibitor was added along with the knockdown of KRAS and ERK2. Addition of LY completely inhibited the KRAS or ERK2 knockdown mediated phosphorylation of Akt (Fig. 3.8). This confirms that's knockdown of MAPK pathway induces activation of PI3K/Akt pathway.

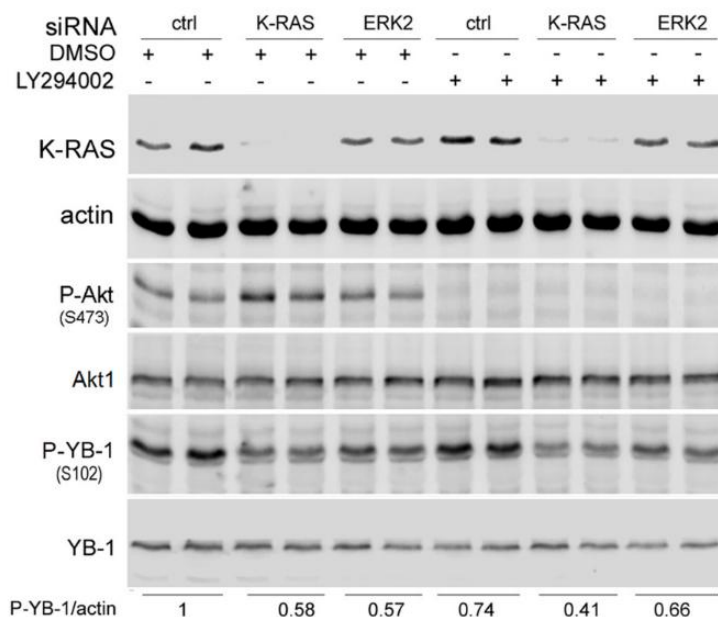


**Fig. 3.8 Inhibition of MAPK pathway activates PI3K pathway.** MDA-MB-231 cells were transfected with control-siRNA (ctrl-siRNA) and the indicated specific siRNAs with and without LY. Seventy-two hours after transfection, protein samples were isolated. The phosphorylation and expression of the indicated proteins were analysed by Western blotting. The densitometry analysis shows the mean ratio of P-YB-1/YB-1  $\pm$  SD normalized to 1 under the ctrl-siRNA conditions without LY treatment. n=2 in one experiments.

### 3.1.5 Mutated *KRAS* induces constitutive phosphorylation of YB-1 predominantly through MEK/ERK pathway in cytoplasmic and nuclear fractions.

YB-1 is found to be present in cytoplasm and nucleus of the BCC. It is reported that under stress conditions like exposure to ionizing radiations or xenotoxins, cytoplasmic YB-1 translocates to the nucleus and regulates the transcription of several essential genes (Koike et al., 1997). Thus, the next step was to explore the levels of P-YB-1 and underlying signaling pathway in nucleus and cytoplasm of the *KRAS*(G13D)-mutated MDA-MB-231 BCC. For this purpose, cells were treated with MEK1/2 inhibitor U0126 and PI3K inhibitor LY for 2 hours and protein lysate was prepared from the nuclear and cytoplasmic fractions.

The data presented in Fig. 3.9 shows that MEK1/2 inhibitor U0126 strongly inhibited P-ERK1/2 and phosphorylation of YB-1 in both cytoplasmic and nuclear fractions. The inhibition of PI3K by LY was strong in both fractions as seen by the inhibition of Akt (Fig. 3.9) however the inhibition of P-YB-1 by PI3K inhibitor was very mild in both cytoplasmic and nuclear fractions. Inhibition of MEK/ERK pathway activates the PI3K pathway as seen

by increase in phosphorylation of Akt only in the cytoplasmic fraction and not in the nuclear fraction of the cell. Therefore, MEK/ERK was confirmed as the predominating pathway regulating the phosphorylation of YB-1 in both nuclear and cytoplasmic fractions in *KRAS* mutated BCC.

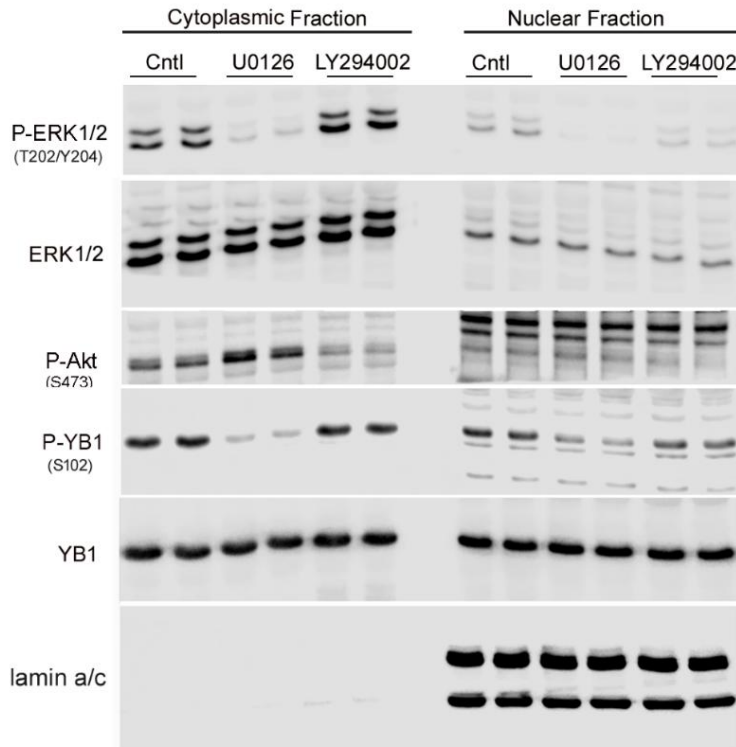


**Fig. 3.9 Mutated *KRAS* induces constitutive phosphorylation of YB-1 predominantly through MEK/ERK pathway in cytoplasmic and nuclear fractions.** MDA-MB-231 cells were treated with DMSO (vehicle), the MEK1/2 inhibitor U0126 and the PI3K inhibitor LY294002 (LY). Two hours after treatment with the indicated inhibitors, nuclear and cytoplasmic fractions were separated and the protein samples were subjected to SDS-PAGE. The phosphorylation and expression of the indicated proteins were analysed by Western blotting.

### 3.1.6 PTEN mutation dominates over *KRAS* mutation to control the constitutive phosphorylation of YB-1 through PI3K signaling pathway

PTEN is a tumor suppressor gene and one of the most frequently mutated genes in a variety of human tumors, including those of the breast (Hopkins et al., 2014, Kechagioglou et al., 2014). *KRAS*(G13D)-mutated MDA-MB-453 cells harbours an additional loss of function mutation in PTEN. PTEN regulates cell proliferation by inhibiting Akt activity through deactivating phosphatidylinositol (3,4,5)-trisphosphate. Therefore, the loss of function mutation in PTEN results in enhanced phosphorylation of Akt. Activated Akt in PTEN wild-type MDA-MB-231



and PTEN-mutated MDA-MB-453 was evaluated. Western blot data as well as the related densitometry has been presented in Fig. 3.10. As expected high level of basal Akt phosphorylation was observed in PTEN mutated MDA-MB-453 cells as compared to PTEN wild-type MDA-MB-231 (Fig. 3.10).

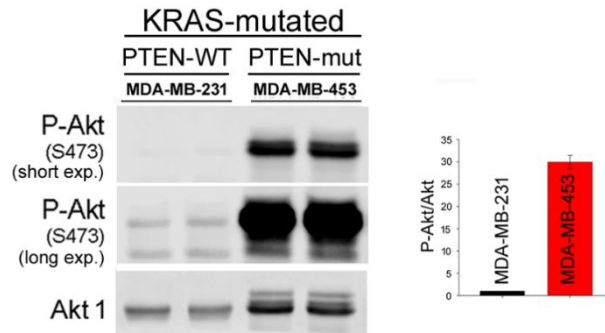


**Fig. 3.10 PTEN mutation dominates mutated *KRAS* for a constitutive phosphorylation of YB-1 through PI3K signaling pathway** Protein samples were isolated from 2 independent cultures of the indicated cells and the levels of P-Akt (S473) and Akt1 were detected by Western blotting. The phosphorylation and expression of the indicated proteins were analysed by Western blotting. The histogram shows the densitometry values of the mean ratio of P-Akt/Akt  $\pm$  SD normalized to 1; n=2 from one experiment.

As show by previous experiments, *KRAS* mutation leads to hyperactivation of MEK/ERK pathway. It was expected that *KRAS*(G13D)-mutated/PTEN mutated cells will also show the dominating role of MEK/ERK pathway in phosphorylation of YB-1. In contrast, knocking down of *KRAS* in *KRAS*(G13D)-mutated/PTEN mutated MDA-MB-453 cells showed no inhibitory effect on ERK1/2 phosphorylation and its downstream target YB-1. *KRAS* knockdown in MDA-MB-453 cells also did not induce the activation of the PI3K pathway in contrast to MDA-MB-231 cell line. This indicates that MEK/ERK pathway is not involved in the phosphorylation of YB-1 in *KRAS* mutated cells with additional PTEN mutation (Fig. 3.11).

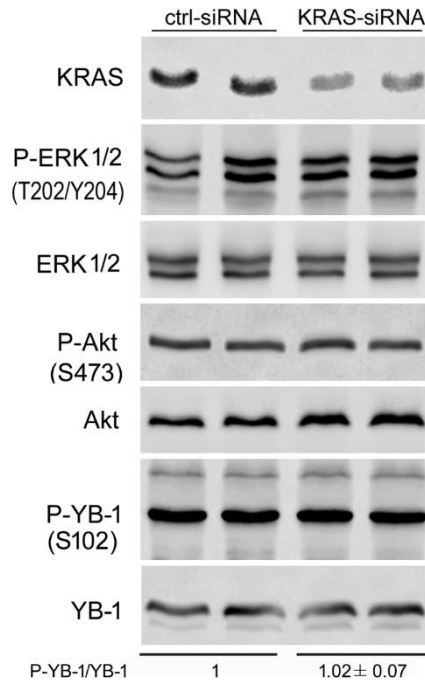


**Fig. 3.11 KRAS knockdown does not affect YB-1 phosphorylation in KRAS mutated cells with additional PTEN mutation.** MDA-MB-453 cells were transfected with control-siRNA (ctrl-siRNA) and the KRAS-siRNA. Seventy-two hours after transfection protein samples were isolated. The phosphorylation and expression of the indicated proteins were analysed by Western blotting. The densitometry analysis shows the mean ratio of P-YB-1/YB-1  $\pm$  SD normalized to 1 under the ctrl-siRNA conditions. n=2 from one experiment.

### 3.1.7 Dual targeting of MAPK and PI3K is an efficient approach to block YB-1 phosphorylation in KRAS(G13D)-mutated BCC expressing PTEN wild-type or PTEN-mutation

From the previous experiments, it was established that MEK/ERK is the dominating pathway involved in the phosphorylation of YB-1 in KRAS-mutated/PTEN wild-type cells whereas PI3K is probably the major pathway in KRAS/PTEN double mutated cells. As shown in MDA-MB-231 cells, inhibition of MER/ERK pathway resulted in the activation of PI3K/Akt pathway. Next it was tested if a crosstalk exists between the MAPK and PI3K pathways. To evaluate this crosstalk in KRAS-mutated/PTEN wild-type MDA-MB-231 cells, both the MEK/ERK and PI3K pathways were inhibited simultaneously by combine treatment of LY and PD for two hours. Interestingly, the dual targeting of both pathways inhibited phosphorylation of YB-1 much stronger than single targeting of either of the pathway. Fig. 3.12 shows that LY completely inhibited phosphorylation of its downstream target Akt, which was further confirmed by the inhibition of phosphorylation of PRAS40, which is one of the downstream target of Akt. But LY inhibited phosphorylation of YB-1 only about 10%.

Furthermore, PD strongly inhibited phosphorylation of ERK1/2, and RSK. The inhibition of P-YB-1 by PD was about 35-40%. As shown earlier (Fig. 3.6), inhibition of P-ERK1/2 showed stimulation of PI3K pathway as seen by the activation of Akt. Interestingly, dual targeting of both the pathways strongly inhibited YB-1 phosphorylation, which is about 75 - 80%. This effect is much stronger than the additive effect of the single targeting of PI3K or MAPK pathway in MDA-MB-231 (Fig. 3.12)

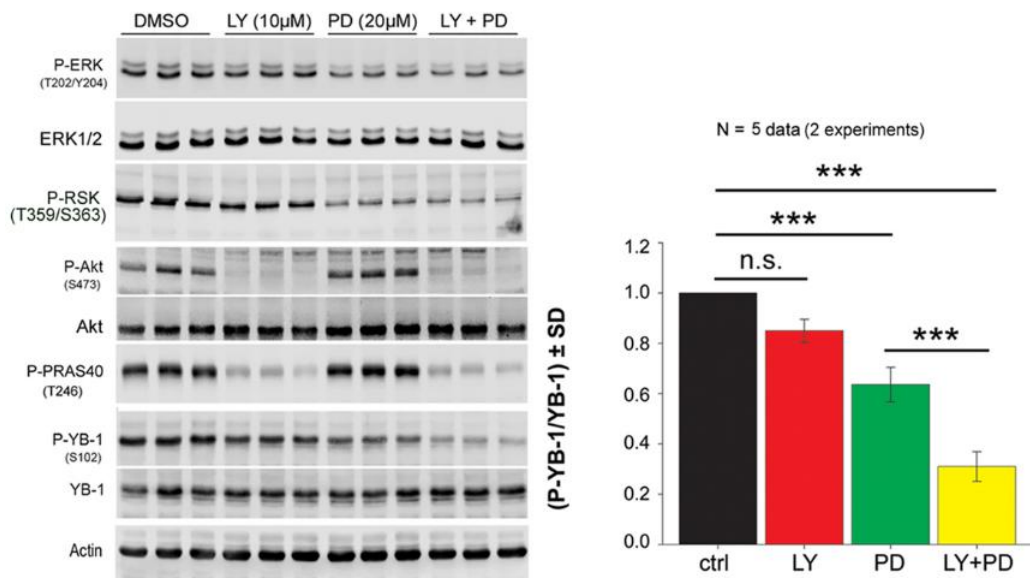


**Fig. 3.12 Dual targeting of MAPK and PI3K is an efficient approach to block YB-1 phosphorylation in *KRAS(G13D)*-mutated-*PTEN* wild-type BCC.** *KRAS(G13D)*-mutated MDA-MB-231 cells were treated with the PI3K inhibitor LY (10 μM), MEK inhibitor PD (20 μM) and a combination of LY and PD for 2 hours. Protein samples were isolated, and the indicated proteins were detected by Western blotting. Protein samples from the same treatment conditions were isolated from 3 parallel cultures. Histogram represents the mean P-YB-1/YB-1 ratio normalized to 1 in DMSO treated condition (\*\*\*) $p < 0.001$ , Student's t-test;  $n = 5$  from 2 independent experiments.

Next, the function of MAPK and PI3K pathway and the potential crosstalk between two pathways on YB-1 phosphorylation was investigated in *KRAS/PTEN* mutated MDA-MB-453 cells. As shown in Fig. 3.13, in contrast to MDA-MB-231 cells, inhibition of PI3K pathway by LY strongly inhibited phosphorylation of YB-1 by about 43% in MDA-MB-453 cells. Interestingly, inhibition of ERK1/2 by PD stimulates the phosphorylation of Akt but showed no inhibitory effect on the phosphorylation of YB-1. This observation points towards the fact that inhibition of one signaling pathway is actually activating the other signaling pathway as a rescue mechanism.

As a result, similar to MDA-MB-231 cells (Fig. 3.12), dual targeting of both the pathways inhibited phosphorylation of YB-1 much stronger than single targeting in *KRAS*/*PTEN* double mutated cells as well. These results indicates that irrespective of the dominating pathway responsible for the phosphorylation of YB-1, dual targeting is an efficient approach to target phosphorylation of YB-1 by eliminating the crosstalk operating between the two pathways.

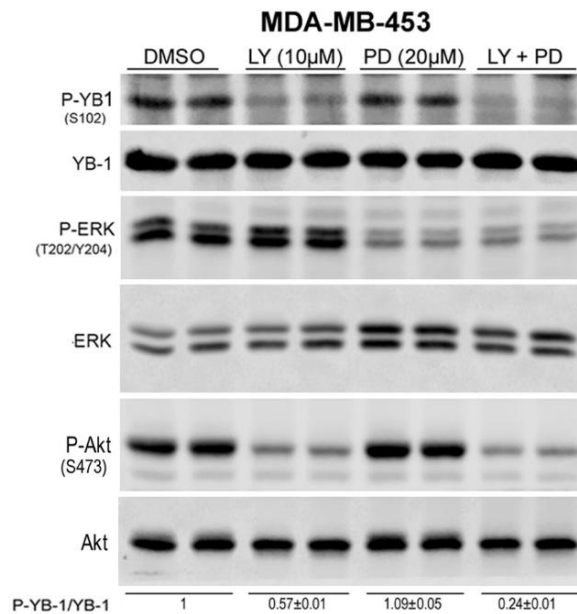


**Fig. 3.13 Dual targeting of MAPK and PI3K is an efficient approach to block YB-1 S102 phosphorylation in *KRAS*(G13D)/*PTEN*-mutated BCC.** MDA-MB-453 were treated with the PI3K inhibitor LY (10 μM), MEK inhibitor PD (20 μM) and a combination of LY and PD for 2 hours. Protein samples were isolated, and the indicated proteins were detected by Western blotting. Protein samples from the same treatment conditions were isolated from 2 parallel cultures. The densitometry values represent the mean P-YB-1/YB-1 ratio normalized to 1 in DMSO treated condition.

### 3.1.8 Constitutive YB-1 phosphorylation in *KRAS*(G13D)-mutated cells is independent of Akt

So far, the obtained data indicates that PI3K pathway plays an important role in the phosphorylation of YB-1 mainly due to the crosstalk with MEK/ERK pathway. Akt is the major downstream substrate of PI3K. Data from dual targeting of PI3K and MEK showed significantly stronger inhibition of YB-1 phosphorylation as compared to the single targeting. Therefore, it was expected that Akt inhibitor MK2206 (MK) will have similar effect on phosphorylation of YB-1 when combined with MEK inhibitor PD. The data presented in Fig.

3.14 showed that single targeting of MK (10 $\mu$ M; 2h) had no inhibitory effect on the phosphorylation of YB-1, although it strongly inhibits P-Akt and its downstream target P-PRAS40. In line with the data shown before in Fig. 3.12, PD showed strong inhibition of P-YB-1 and consequent stimulation of P-Akt. The inhibitory potential of PD was checked by the strong inhibition of P-ERK1/2 and P-RSK, the downstream targets of MEK and ERK1/2, respectively. In contrast to the data obtained by PI3K inhibition, the combination of MK and PD showed no further inhibition of phosphorylation of YB-1 in comparison to the PD treatment alone (Fig. 3.14 histogram). This data indicates that Akt might not be involved in the PI3K mediated phosphorylation of YB-1. To further confirm this conclusion, role of each Akt isoform on YB-1 phosphorylation was investigated by using genetic approaches in the subsequent experiments.

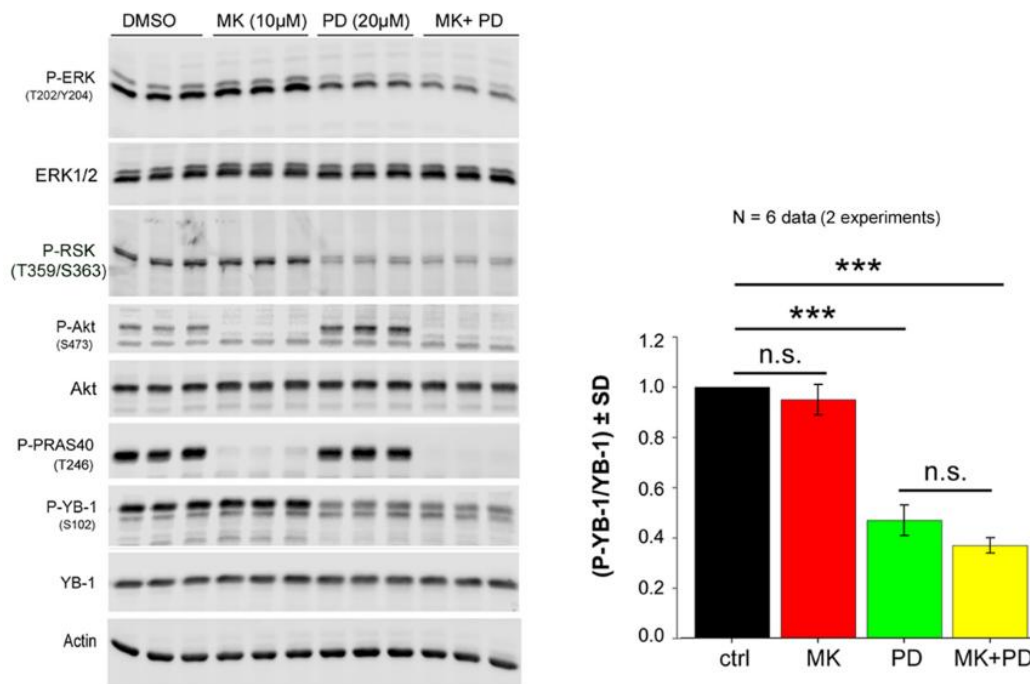


**Fig. 3.14 Constitutive YB-1 phosphorylation in *KRAS*(G13D)-mutated cells is independent of Akt.** MDA-MB-231 cells were treated with the Akt inhibitor MK2206 (MK, 10  $\mu$ M), PD98059 (PD, 20  $\mu$ M) and combination of MK and PD for 2 hours. Control cells (ctrl) received DMSO as the vehicle. Protein samples were isolated, and the indicated proteins were detected by Western blotting. Protein samples exposed to the same treatment conditions were isolated from 3 parallel cultures. Histogram shows the mean P-YB-1/YB-1 ratio  $\pm$  SD normalized to 1 in DMSO treated control condition (\*\*\*) $p$ <0.001, Student's t-test;  $n$ =6 in 2 independent experiments). n.s.: not significant

Akt isoforms (Akt1, Akt2 & Akt3) were knockdown by using siRNA against specific isoforms. The efficiency of knockdown was checked by detecting the total protein of each Akt isoform as shown in the Fig. 3.15. None of the Akt isoform knockdown showed any inhibitory effect on YB-1 phosphorylation. In contrast, a significant increase in the level of P-YB-1 was observed after knocking down of Akt 2 and Akt3 isoforms (Fig. 3.15 histogram).

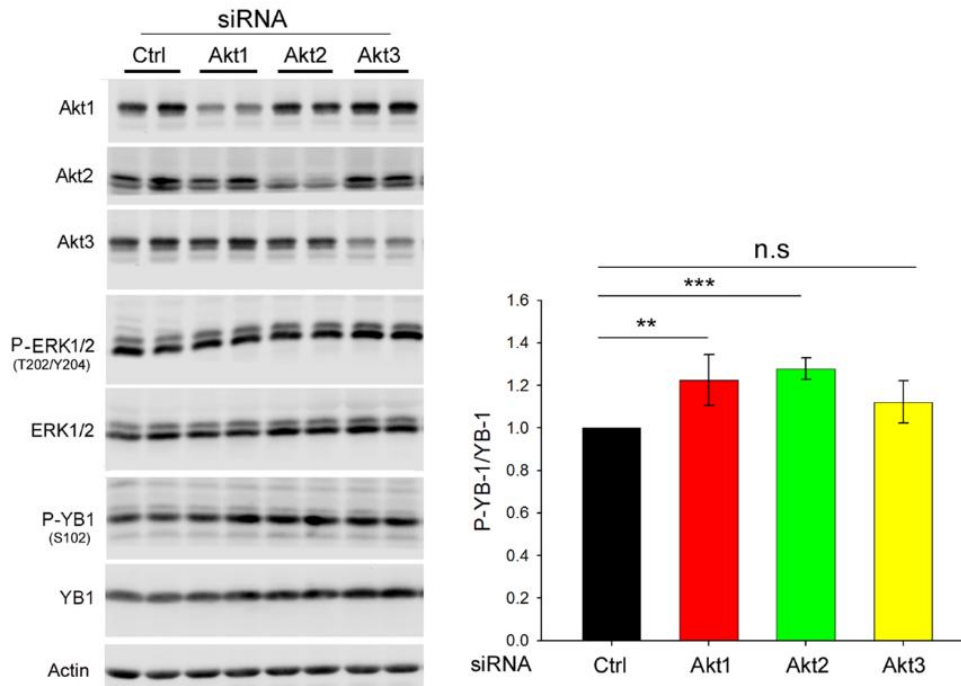


**Fig. 3.15 Constitutive YB-1 phosphorylation in *KRAS(G13D)*-mutated cells is independent of Akt isoforms.** MDA-MB-231 cells were transfected with control-siRNA (ctrl-siRNA) and the siRNAs against indicated Akt isoforms. Seventy-two hours after transfection protein samples were isolated. The phosphorylation and expression of the indicated proteins were analysed by Western blotting. The densitometry analysis depicted in the histogram shows the mean ratio of P-YB-1/YB-1  $\pm$  SD normalized to 1 under the ctrl-siRNA conditions (\*\* $p < 0.01$ , \*\*\* $p < 0.001$ , Student's t-test)  $n=5$  from two independent experiments (n.s. = not significant).

To further check the role of Akt isoforms in YB-1 phosphorylation, stably knockdown Akt isoforms using shRNA in MDA-MB-231 cells were used. Data shown in Fig. 3.16 indicates that knockdown of none of the Akt isoforms inhibited basal phosphorylation of YB-1. Furthermore, a rescue experiment was performed where the GFP tagged Akt isoforms were transiently overexpressed in the corresponding Akt knockdown cells. The data presented in Fig.3.17 shows that overexpression of none of the Akt isoforms had any effect on the phosphorylation of YB-1. Together, it can be concluded that PI3K mediated YB-1 phosphorylation is independent of Akt activity.

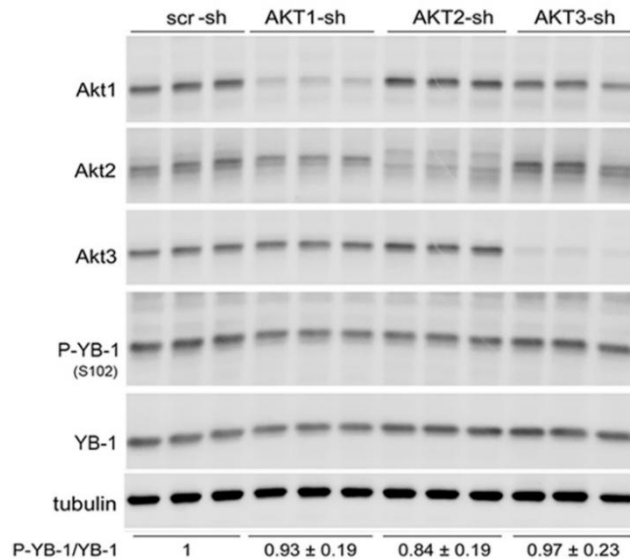


**Fig. 3.16 Constitutive YB-1 phosphorylation in *KRAS*(G13D)-mutated cells is independent of Akt isoforms.** Protein samples were isolated from MDA-MB-231 cells stably transfected with scramble-shRNA (scr-sh), Akt1-shRNA, Akt2-shRNA and Akt3-shRNA. Protein samples were isolated and subjected to SDS Page. The indicated proteins were detected by Western blotting. Protein samples were isolated from 3 parallel cultures. Densitometry values represents the mean P-YB-1/YB-1 ratio  $\pm$  SD normalized to 1 in scramble-shRNA cells (n= 6 data from 2 independent experiments).

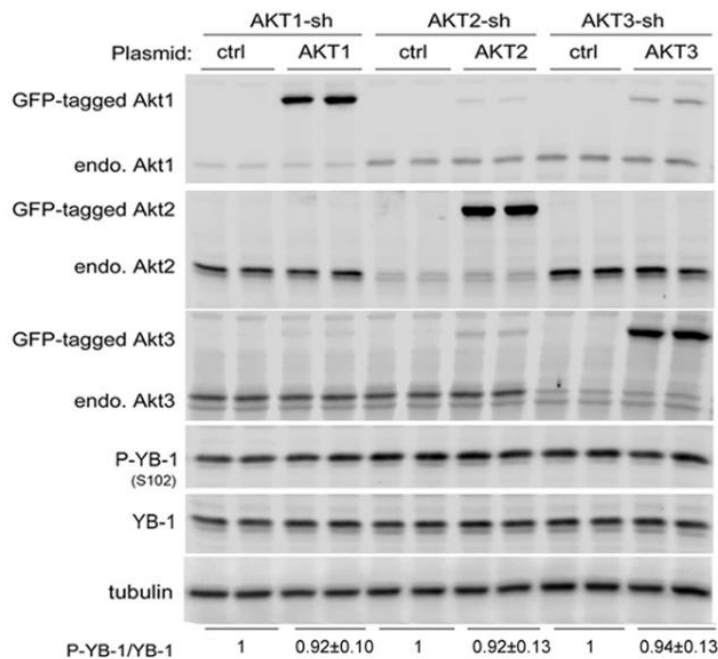


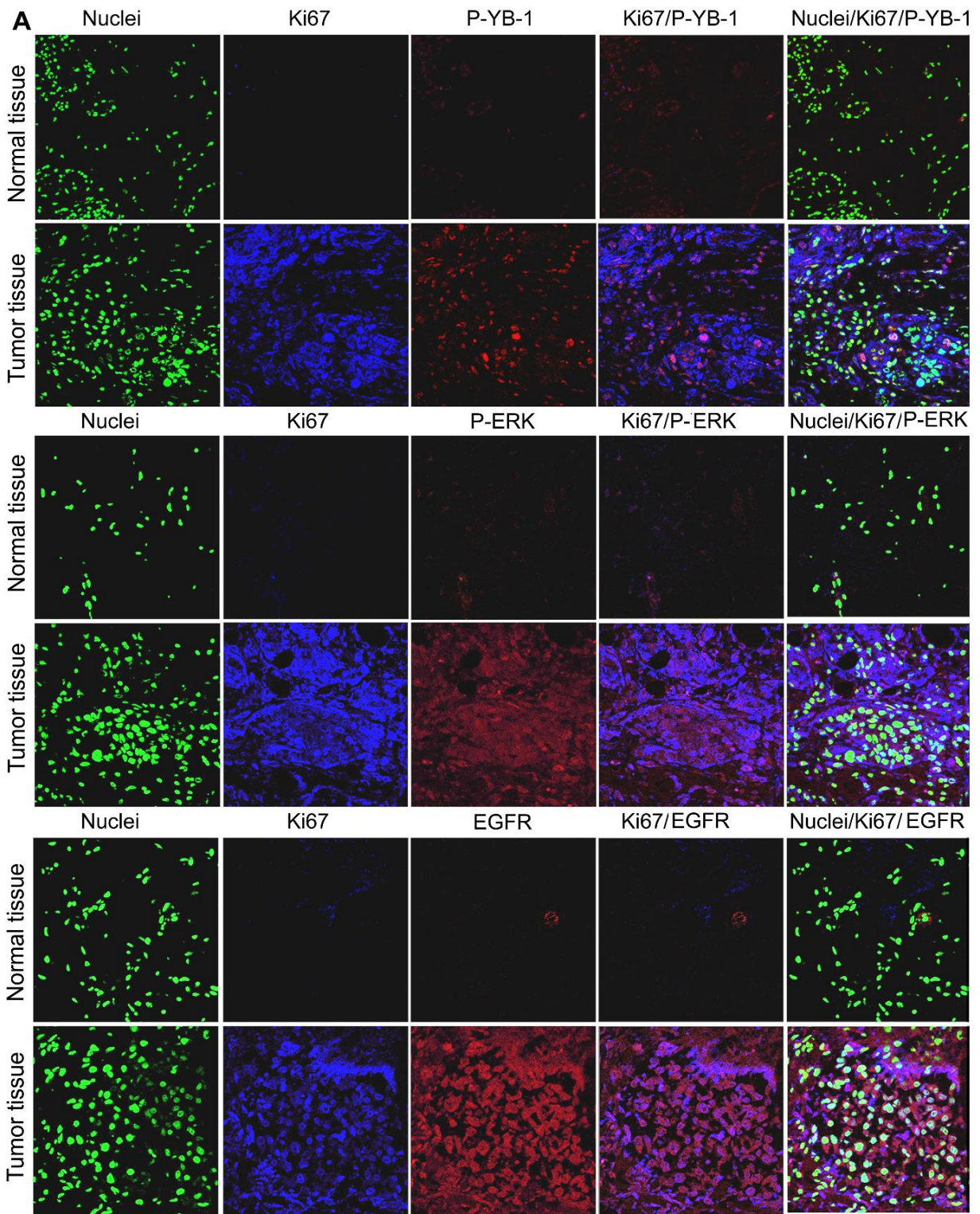
**Fig. 3.17 Constitutive YB-1 phosphorylation in *KRAS*(G13D)-mutated cells is independent of Akt isoforms.** MDA-MB-231 cells stably knockdown of Akt1, Akt2 or Akt3 were transiently transfected with plasmid expressing GFP-tagged-Akt1, -Akt2 or -Akt3 respectively. Forty-eight hours after transfection, protein samples were isolated and the indicated proteins were detected by Western blotting. Protein samples exposed to the same treatment conditions were isolated from 2 parallel cultures. Densitometry values represent the mean P-YB-1/YB-1 ratio  $\pm$  SD normalized to 1 in ctrl-plasmid transfected cells.

### **3.1.9 A positive correlation exists between P-YB-1 and P-ERK as well as expression of EGFR in the tissue samples from breast cancer patients**

The *in vitro* data so far has confirmed that MEK/ERK pathway is the major pathway regulating the phosphorylation of YB-1 in PTEN wild-type *KRAS* mutated BCC. To check the activation of this pathway in breast cancer patients, tumor tissues were collected from six breast cancer patients undergoing surgery, excluding samples from patients with neo-adjuvant chemo-/radiotherapy. Access to normal tissue was limited to only one patient (PT1). The immunofluorescence staining data obtained with the help of Ms Birgit Fehrenbacher (Department of Dermatology, University of Tuebingen) presented in Fig. 3.18 A, showed high levels of P-ERK and P-YB-1 as well as the over expression of EGFR in tumor tissue in comparison to the corresponding normal tissue obtained from PT1. The staining pattern of the other two tumor samples showing a high level of P-ERK and P-YB-1 with the overexpression of EGFR is shown in Fig. 3.18 B.



PT #1



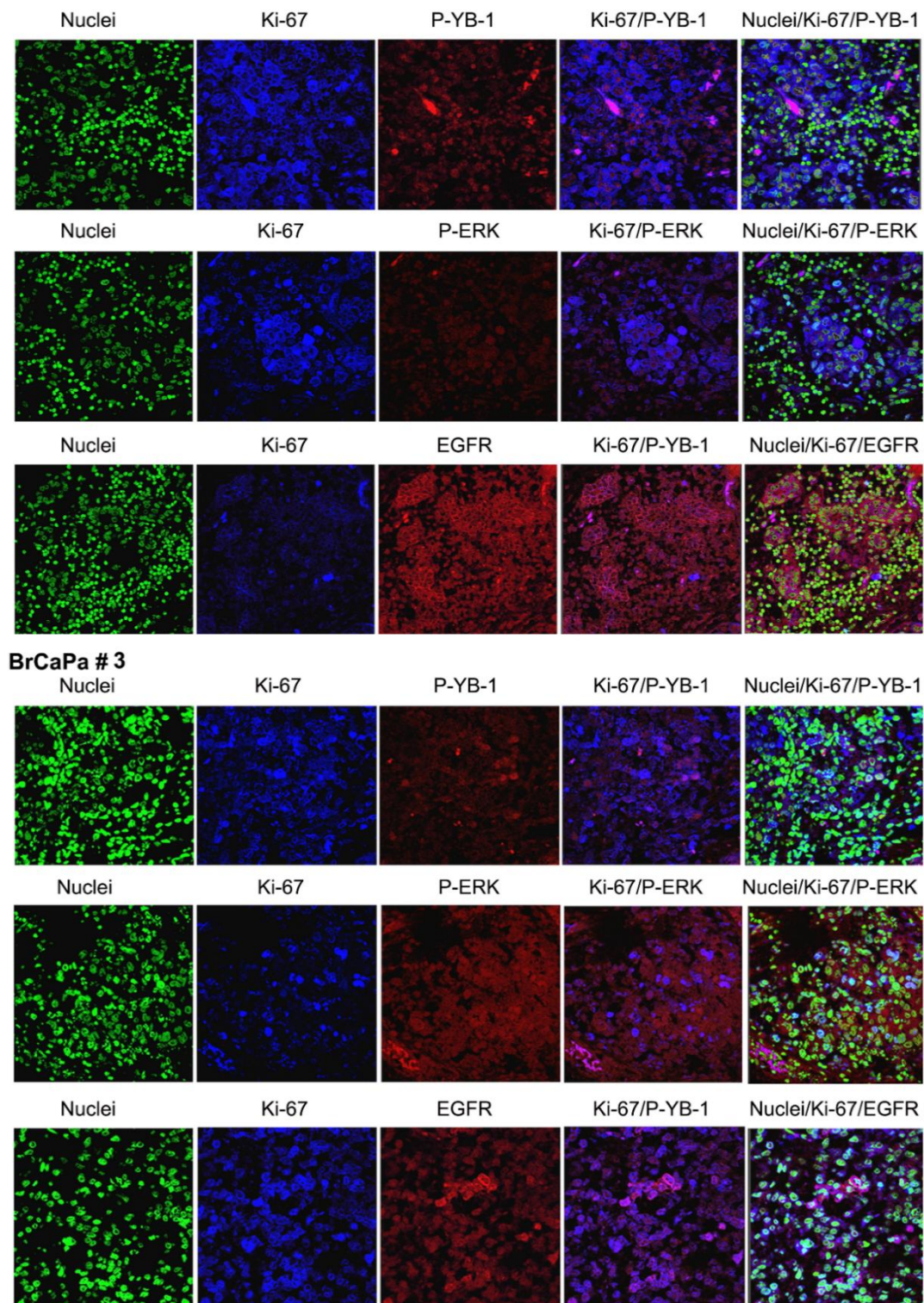
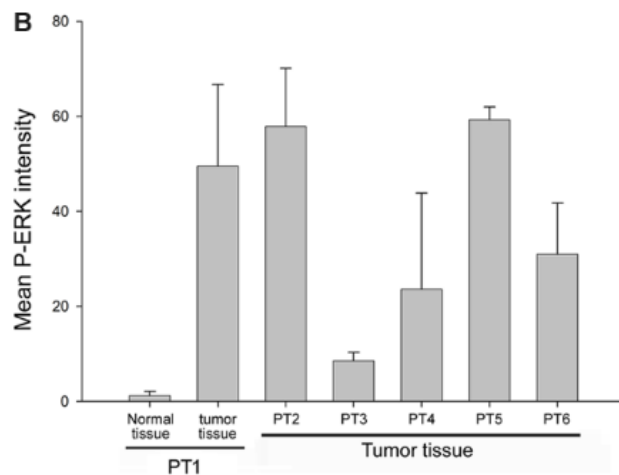
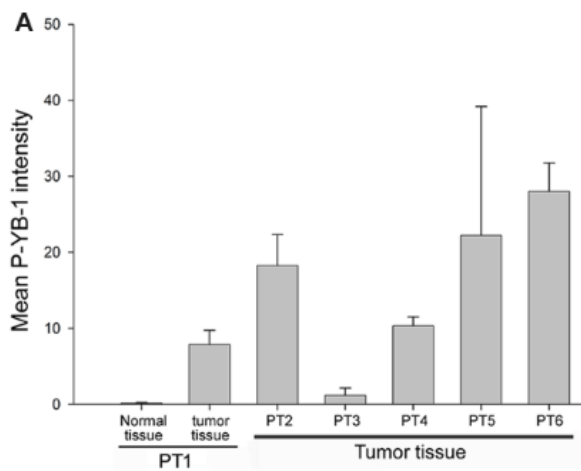


**Fig. 3.18 A positive correlation exists between P-YB-1 and P-ERK as well as expression of EGFR in the tissue samples from breast cancer patients** **A)** Paraffin-embedded sections were used for immunofluorescence staining of P-ERK1/2, P-YB-1 and EGFR in tumor tissues and the normal tissue from patient number 1 (PT1) and in tumor tissues from PT2 and PT3 **(B)**. Nuclei were stained with YO-PRO. Ki67 was stained as an indicator of cell proliferation. The sections were analysed with the confocal laser scanning microscope at 250x for P-YB-1 and 400x magnification for P-ERK1/2 as well as EGFR. This work was performed with the help of Ms Birgit Fehrenbacher, Department of Dermatology, University of Tuebingen.

According to the pathological data presented in the table 1, two out of six tumors were TNBC and the remaining four were non-TNBC. The graphs below shows, mean staining levels of P-YB-1 (Fig. 3.19 A), P-ERK (Fig. 3.19 B) and EGFR (Fig. 3.19 C). Pearson correlation coefficient test performed between P-YB-1 and P-ERK showed moderate positive correlation between P-YB-1 and EGFR. A strong positive correlation was observed between P-ERK and EGFR.

**Tab. 1**

Pts. ID	Cancer type	Grade	Stage	Metastasis	Lymphatic invasion	Vascular invasion	Estrogen receptor	Progesteron receptor	Her2 receptor
PT1	Duct. inv.	2	pT2	Yes	L1	no	negative	negative	positive
PT2	Duct. inv.	3	pT2	Yes	L1	V1	negative	negative	positive
PT3	Duct. inv.	3	pT4b	Yes	L1	no	positive	positive	negative
PT4	-	-	-	-	-	-	-	-	-
PT5	Duct. inv.	3	pT3	Yes	L1	no	negative	negative	negative
PT6	Duct. inv.	2	pT2	Yes	L1	no	negative	negative	negative



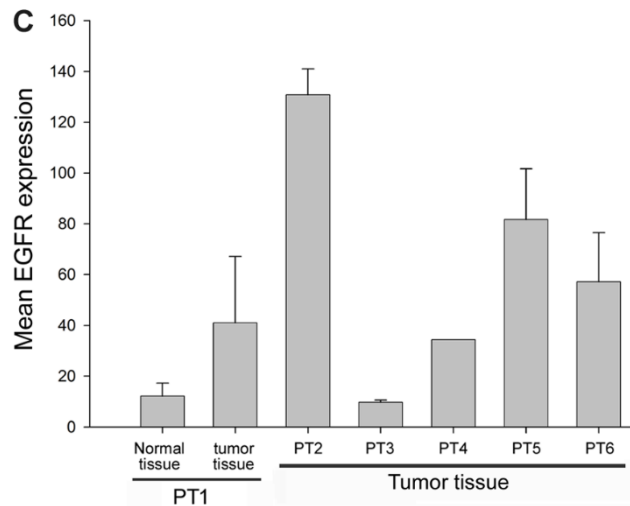


**Fig. 3.19 A positive correlation exists between P-YB-1 and P-ERK as well as expression of EGFR in the tissue samples from breast cancer patients.** Table.1 shows the pathological data of all the six patients. The mean intensity of fluorescence staining for (A) P-YB-1 (B), P-ERK1/2 and (C) EGFR was analysed in 3 randomly selected areas from staining sections under fluorescence microscope. Pearson correlation coefficient tests revealed a positive moderate correlation between P-ERK1/2 and P-YB-1 ( $r=0.51$ ), a positive moderate correlation between P-YB-1 and EGFR ( $r=0.61$ ) and a positive strong correlation between P-ERK1/2 and EGFR ( $r=0.81$ ).

### 3.2 Role of YB-1 in proliferation of *KRAS(G13D)*-mutated BCC

YB-1 plays an important role in cell proliferation by regulating cell cycle progression from G1 to S phase in cancer (Basaki et al., 2010). Overexpression of YB-1 is reported in different cancers including breast cancer (Maurya et al., 2017, Wang et al., 2015). Therefore, role of YB-1 in cell proliferation was tested in *KRAS(G13D)*-mutated TNBC cells. As shown in the previous section (Fig. 3.12), dual targeting of PI3K and MEK is an efficient approach to block phosphorylation of YB-1. In the further experiments it was investigated if this approach would effectively inhibit proliferation of *KRAS(G13D)*-mutated breast cancer cells. Along with the breast cancer cell line used in the study, NM2C5 melanoma cell line was also investigated. NM2C5 cells are known to have heterogenous mutation (V600E) in BRAF and shows high level of P-YB-1. RAF is downstream of RAS therefore these cells could be compared with the *KRAS* mutated BCC. YB-1 knockdown and knockout approaches were used to check the role of YB-1 in proliferation.

### **3.2.1 Dual targeting of PI3K and MEK is an efficient approach to block proliferation of *KRAS(G13D)*-mutated BCC in a YB-1-dependent manner**

MDA-MB-231 and MDA-MB-453 cells were treated with the PI3K inhibitor LY, MEK inhibitor PD and combination of the two inhibitors. Cells were counted on day 1, 2, 3 and 5 after inhibitors treatment. As shown in the Fig. 3.20 A, combination of both inhibitors showed a strong antiproliferative effect on MDA-MB-231 cells, which was significantly more than the effect of either of the inhibitor alone. This was also evident in population doubling time (PDT) calculated for every condition in each cell line. The cells were collected from all groups on day 5 of counting and Western blotting was performed. The Western blot data showed that the pattern of inhibition of cell proliferation by single or combination treatment of the inhibitors was in correlation with the level of inhibition of phosphorylation of YB-1 by the inhibitors (Fig. 3.20 B). Previous experiments showed that after short-term (2 hours) treatment with the inhibitors, PD mediated inhibition of P-YB-1 was stronger (35-40%) than LY (10%). Interestingly in long-term (5 days) treatment with inhibitors in the proliferation assay, LY inhibited P-YB-1 much stronger than PD, which is also seen by inhibition of P-RSK upstream to YB-1. Nevertheless, the combination of the two inhibitors had much stronger inhibitory effect on P-YB-1. The long-term treatment with LY also showed inhibition of expression levels of total YB-1 protein which was also correlated with the inhibition of EGFR expression (densitometry Fig. 3.20 B).

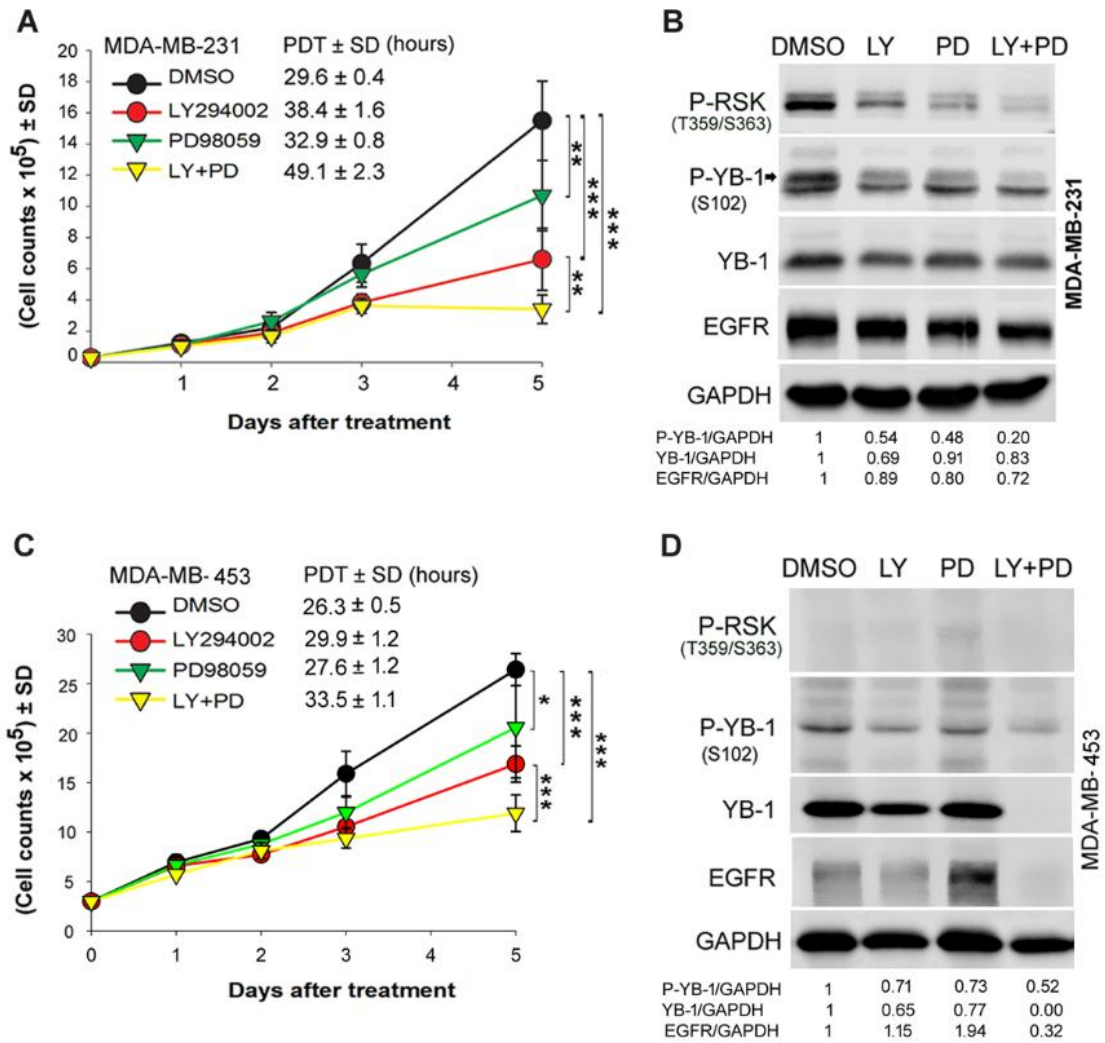


**Fig. 3.20 Dual targeting of PI3K and MEK is an efficient approach to block proliferation of *KRAS*(G13D)-mutated BCC in a YB-1-dependent manner.** Proliferation assay was performed in MDA-MB-231 (A) and MDA-MB-453 (C) cell lines. Cells were plated in 6-cm culture plates ( $30 \times 10^3$ ) as described in Methods section. 24 hours after plating, cells were treated with the PI3K inhibitor LY (10  $\mu$ M), MEK inhibitor PD (20  $\mu$ M) and combination of both inhibitors. The concentration of vehicle (DMSO) was similar under all conditions, including the control (0.2%). (A & C) The cells were counted on the indicated days after treatment and the graph was plotted. Asterisks indicates significant differences in PDT between the indicated treatment conditions (\* $p < 0.05$ , \*\* $p < 0.01$ , and \*\*\* $p < 0.001$ , Student's t-test;  $n = 6$  data, 2 experiments). (B & D) Protein samples were isolated on day 5 after treatment and the levels of indicated proteins were detected by Western blotting. Densitometry values represent the P-YB-1/GAPDH, YB-1/GAPDH and EGFR/GAPDH ratios normalized to 1 in the DMSO-treated control. GAPDH was detected as the loading control. PDT: population doubling time

Similarly, in proliferation assay of MDA-MB-453 cells, LY treatment showed much stronger antiproliferative effect than PD. The combination effect of LY and PD was significantly stronger than the single treatment. PDT (Fig. 3.20C) showed a significant increase in the combination treatment when compared to single treatments. The Western blotting was

performed with the cells counted on day 5. Interestingly a detectible amount of P-RSK was not seen in these cells (similar to Fig. 3.1 in the previous section). The LY mediated inhibition of P-YB-1 was stronger than the effect of PD and dual targeting was much stronger than single treatment. LY mediated suppression of YB-1 expression was much pronounced, specifically in the combination treatment, where no detectible amount of YB-1 was seen. Inhibition of YB-1 expression was also seen to be correlated with the expression of EGFR, which is obvious by the densitometry values shown in Fig. 3.21D.

### 3.2.2 Reactivation of PI3K or MEK/ERK pathways after long-term treatment with LY and PD

It is known that long-term (24 h) inhibition of PI3K leads to reactivation of Akt in KRAS-mutated lung cancer cells through MAPK/ERK pathway (Toulany et al., 2014, Toulany et al., 2016). Here, it could be shown that continues inhibition of PI3K or MEK up to 5 days leads to Akt reactivation in KRAS-mutated BCC in association with enhanced phosphorylation of ERK1/2. PI3K inhibition also stimulated ERK1/2 phosphorylation (Fig. 3.21). This pointed again towards the presence of a dynamic crosstalk between these two pathways, which regulates the cell proliferation and growth of KRAS mutated BCC.

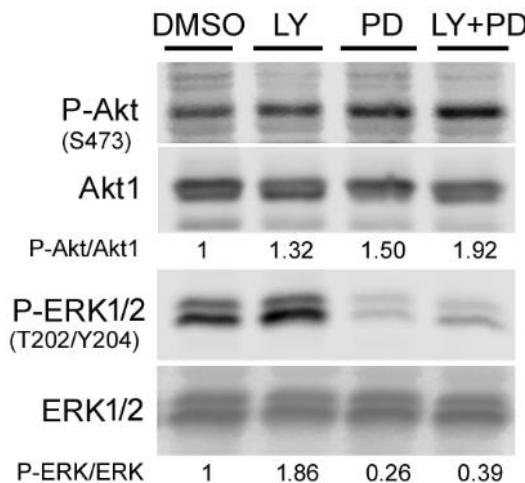


**Fig. 3.21 Reactivation of PI3K or MEK/ERK pathway following long-term inhibition of the pathways.** MDA-MB-231 cells were plated in 6-cm culture plates ( $30 \times 10^3$  cells) as described in Materials and Methods. 24 hours after plating cells were treated with the PI3K inhibitor LY (10  $\mu$ M), MEK inhibitor PD (20  $\mu$ M) or the combination of both inhibitors. The concentration of vehicle (DMSO) was similar under all conditions, including the control (0.2%). Protein samples were isolated on day 5 after treatment, and the levels of indicated proteins were detected by Western blotting. Densitometry values represent the P-Akt/Akt and P-ERK/ERK ratios normalized to 1 in the DMSO-treated control.

### 3.2.3 Dual targeting of PI3K and MEK is also an efficient approach to block proliferation of BRAF(V600E) mutated melanoma cells in a YB-1-dependent manner

RAF is the downstream component of KRAS signaling and is frequently mutated in melanoma. Next, it was examined whether mutation in BRAF in melanoma cells similar to KRAS mutation in BCC also renders the hyper activation of RAS-RAF-MEK-ERK pathway. BRAF(V600E) mutated NM2C5 cells were plated for proliferation assay and treated on second day with the LY and PD alone and in combination (as in previous experiments). Cells were counted on day 1, 2, 3 and 5 after treatment. Similar to KRAS mutated BCC line, dual targeting of both MEK and PI3K pathway inhibited the cell proliferation significantly stronger than single targeting of either of the pathway (Fig. 3.22 A). Interestingly, the long-term effect of single targeting was much different than the BCC lines shown above. PD inhibited cell proliferation much strongly than LY. The Western blotting was performed from the protein obtained from treated cells on day 5. The pattern of inhibition of P-YB-1 by single or dual treatment was in line with the effect of the treatments on proliferation (Fig. 3.22 B). As shown by Western blotting, P-RSK was strongly inhibited by PD and LY+PD, which results in strong or complete inhibition of P-YB-1 and suppression of cell proliferation in these groups. Inhibition of P-RSK was also seen in the LY condition when compared to the DMSO treated control condition. Similar to the results obtained from BCC lines, long-term treatment with inhibitors resulted in inhibition of total protein expression of YB-1 and EGFR.

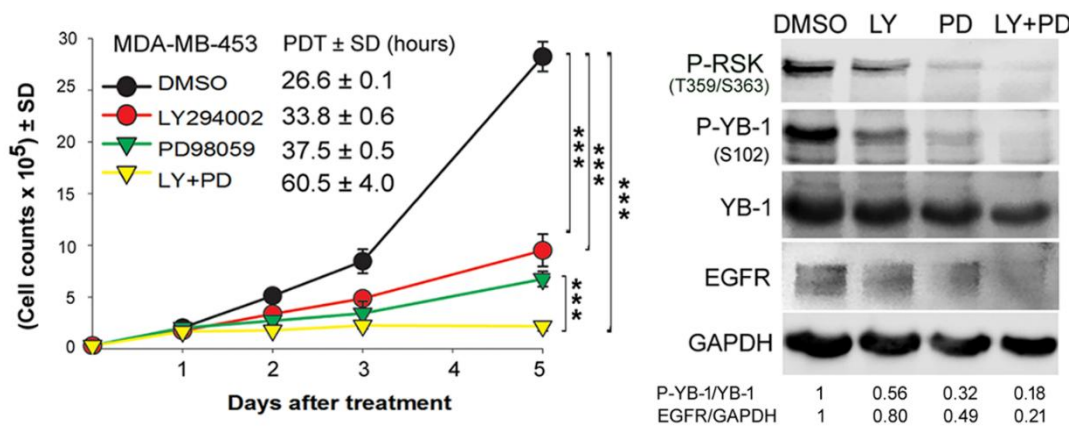


**Fig. 3.22 Dual targeting of PI3K and MEK is an efficient approach to block proliferation of BRAF(V600E)-mutated melanoma cells.** NM2C5 cells were plated in 6-cm culture plates ( $30 \times 10^3$  cells) as described in Materials and Methods. Twenty-four hours after plating, cells were treated with the PI3K inhibitor LY (10  $\mu$ M), MEK inhibitor PD (20  $\mu$ M) or the combination of both inhibitors. The concentration of vehicle (DMSO) was similar in all conditions, including the control (0.2%). Protein samples were isolated on day 5 after treatment and the levels of indicated proteins were detected by Western blotting. Densitometry values represent the P-YB-1/YB-1 and EGFR/GAPDH normalized to 1 in the DMSO-treated control. GAPDH was detected as



loading control. Asterisks indicate significant differences in PDT between the indicated treatment conditions (\*\* $p < 0.001$ , Student's t-test;  $n = 6$  data from 2 experiments). PDT: population doubling time.

### 3.2.4 YB-1 knockdown by siRNA strongly inhibits the cell proliferation in *KRAS* mutated BCC

The data so far indicate that PI3K and MEK pathways are regulating the cell proliferation through phosphorylation of YB-1. To confirm this observation, YB-1 was knocked down by siRNA in MDA-MB-231. Effect of LY, PD and the combination of LY and PD on cell proliferation was tested in control-siRNA and YB-1 siRNA transfected cells (Fig.3.23 C). In control siRNA group, dual treatment of LY and PD inhibited the proliferation much strongly than single treatment while in YB-1 knockdown cells there was no further antiproliferative effect of LY, PD or the combination of the inhibitors (Fig.3.23 B). This data indicates that the antiproliferative effect of inhibition of PI3K and MAPK pathway is YB-1 dependent.

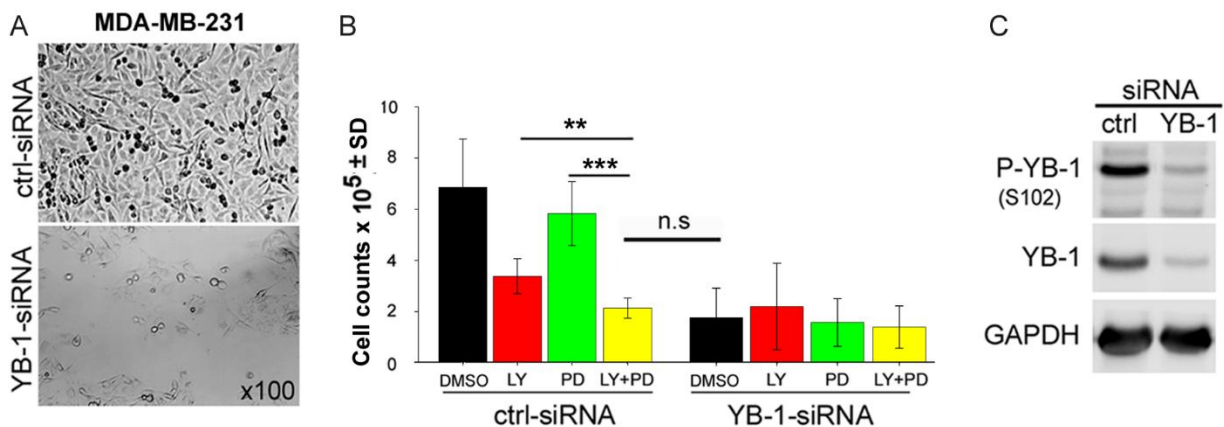


**Fig. 3.23 YB-1 knockdown by siRNA strongly inhibits the cell proliferation in *KRAS* mutated BCC.** MDA-MB-231(G13D) cells were transfected with 50 nM control (ctrl) siRNA or YB-1-siRNA, and 24 h after transfection, the cells were treated with the indicated inhibitors. (A) Representative image from control-siRNA (ctrl-siRNA) and YB-1 siRNA transfected cells. (B) Thereafter, the cells were counted on day 6 and the results were graphed. Asterisks indicate significant differences between the indicated treatment conditions (\*\* $p < 0.01$ , and \*\*\* $p < 0.001$ , Student's t-test;  $n = 6$  data points, 2 experiments). (C) Protein was isolated on day 6 from Ctrl-siRNA and YB-1 siRNA transfected/DMSO treated conditions and Western blotting was performed. GAPDH was used as loading control.

### 3.2.5 YB-1 knockout in MDA-MB-231 and NM2C5 cells by CRISPR/Cas9

To further confirm the role of YB-1 in cell proliferation of *KRAS*(G13D)-mutated BCC and RAF-mutated melanoma cells, YB-1 knockout (KO) cells were prepared by CRISPR/Cas9

technology as described in Methods section. The expression of YB-1 was checked immediately after viral transduction in the total cells. Cell were then kept in selection marker and clonal selection was performed to isolate the clones showing the knockout of YB-1. As shown in the Fig. 3.24, YB-1 was knocked out in clones 5, 6, 10 and 12. YB-1 KO clone 5 and 10 were used for further experiments. In NM2C5 cells clone 27, 29 and 33 showed knockout of YB-1 out of 13 clones tested for YB-1 expression. Out of these clones, YB-1 KO clone 27 and 33 were used for further experiments.

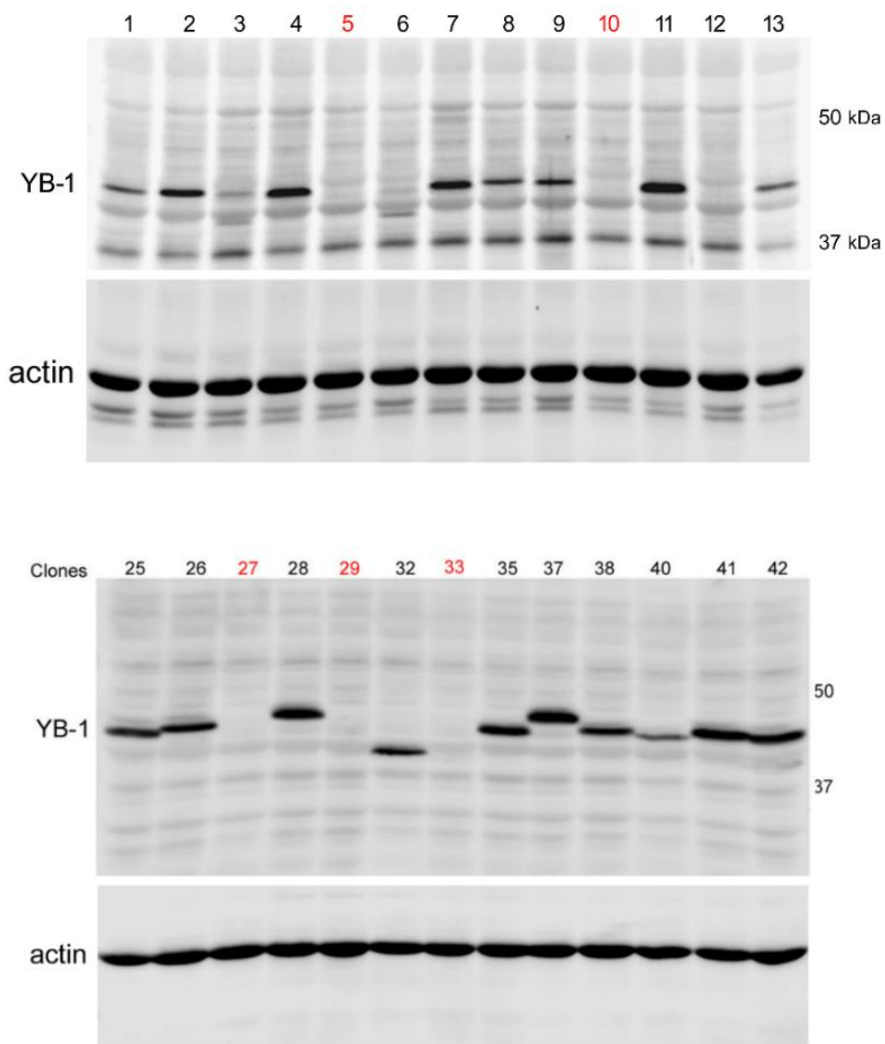


**Fig. 3.24 CRISP/Cas9 mediated YB-1 knockout in MDA-MB-231 cells.** YB-knockout was performed by using CRISP/Cas9 as described in method section. Knockout efficiency was tested by Western blotting in indicated clones. Actin was used as the loading control.

### 3.2.6 Dual targeting of MEK/ERK and PI3K pathways strongly inhibits proliferation through YB-1

YB-1 knockout clones were used to confirm that YB-1 is essential for cell proliferation and MAPK and PI3K signaling pathways converge on YB-1 to regulate proliferation of *KRAS* mutated BCC. MDA-MB-231 parental and two YB-1 knockout clones 5 and 10 were treated with LY and PD alone and in combination and cells were counted on day 5 of treatment. The data in the Fig.3.25 A shows that in YB-1 knockout clones there is no further antiproliferative effect of the inhibitors treatment either alone or in combination. The table Fig. 3.25 B shows the p-value of the groups in vertical column with the indicated treatment on the horizontal row. The p-values of combine treatment of LY and PD in the parental MDA-MB-231 cells showed significantly strong inhibition of cell proliferation ( $p < 0.05$ ). Single treatment of the respective inhibitors was also significant ( $p < 0.05$ ). Whereas in YB-1 KO clone 5 and 10 there was no significant inhibition of cell proliferation by any of the inhibitors alone or in combination. This data again indicates that MEK/ERK and PI3K pathways regulates cell proliferation through YB-1.

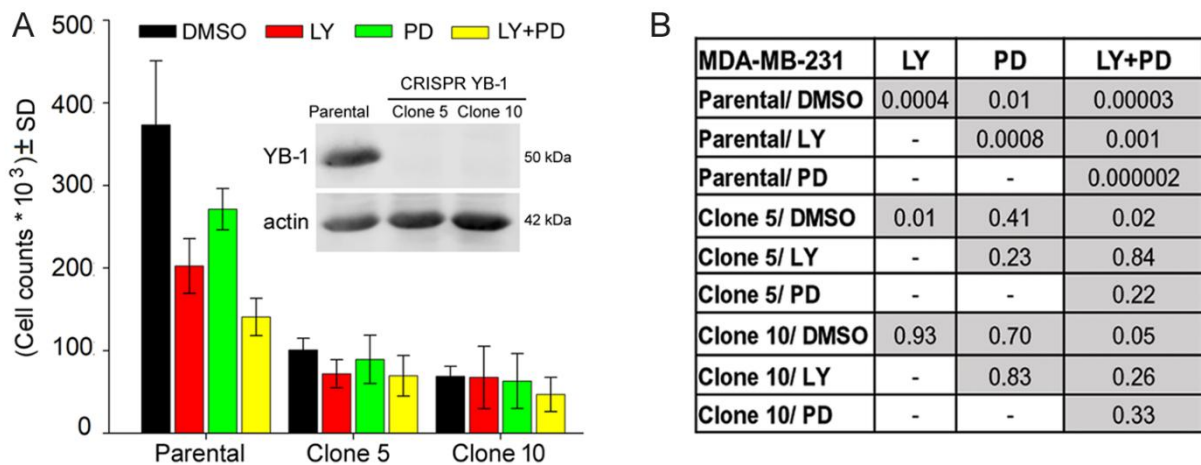


**Fig. 3.25 Dual targeting of MEK/ERK and PI3K pathway strongly inhibits proliferation through YB-1.** (A) parental MDA-MB-231 and YB-1 knockout clone 5 and clone 10 were plated ( $3 \times 10^4$  cells) in 6-cm culture dishes and treated with PI3K inhibitor LY (10  $\mu$ M), MEK inhibitor PD (20  $\mu$ M) or a combination of both inhibitors after 24 hours. The concentration of vehicle (DMSO) was similar under all conditions, including the control (0.2%). Cells were counted 5 days after treatment, and the results were graphed. The histogram shows the mean number of cells  $\pm$  SD (6 data points, 2 independent experiments). Western blot data show knockout of YB-1 in clone 5 and 10. (B) Statistical analyses table shows the degree of significance of the antiproliferative effect of the indicated inhibitors in parental and YB-1 knockout clones.

### 3.2.7 Dual targeting of MEK/ERK and PI3K pathways does not regulates proliferation entirely through YB-1 in BRAF(V600E) melanoma cells

In contrast to *KRAS*(G13D)-mutated BCC, BRAF(V600E) mutated melanoma NM2C5 cells showed a further inhibition of proliferation after treatment with LY and PD alone or the combination of both inhibitors in YB-1 knockout clones. As shown in Fig. 3.26 A there is strong reduction of cell proliferation in YB-1 KO clone 27 and 33 DMSO condition when compared to the Parental DMSO condition. Treatment with LY and PD could further inhibit the proliferation both in parental and YB-1 KO clone 27 and clone 33. The combination treatment also showed further antiproliferative effect in both the parental and YB-1 KO clones. This is also reflected in Fig. 3.26 B by comparing p-values between different groups.

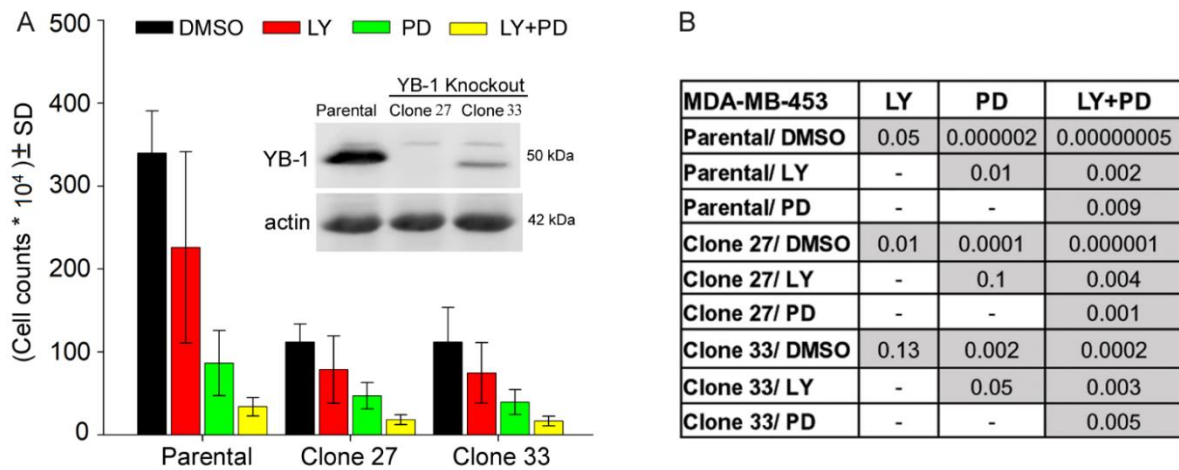


**Fig. 3.26 Dual targeting of MEK/ERK and PI3K pathways does not regulates proliferation entirely through YB-1 in BRAF(V600E) melanoma cells.** Parental NM2C5 and YB-1 knockout clone 27 and 33 were plated ( $3 \times 10^4$  cells) in 6-cm culture dishes and treated with PI3K inhibitor LY (10  $\mu$ M), MEK inhibitor PD (20  $\mu$ M) or the combination of both inhibitors after 24 hours. The concentration of vehicle (DMSO) was similar under all conditions, including the control (0.2%). (A) Cells were counted 5 days after treatment and the results were graphed. The histogram shows the mean number of cells  $\pm$  SD (6 data points, 2 independent experiments). Western blot data shows knockout of YB-1 in clone 27 and 33. (B) Statistical analyses show the degree of significance of the antiproliferative effect of the indicated inhibitors in NM2C5 parental and YB-1 knockout cells (Student's t-test).

### 3.2.8 Dual targeting of MEK/ERK and PI3K pathways has no effect on cell proliferation in *KRAS* wild-type BCC

The data so far showed that PI3K and MAPK pathways regulates cell proliferation through YB-1 in *KRAS* (G13V) mutated breast cancer cells. Next, the effect of dual targeting of MEK/ERK and PI3K pathways on cell proliferation in *KRAS* wild-type breast cancer cell was

tested. For this purpose, SKBR3 cells were treated with the single and the combination of LY and PD and proliferation assay was performed. Cells were counted on day 1, 2, 3 and 5 after treatment. Data obtained showed that in *KRAS* wild-type SKBR3 cells, both the single treatment or dual treatment strongly inhibited proliferation of cells and there was no beneficial effect of dual targeting. Due to the very strong antiproliferative effect of the inhibitors, protein isolation was not possible to detect P-YB-1 status in these cells.

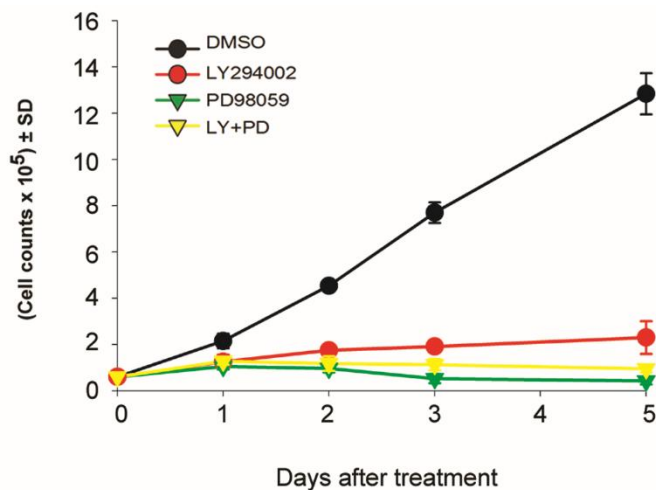


**Fig. 3.27 Dual targeting of PI3K and MEK has no effect on cell proliferation in *KRAS* wild-type BCC.** Proliferation assay was performed after treating the SKBr3 cells with the PI3K inhibitor LY294002 (10 $\mu$ M), MEK inhibitor PD98059 (20 $\mu$ M) and the combination of the both inhibitors as described in Methods section. Concentration of vehicle (DMSO) in all conditions including control was similar (0.2%). Each data-point represents mean number of cells from 3 parallel culture in one experiment.

Furthermore, effect of dual targeting of MEK and PI3K on proliferation of HBL-100 cells was tested. HBL-100 cells are de novo transformed breast epithelial cells derived from the milk of the normal lactating woman. Because of their non-cancerous origin, these cells can be compared with the normal cells. Surprisingly, both the single or dual treatment showed no antiproliferative effect on HBL-100 cells. Western blot data from the protein isolated on day 5 also showed no inhibition of phosphorylation of YB-1 by LY and PD alone or in combination (densitometry values in Fig.3.28 B).

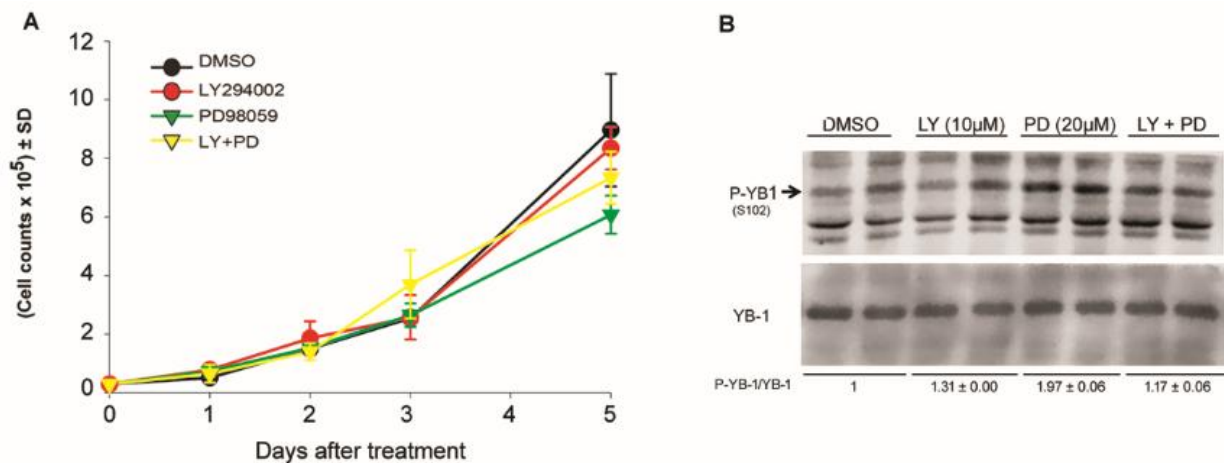


**Fig. 3.28 Dual targeting of PI3K and MEK has no effect on cell proliferation in *KRAS* wild-type cells.** Proliferation assay was performed after treating the HBL-100 cells with the PI3K inhibitor LY294002 (10μM), MEK inhibitor PD98059 (20μM) and the combination of the both the inhibitors as described in Methods section. Concentration of vehicle (DMSO) in all conditions including control was similar (0.2%). (A) Cells were counted at the indicated time points. Each data-point represents mean number of cells from 3 parallel culture in one experiment. (B) Protein samples isolated on day 5 were subjected to SDS-PAGE and level of phospho-YB-1 and YB-1 was analysed by Western blotting. Densitometry values represent the P-YB-1/YB-1 normalized to 1 in the DMSO-treated control.

### 3.2.9 P-YB-1 strongly regulates cell proliferation of *KRAS*(G13D)-mutated BCCs

Rescue experiment was performed to show whether co-targeting of MEK and PI3K has cytostatic or cytotoxic effect. For this purpose, MDA-MB-231 cells were treated with the combination of LY and PD for 7 days. Thereafter, medium was changed to fresh medium with the inhibitors in group 1 and without the inhibitors in group 2 and cells were allowed to grow till day 12. The cells were counted on day 12. The data obtained showed (Fig. 3.39; histogram) that the group 1 with the inhibitors treatment for 12 days had strong inhibition of cell proliferation but when the inhibitors were removed after 7 days the cell started growing again in group 2. This confirms the cytostatic rather than cytotoxic effect of YB-1 in *KRAS*(G13D)-mutated BCCs.

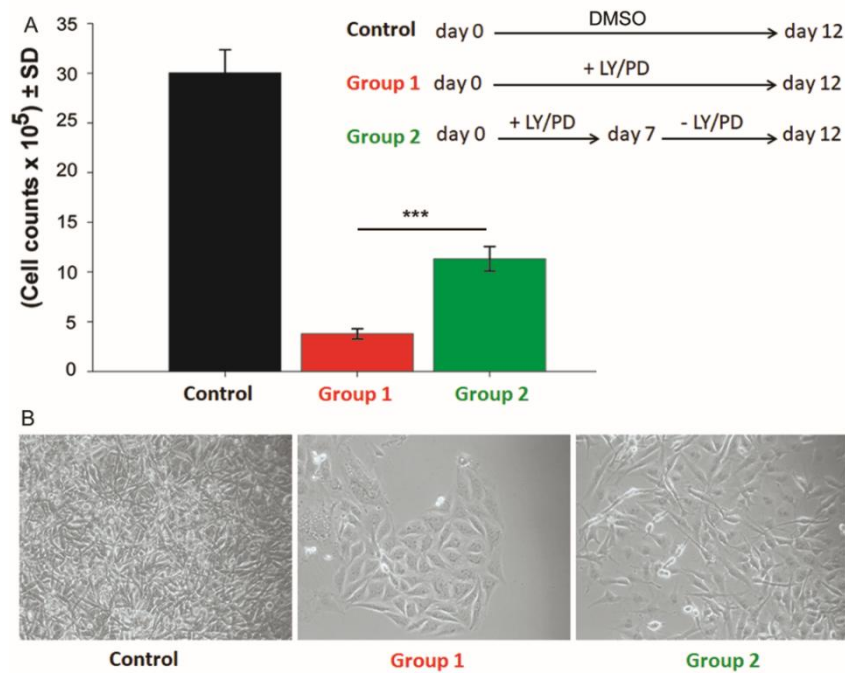


**Fig. 3.29 P-YB-1 regulates cell proliferation of *KRAS*(G13D)-mutated BCC.** MDA-MB-231 cells were plated in 6-cm culture plates ( $30 \times 10^3$  cells) as described in Methods. Twenty-four hours after plating, cells were treated with the combination of PI3K inhibitor LY (10  $\mu$ M) and MEK inhibitor PD (20  $\mu$ M). Concentration of vehicle (DMSO) in all conditions including control was similar (0.2%). On day 7, medium was changed with fresh medium containing inhibitors in group 1 (LY+PD) and without the inhibitors in the group 2 until day 12. (A) The cells were counted on day 12 and the results were graphed. (B) Representative images of cells under different treatments with 200x magnification.

### 3.3 Role of YB-1 in DNA DSB repair and radioresistance:

Efficient DNA repair mediates radioresistance in cancer cells. YB-1 is reported to influence DNA repair process (Kim et al., 2013). Many studies have shown that YB-1 regulates repair of single strand DNA break by mismatch repair (Gaudreault et al., 2004) (Fomina et al., 2015) and base excision repair (Das et al., 2007), (Alemasova et al., 2016). It has been shown that YB-1 is involved in DNA DSB repair (Toulany et al., 2011). However, the mechanism of YB-1 mediated DSB repair has not been reported. It is also not known, which of the DSB repair pathways is(are) regulated by YB-1. DSB are repaired through two major repair pathways: NHEJ and HR. NHEJ is further divided into two subgroups; DNA-PKcs dependent classical-NHEJ (C-NHEJ) and PARP dependent alternate-NHEJ (A-NHEJ). HR specifically needs a sister chromatid as a template to repair the damaged sequence. Therefore, HR is carried out predominantly during the S and G<sub>2</sub> phases of the cell cycle. HR is highly accurate and error free repair pathway in contrast to NHEJ, which is prone to mutations. In this section of the

thesis, the data regarding the role of YB-1 in DNA DSB repair and radioresistance is presented in detail.

### 3.3.1 YB-1 stimulates repair of ionizing radiation induced DNA DSB

DNA DSB are immediately marked by phosphorylation of the histone subunit H2AX on serine 139 (Ser-139) at the damaged site, followed by localization of Ku70/80 or MRN complex. The phosphorylated histone subunit is known as  $\gamma$ H2AX. It becomes dephosphorylated again to H2AX on the repair of the damaged DSB. Therefore, the level of  $\gamma$ H2AX represents the amount of residual DNA damage after irradiation or other kind of genotoxic stress. Monitoring frequency of  $\gamma$ H2AX foci is used as a tool to calculate the residual DNA DSB at different time points after irradiation.

The parental MDA-MB-231 and CRISPR/Cas9 mediated YB-1 knockout clone 5 and 10 were exposed to single dose of 4 Gy during sub-confluent and confluent stages.  $\gamma$ H2AX immunostaining was performed 24 hours' post-treatment. YB-1 knockout clone 5 and clone 10 showed a significant increase in the residual  $\gamma$ H2AX foci when irradiated at confluent or sub-confluent stages in comparison with the parental cells. Interestingly in sub-confluent group both the YB-1 knockout clones showed relatively enhanced residual  $\gamma$ H2AX foci as compared to the confluent cells. This increase in the residual  $\gamma$ H2AX foci in sub-confluent cells indicates DSB repair in G2 and S phase through HR.

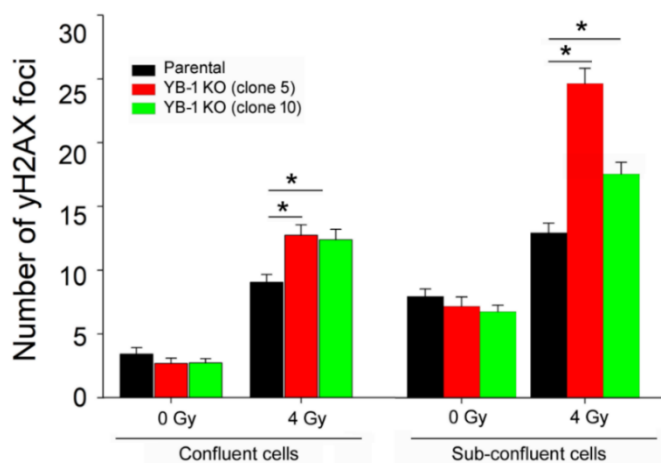


**Fig. 3.30 YB-1 stimulates repair of ionizing radiation induced DNA DSB.** Parental MDA-MB-231 cells and YB-1 knockout clone 5 and 10 were irradiated with 4 Gy during confluent and sub-confluent status. Twenty-four hours after radiation immunofluorescence staining was performed for  $\gamma$ H2AX as described in method section. Residual  $\gamma$ H2AX foci were counted in total of 200 nuclei from 2 experiments. Asterisk indicate significant differences between the indicated conditions (\*p<0.05; Student's t-test). KO: knockout.



### 3.3.2 YB-1 induces radioresistance in *KRAS(G13D)*-mutated BCC

The effective DNA repair is associated with radioresistance in cancer cells. Thus, on the bases of the role of YB-1 in DNA DSB repair, effect of YB-1 knockout on radiosensitivity was investigated. Colony formation assay was performed in MDA-MB-231 parental and YB-1 knockout clone 5 and 10, as described in the method section. The data presented in Fig 3.31 indicates that YB-1 knockout leads to strong radiosensitization in both knockout clones.

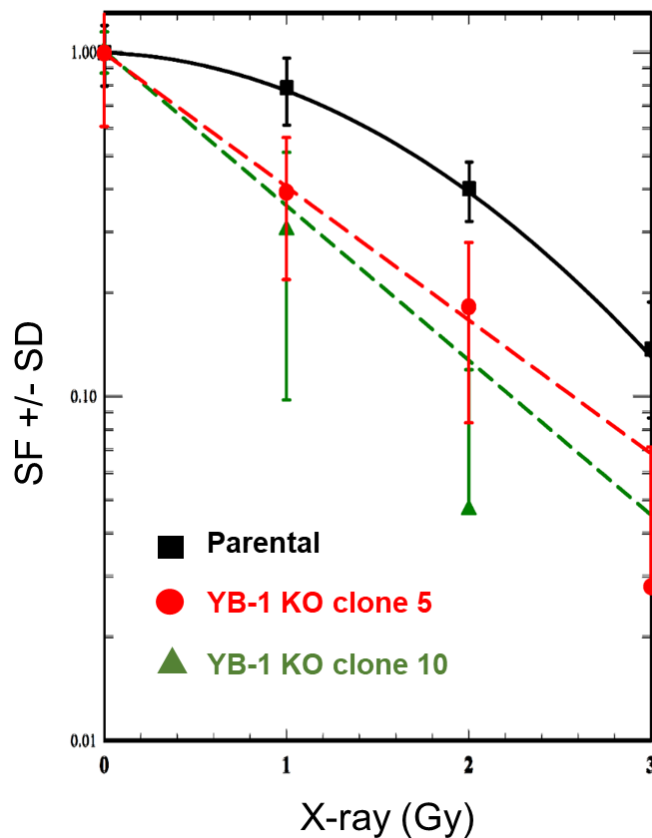


**Fig. 3.31 YB-1 knockout induces radiosensitization in *KRAS(G13D)*-mutated BCC.** Colony formation assay was performed as described in Methods section in MDA-MB-231 parental and YB-1 knockout clone 5 and 10. Pre-plated cells were irradiated with single dose of 0, 1, 2, and 3 Gy. Twelve days later colonies were stained and the colonies with more than 50 cells were counted. The clonogenic fraction of irradiated cells was normalized to the plating efficiency of non-irradiated controls. The experiments were repeated 3 times with n=6 in each experiment, total n= 18), Mean D37 values of 3 experiments: Parental-2.25±0.2, KO5-1.26±0.2 and KO10-1.26±0.3. KO: knockout.

### 3.3.3 YB-1 stimulates DNA DSB repair through HR and A-NHEJ repair pathways

YB-1 strongly regulates DNA DSB repair as demonstrated in the previous experiments. DNA DSB repair assay was performed in osteosarcoma cell line with stable expression of DSB repair constructs for specific DSB repair pathway (Gunn and Stark, 2012) to uncover the underlying DSB repair pathways regulated by YB-1. siRNA mediated knockdown of YB-1 was performed. Forty-eight hours after transfecting cells with YB-1 siRNA, cells were transfected with non-inducible plasmid expressing I-sceI endonucleases to produce DSB in DNA. Flowcytometry was carried out 24 hours after endonuclease expression. Cells were synchronized in S/G2 phase in the experiments tested for HR. The data showed a significant decrease in the HR mediated DNA repair in YB-1 knockdown condition (Fig. 3.32 A). However, no effect on the C-NHEJ repair was observed after YB-1 knockdown (Fig.3.32 B). Interestingly YB-1 knockdown showed a strong inhibition of A-NHEJ repair pathway (Fig.3.32 C). This data indicate that YB-1 might regulate DSB repair specifically through HR and A-NHEJ pathways.

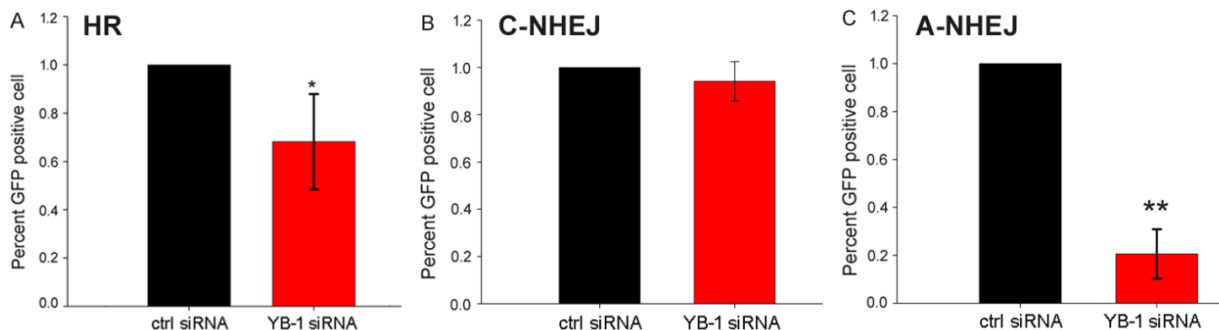


**Fig. 3.32 YB-1 regulates DNA DSB repair through HR and A-NHEJ repair pathways.** U2OS osteosarcoma cells with specific repair constructs for (A) HR repair pathway, (B) C-NHEJ pathway pathway and (C) A-NHEJ pathway were transfected with control siRNA (ctrl siRNA) or YB-1-siRNA. Forty-eight hours after transfection, cells were transfected with a non-inducible I-sceI endonuclease plasmid. Flowcytometry was performed after 24 hours. Graphs were prepared from percentage of GFP positive cells. (HR: n=5, 3 experiments; C-NHEJ: n=6, 2 experiments; A-NHEJ: n=11, 4 experiments). Asterisk indicate the significant differences between ctrl-siRNA and YB-1-siRNA transfected cells (\*p<0.05, \*\*p<0.01 Student's t-test).

### 3.3.4 YB-1 regulates DNA DSB repair through HR

Based on the data obtained from osteosarcoma cells expressing different repair constructs, it could be concluded that YB-1 stimulates repair of DNA DSB through HR and A-NHEJ pathways.  $\gamma$ H2AX assay was performed in the presence of B02 (5  $\mu$ M, 2 hours) as Rad51 inhibitor to confirm the involvement of YB-1 in homologous recombination repair pathway.. Similar to the data shown in Fig. 3.30, YB-1 knockout clones showed significantly increased residual DSBs as compared to the parental cells (Fig. 3.33). However, inhibition of HR by B02 in parental cells significantly enhanced the residual DNA damage after irradiation, which was similar to the levels of residual DNA damage in YB-1 knockout cells. As shown in the Fig. 3.34, no significant difference was observed between parental cells after B02 treatment and YB-1 knockout cells with or without the inhibitor treatment. YB-1 knockout cells showed no effect of B02 treatment as no further increase in residual  $\gamma$ H2AX foci was observed. This could indicate that the DSB repair through HR is regulated by YB-1.

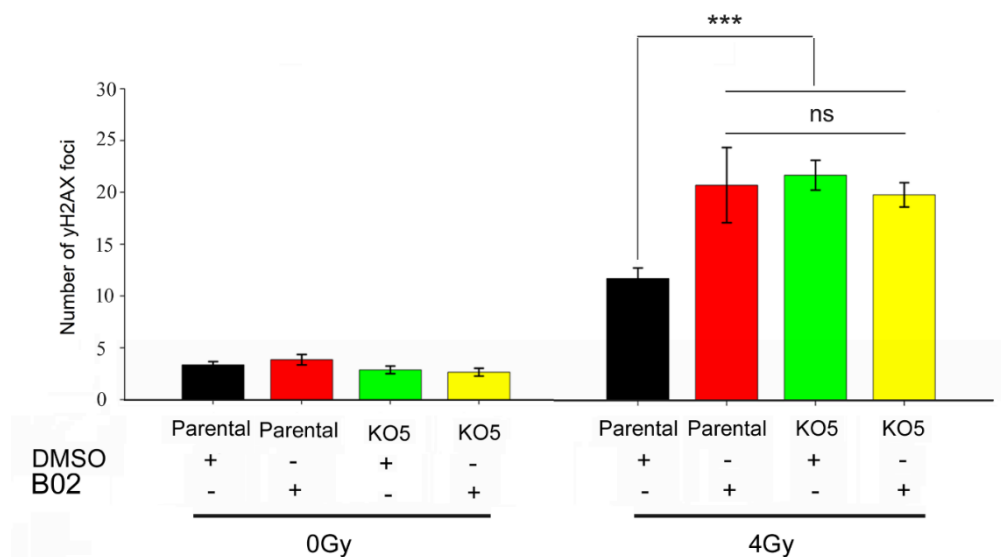


**Fig. 3.33 YB-1 regulates DNA DSB repair through HR.** MDA-MB-231 parental and YB-1 knockout clone 5 was treated with DMSO or B02 for 2 hours. The cells were then irradiated with 4 Gy and 24 hours after radiation immunofluorescence staining was performed for  $\gamma$ H2AX, as described in the Method section. Residual  $\gamma$ H2AX foci were counted in total of 150 nuclei from 2 experiments. Asterisk indicate the significant differences between the indicated conditions (\*\*\*)  $p < 0.001$ ; Student's t-test). ns denotes no significant difference between Parental+B02 as compared with KO5 with or without B02. KO: knockout.

It was further investigated whether the differential effect of B02 on DSB repair in MDA-MB-231 parental and YB-1 knockout cells differentially affects post-irradiation cell survival. To this end, clonogenic assay was performed in the parental and YB-1 knockout clones 5 and 10. The data presented in Fig. 3.34 showed that B02 induces radiosensitization in parental cells to the same levels as in YB-1 knockout clones 5 and 10.

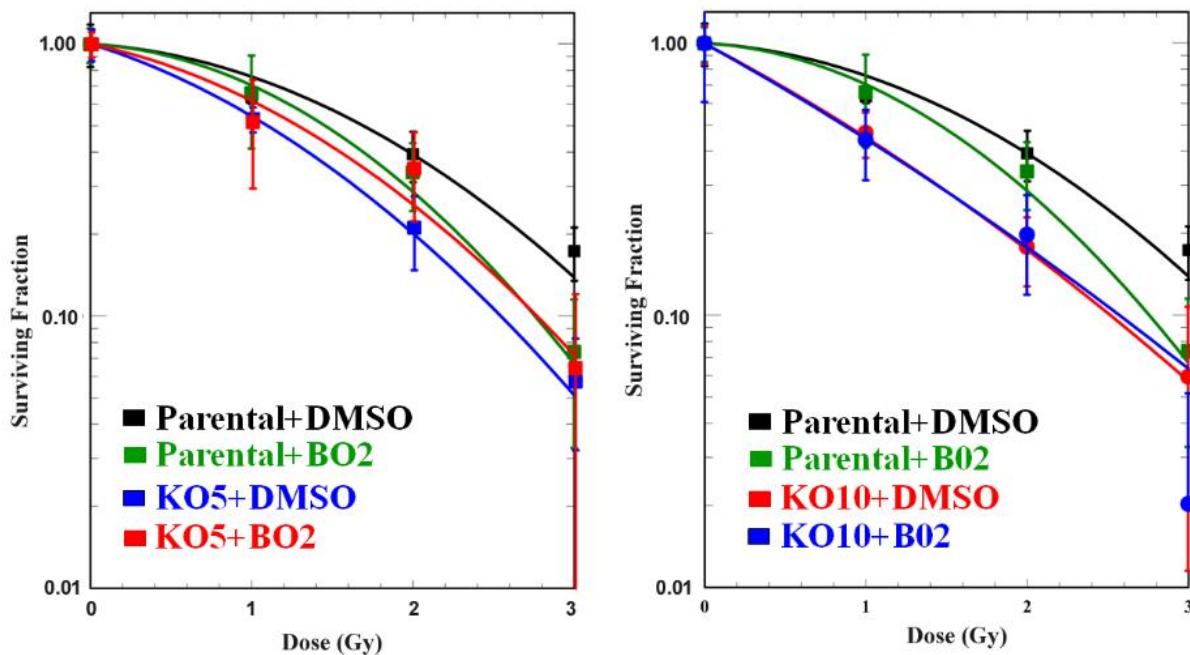


**Fig. 3.34 YB-1 regulates repair of DNA DSB through HR.** Colony formation assay was performed as described in Methods section in MDA-MB-231 parental and YB-1 knockout clone 5 and 10. Twenty-four hours after plating, cells were treated with DMSO or B02 for 2 h and irradiated with single dose of 0, 1, 2, and 3 Gy. After 12 days, colonies were stained and the colonies with more than 50 cells were counted. The surviving fraction (SF) of irradiated cells was normalized to the plating efficiency of non-irradiated controls. The experiments were repeated 2 times with n=6 in each experiment, total n= 12. The above figure is representation of one of the two experiments. Mean D37 values from two experiments are as follow: Parental- $2.2 \pm 0.3$ , Parental+B02= $1.8 \pm 0.1$ , KO5= $1.5 \pm 0.1$ , KO5+B02= $1.6 \pm 0.0$ , KO10= $1.3 \pm 0.2$ , KO10+B02= $1.3 \pm 0.3$ . KO: knockout.

### 3.3.5 YB-1 knockout cells shows enhanced dependency on C-NHEJ repair pathway

To further confirm the lack of role of YB-1 in regulating C-NHEJ repair pathway,  $\gamma$ H2AX assay was performed in the presence of Nu7441, which inhibits DNA-PKcs kinase activity, which is crucial for C-NHEJ repair pathway. To this end, cells were treated with Nu7441 (5 $\mu$ M, 2 hours) followed by 4 Gy irradiation.  $\gamma$ H2AX foci assay was performed 24 hours after radiation. The data presented in Fig.3.35 shows that the presence of Nu7441 in 4 Gy treatment group, drastically increased the residual  $\gamma$ H2AX foci in the parental as well as YB-1 knockout cells. Interestingly the YB-1 knockout clones showed significant increase in frequency of residual DSB as compared to the parental cells.

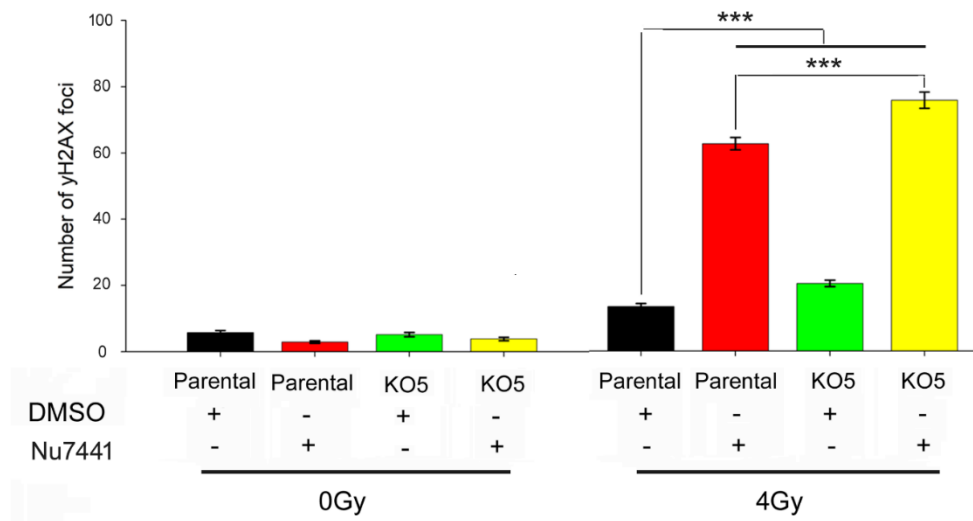


**Fig. 3.35: YB-1 knockout cells shows enhanced dependency on C-NHEJ repair pathway** MDA-MB-231 parental and YB-1 knockout clone 5 were treated with DMSO or Nu7441 (5  $\mu$ M) for 2 hours and irradiated with 4 Gy. Twenty-four hours after radiation,  $\gamma$ H2AX assay was performed. Residual  $\gamma$ H2AX foci were counted in total of 150 nuclei from 2 independent experiments. Asterisks indicate significant differences between the indicated radiation conditions (\*\* $p$ <0.001, Student's t-test). KO: knockout.

### 3.3.6 YB-1 regulates DSB repair through A-NHEJ repair pathway

Data from the repair assays showed that YB-1 also regulate DNA DSB repair by A-NHEJ repair pathway. PARP activity is essential for A-NHEJ repair pathway. Thus, role of YB-1 in DSB repair through A-NHEJ was investigated in the presence and absence of PARP inhibitor

talazoparib. The parental and YB-1 knockout clones 5 were treated with DMSO or talazoparib (25 nM, 2 hours).

Similar to the data shown in Fig. 3.30, the data presented in Fig. 3.36 shows that residual DSB were increased in YB-1 knockout cells in comparison to the parental cells after 4 Gy IR. In parental cells, talazoparib treatment drastically enhanced the amount of residual DNA damage which was similar to its level in YB-1 knockout cells. Interestingly, there was no further increase in the residual DNA damage in YB-1 knockout cells after talazoparib treatment

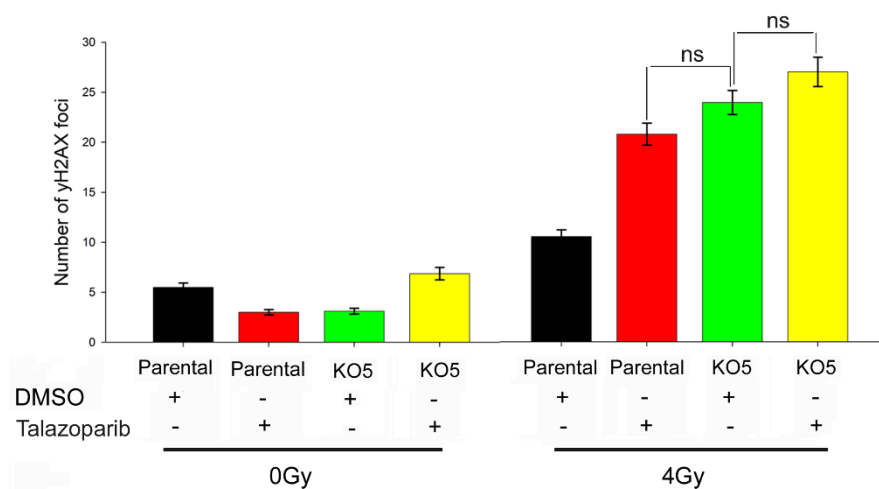


**Fig. 3.36 YB-1 regulates DSB repair through A-NHEJ repair pathway.** MDA-MB-231 parental and YB-1 knockout clone 5 were treated with DMSO or talazoparib for 2 hours and irradiated with 4 Gy. Twenty-four hours after irradiation, immunofluorescence staining was performed for  $\gamma$ H2AX. Residual  $\gamma$ H2AX foci were counted in total of 150 nuclei from two experiments. ‘ns’ denotes no significant difference between the indicated conditions. KO: knockout

### 3.3.7 Phosphorylation of YB-1 at Ser-102 is essential for regulating DSB repair and radioresistance

To confirm the role of YB-1 in DNA DSB repair, wild-type YB-1 was overexpressed in YB-1 knockout clone 5 and 10. Twelve clones were evaluated for the expression of exogenous YB-1 in YB-1 knockout clone 5. The Western blot in the Fig. 3.37 shows the overexpression of wild-type YB-1 in clone 1, 3, 4, 7 and 10. Similarly, out of nine clones evaluated in YB-1 knockout clone 10 for YB-1 overexpression; clone 1, 4 and 8 showed expression of exogenous wild-type YB-1

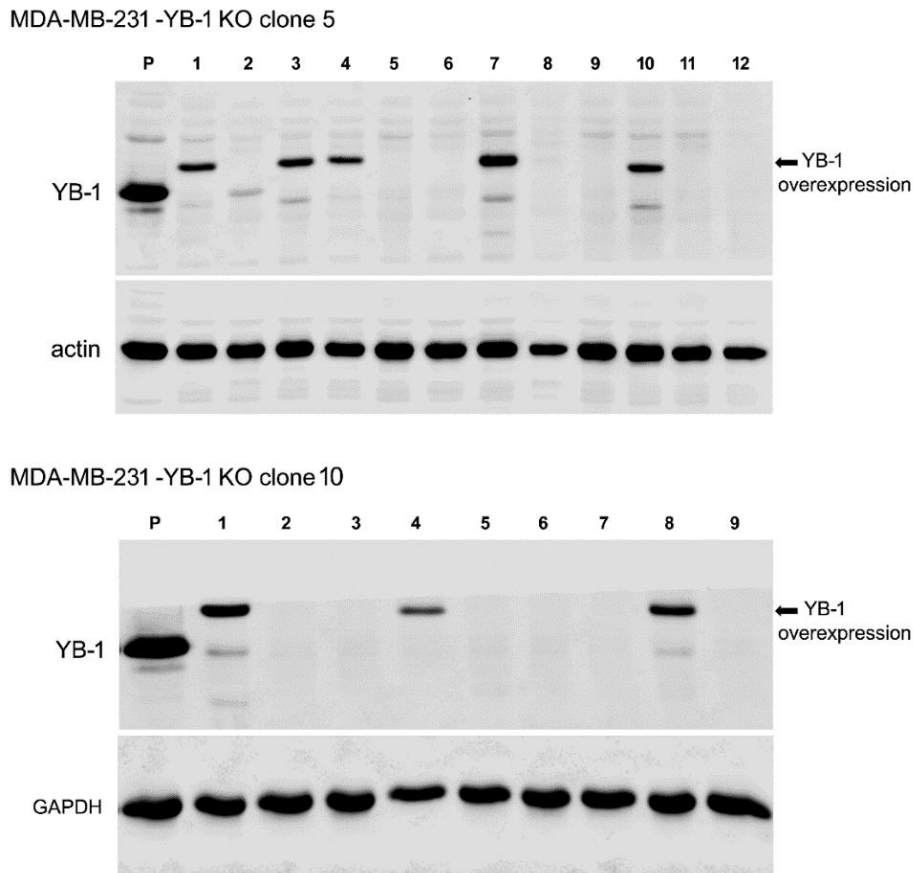


**Fig. 3.37 Overexpression of YB-1 in YB-1 knockout clones 5 and 10 in MDA-MB-231 cells.** YB-1 overexpression was performed by using viral transduction with the help Dr Corinna Kosnofel, Department of Dermatology, University of Tuebingen as described in Method section. Exogenous YB-1 expression was evaluated by Western blotting in indicated clones. Actin and GAPDH were used as loading controls in clone 5 and 10, respectively.

To check if the phosphorylation of YB-1 is crucial for DSB repair, phospho-site mutant YB-1 (S102A) is expressed in YB-1 knockout clone 5. Twelve clones were evaluated for the expression of exogenous YB-1(S102A) in YB-1 knockout clone 5. The western blot in the Fig. 3.38 showed the expression of phospho-site mutant YB-1(S102A) in clone 1, 3, and 5.

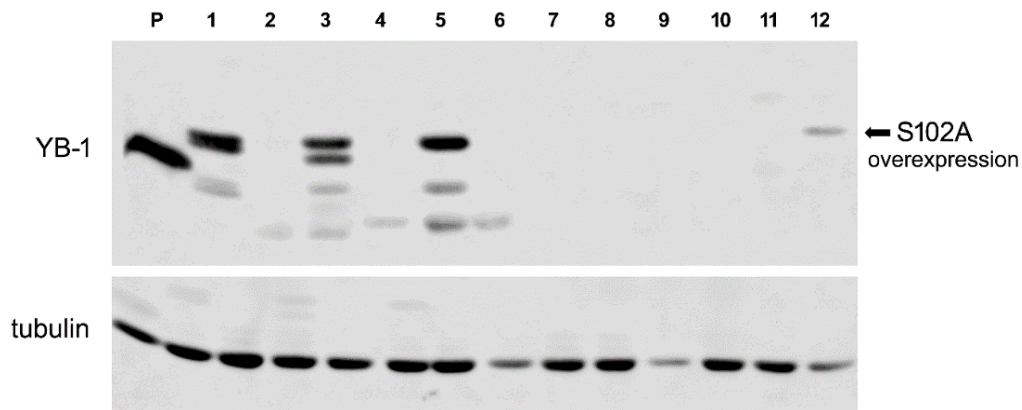


**Fig. 3.38: Expression of phospho-site mutant YB-1(S102A) in YB-1 knockout clone 5 of MDA-MB-231 cells.** YB-1(S102A) expression was performed by viral transduction with the help Dr Corinna Kosnofel, Department of Dermatology, University of Tuebingen as described in method section. Exogenous P-YB-1(S102A) expression was checked by Western blotting in indicated clones. Tubulin was used as the loading control.

By performing rescue experiments using YB-1 wild-type and YB-1(S102A) expressing clones, effect of YB-1 and its phosphorylation at Ser-102 on DSB repair as well as post-irradiation cell survival was investigated. As shown before (Fig. 3.30), YB-1 knockout clone 5 and 10 showed significant increase in the residual DNA damage as compared to parental cells (Fig.3.39). Expression of wild-type YB-1 in YB-1 knockout clone 5 enhanced DSB repair capacity to the levels similar to the parental cells. This effect was not observed after expression of YB-1(S102A) site mutant in YB-1 knockout clones.

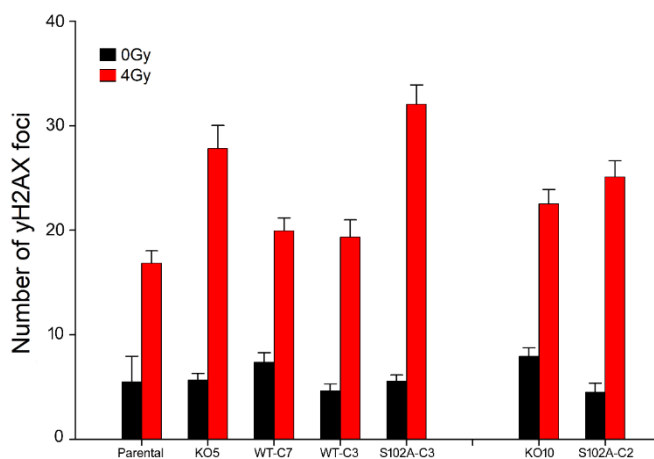
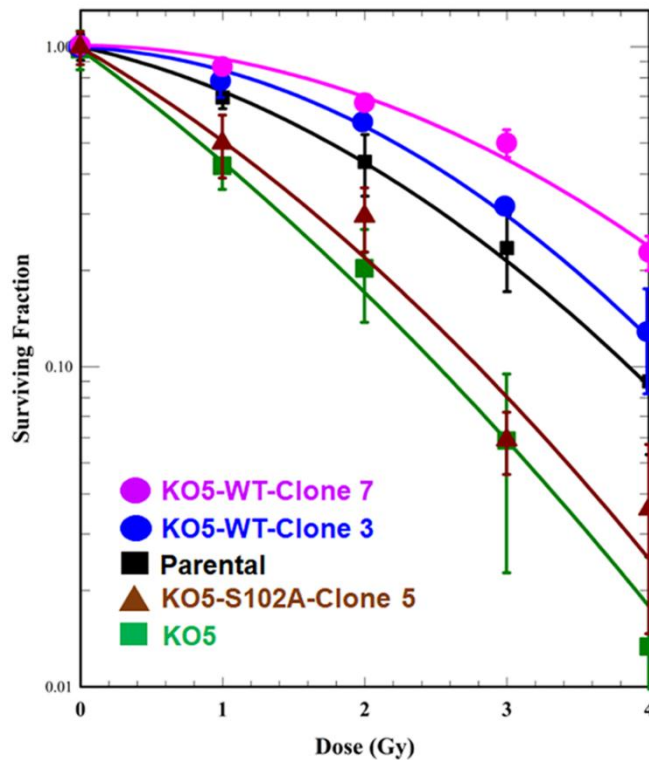


**Fig. 3.39: Phosphorylation of YB-1 at Ser-102 is essential for regulating DNA DSB repair.** MDA-MB-231 parental, YB-1 knockout clones 5 and 10, YB-1 knockout clone 5 overexpressing wild-type YB-1 (clones 3 and 7) and YB-1 knockout clone 5 and 10 overexpressing YB-1 (S102A) were irradiated with 4 Gy. Twenty-four hours after radiation,  $\gamma$ H2AX assay was performed. Residual  $\gamma$ H2AX foci were counted in total of 100 nuclei from one experiment. KO: knockout.









Next, the significance of phosphorylation of YB-1 in radioresistance was investigated in indicated YB-1 KO clones expressing YB-1 wild-type and YB-1(S102A) phospho-site mutant. As shown before, the YB-1 knockout clone 5 showed strong radiosensitization. Re-expression of wild-type YB-1 lead to radioresistance comparable to that of parental cells. This effect was not observed after expressing phospho-site mutant YB-1(S102A) (Fig. 3.40).













**Fig. 3.40 Phosphorylation of YB-1 at Ser-102 is essential for stimulating DSB repair and radioresistance** Colony forming assay was performed as described in Methods section in MDA-MB-231 parental, YB-1 knockout clone 5, YB-1 knockout clone 5 overexpressing wild-type YB-1 (clone 3 and 7) and YB-1 knockout clone 5 overexpressing YB-1 phospho-site mutant (S102A) (clone 5). Twenty-four hour after plating, cells were irradiated with single dose of 0, 1, 2, 3 and 4 Gy. Twelve days' later colonies were stained with cresyl-violet stain and the colonies with more than 50 cells were counted. The experiments were repeated 2 times with different overexpression clones  $n=6$  each time, total  $n=12$ . The above figure is the representation of one of the two experiments. D37 values from this experiment are: Parental-2.25, KO5=1.2, KO5 WT overexpression clone 3=2.7, KO5 WT overexpression clone 7=3.3, KO5 S102A phosphor-site mutant overexpression clone 5 =1.4. KO: knockout.

### 3.3.8 Proteomic Study

SILAC based proteomic study was performed to investigate the role of YB-1 on protein expression. MDA-MB-231 parental and YB-1 knockout clone 5 and 10 were cultured in light, medium and heavy labelled culture media for 5 days followed by protein isolation for proteomic analysis. The proteins summarized in the Tab. 2 showed significant up regulation (red arrow) or down regulation (green arrow) in YB-1 knockout clones 5 and 10. These proteins are directly or indirectly involve in DNA repair. Specifically, KAP-1, which is down regulated, is involved in DNA end resection during HR and A-NHEJ.

S.No	Protein	Gene	Expression	Role in DNA repair
1	<b>Acetyl-CoA acetyltransferase, cytosolic</b>	ACAT2	Down regulated in both YB-1 knockout clones 5 and 10 	DNA repair via HR pathway
2	<b>Serine/threonine-protein phosphatase</b>	PPP1CC	Down regulated in both YB-1 knockout clones 5 and 10 	Regulates DDR
3	<b>KAP1</b>	TRIM28	Down regulated in both YB-1 knockout clones 5 and 10 	Regulates DNA end resection process during HR and A-NHEJ mediated DNA DSB repair
4	<b>Thymidylate synthase</b>	TYMS	Down regulated in both YB-1 knockout clones 5 and 10 	Essential for DNA synthesis and repair
5	<b>Protein-glutamine gamma-glutamyltransferase 2</b>	TGM2	Down regulated in both YB-1 knockout clones 5 and 10 	Involves in DNA damage response and Drug resistance
6	<b>Ribonuclease inhibitor</b>	RNH1	Up regulated in both YB-1 knockout clones 5 and 10 	Overexpression of Rnh1 Delays DSB Repair.

7	<b>Galectin-3;Galectin</b>	LGALS3	Up regulated in both YB-1 knockout clones 5 and 10 	DDR response, regulates S/G2 checkpoints
8	<b>Heat shock 70 kDa protein 1</b>	HSPA1A	Up regulated in both YB-1 knockout clones 5 and 10 	possible function in DNA repair
9	<b>Nuclear mitotic apparatus protein 1</b>	NUMA1	Up regulated in both YB-1 knockout clones 5 and 10 	promotes HR
10	<b>Prothymosin alpha</b>	PTMA	Down regulated in both YB-1 knockout clones 5 and 10 	-positively regulated by c-MYC (c-Myc supresses C-NHEJ) -downstream target of c-Myc
11	<b>Integrin beta-1</b>	ITGB1	Up regulated in both YB-1 knockout clones 5 and 10 	interacts with Rad9 and have a role in HR and mismatch
12	<b>Spectrin beta chain, non-erythrocytic 1</b>	SPTBN1	Up regulated in both YB-1 knockout clones 5 and 10 	Involves in DNA repair via HR
13	<b>Glutathione S-transferase Mu 1</b>	GSTM1; GSTM4	Down regulated in both YB-1 knockout clones 5 and 10 	invoves in DNA damage response
14	<b>Dihydropyrimidinase-related protein 2</b>	DPYSL2	Up regulated in both YB-1 knockout clones 5 and 10 	DNA damage response-downstream target of p53
15	<b>Transferrin receptor protein 1</b>	TFRC	Up regulated in both YB-1 knockout clones 5 and 10 	facilitates the formation of DNA double-strand breaks acc.
16	<b>Thymidylate synthase</b>	TYMS	Down regulated in both YB-1 knockout clones 5 and 10 	regulates DNA synthesis and repair

**Tab. 2** Panel of proteins that were up regulated (red arrow) or down regulated (green arrow) in YB-1 knockout clones in SILAC based proteomic study.

Proteomic study revealed KAP-1 as one of the protein, which was significantly down regulated in both YB-1 knockout clones 5 and 10. DNA end resection is an essential step crucial for HR and A-NHEJ repair pathways. KAP-1 is a necessary protein in DNA end resection. The data so far showed that YB-1 stimulates both HR and A-NHEJ repair pathways. Therefore, the role of YB-1 in regulation of HR and A-NHEJ through KAP-1 mediated end resection was investigated in the subsequent experiment.

### 3.3.9 YB-1 knockout results in significant reduction in end resection

Quantitative assessment of DNA end resection is performed by RPA foci assay. Immediately after end resection, the single stranded DNA is coated by RPA protein to protect further DNA degradation. Frequency of RPA foci was analysed at 4 h and 12 h after irradiation. MDA-MB-231 parental cells showed significantly high number of RPA foci at both 4 hours and 12 hours after irradiation as compared to YB-1 knockout clones 5 and 10 (Fig 3.41)

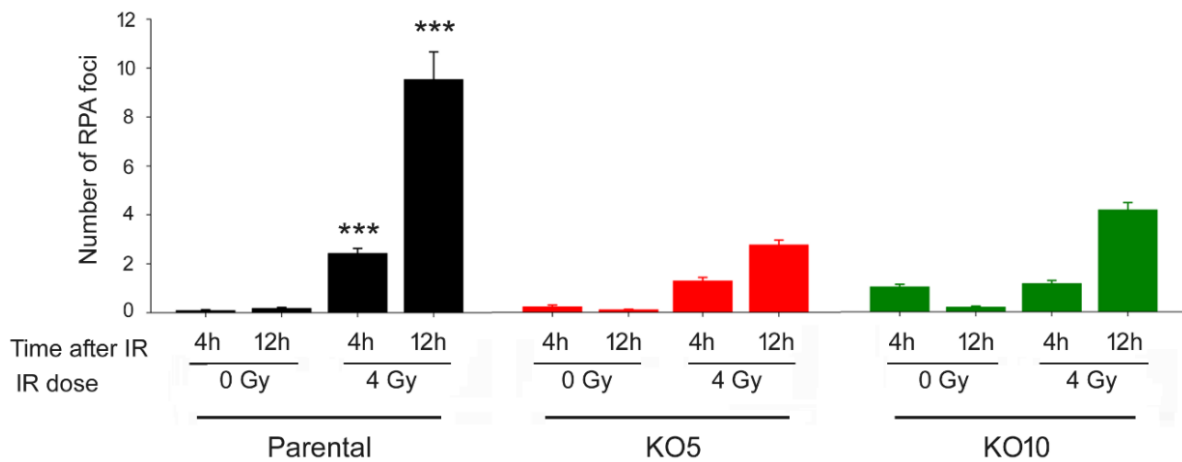


**Fig. 3.41 YB-1 knockout results in significant reduction in end resection as verified through reduced RPA foci.** MDA-MB-231 parental and YB-1 knockout clone 5 and 10 were irradiated with 4 Gy. Four and twelve hours' post-radiation immunofluorescence staining was performed for RPA foci as described in Method section. RPA foci were counted in total of 300 nuclei in 2 experiments. Asterisk indicate significant differences between the frequency of RPA foci in parental cells compared to YB-1 KO clones 5 and 10 as the same time points. (\*\*\*) $p < 0.001$ ; Student's t-test). KO: knockout.

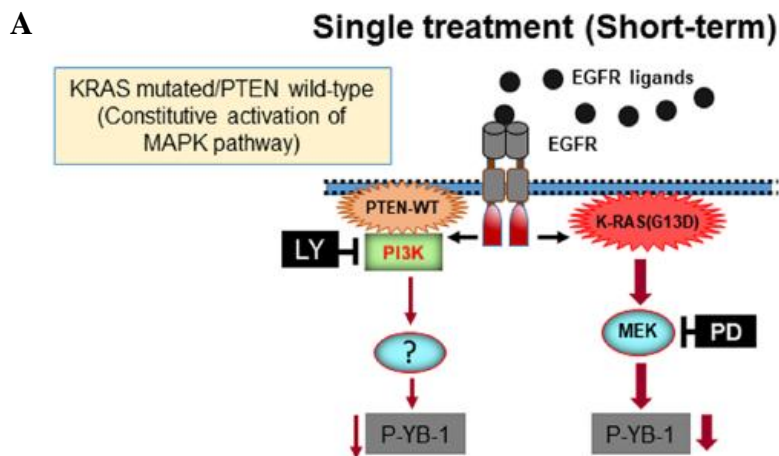
## 4 DISCUSSION

In the present study it has been discovered that YB-1 plays a crucial role in survival of *KRAS(G13D)*-mutated BCC. In *KRAS*-mutated BCC, depending on additional PTEN mutation, either the MAPK pathway or the PI3K pathway plays a major role in YB-1 phosphorylation at Ser-102. Interestingly, independent of either of the dominating pathways, dual targeting of MEK and PI3K is an efficient approach to block YB-1 phosphorylation and cell proliferation when compared to the single targeting strategies. Although Akt is one of the major downstream target of PI3K, phosphorylation of YB-1 was found to be independent of the Akt isoforms. Similar to the *in vitro* data in the tumor tissues from breast cancer patients, phosphorylation of YB-1 and ERK1/2 was found to be markedly high, in association with the overexpression of EGFR. In corresponding normal tissue, phosphorylation of YB-1 and ERK1/2 as well as the expression of EGFR were found to be at very low levels. Present study further showed that the regulation of cell proliferation by PI3K and MAPK pathways depends on expression of YB-1 in *KRAS* mutated BCC. Furthermore, YB-1 is responsible for radioresistance of BCC by stimulating DNA DSB repair through both homologous recombination (HR) and alternate-non homologous end joining (A-NHEJ) pathways. The mechanism of regulation of HR and A-NHEJ pathways by YB-1 is through KAP-1 mediated end resection.

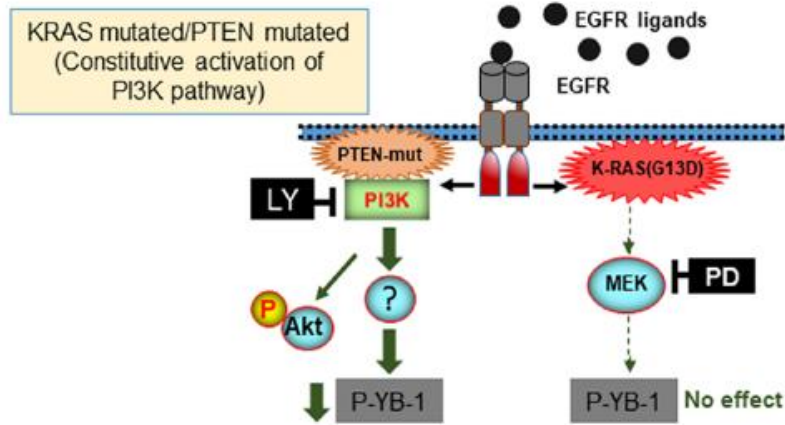
### 4.1 Signaling pathways regulating phosphorylation of YB-1 in *KRAS* mutated BCC

YB-1 is required for the normal development of multiple embryonic organ systems as well as for perinatal survival. Therefore, embryonic tissues show high YB-1 expression (Lu et al., 2005). The level of YB-1 diminishes in almost all organs in adults and found to be completely absent in old age. Cancer cells however, show high level of YB-1 expression, which is associated with poor prognosis and therapy response. Besides that, recent studies have shown that YB-1 needs to be activated/phosphorylated at Ser-102 to perform majority of its functions. Breast cancer cells present a high level of P-YB-1 when compared to normal breast epithelial cells. Furthermore ionizing radiation (IR) and growth factors like epithelial growth factor (EGF) can stimulates the phosphorylation of YB-1 (Toulany et al., 2011) , which as shown in Fig. 3.2 & 3.3 remains elevated for as long as 24 hours post stimulation in *KRAS* wild-type BCC. However, *KRAS(G13D)*-mutated BCC shows a constitutive high level of phosphorylation, which cannot be stimulated further by EGF or IR treatment as evaluated until 24 hours post treatment.

*KRAS* mutation is one of the most common genetic alterations in human tumors (Malumbres and Barbacid, 2003) . It plays a central role in tumor progression and chemoradiotherapy resistance and reduced overall patient survival (Knickelbein and Zhang, 2015) (Jiang et al., 2019, Wang et al., 2017). *KRAS* mutated BCC are highly aggressive (Rachagani et al., 2011) and radioresistance (Minjgee et al., 2011). Several previous studies have proposed that the RAS/MAPK/RSK pathway regulates YB-1 phosphorylation. Furthermore, RAS is involved in YB-1 phosphorylation induced by ionizing radiation in BCC (Toulany et al., 2011). In addition, it is also shown that the ERK is an upstream kinase that regulates YB-1 phosphorylation (Donaubauer and Hunzicker-Dunn, 2016). These findings are further supported by the correlation between the MEK/ERK pathway target genes and YB-1 expression in colorectal cancer (Jurchott et al., 2010). Stratford and colleagues have shown that RSK phosphorylates YB-1 at Ser-102 in breast cancer, which can be inhibited by the RSK inhibitor SL0101 (Stratford et al., 2008). The present study showed that phosphorylation of YB-1 is mainly regulated by RAS/ERK/RSK pathway and slightly regulated by PI3K pathway in *KRAS*(G13D)-mutated and PTEN wild-type BCC as summarized in Fig. 4.1 A.



B



C

### Single/dual treatment (Long-term)

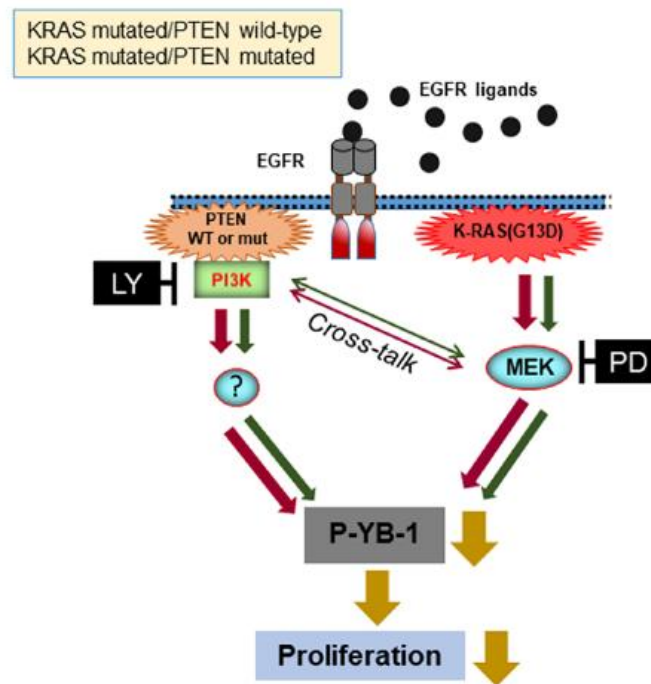


Fig. 4.1 Schematic representation of signaling pathways involved in phosphorylation of YB-1 in *KRAS(G13D)*-mutated/PTEN wildtype (A) and *KRAS(G13D)*-mutated/PTEN mutated (B) BCCs after short-term (2 h) treatment (A & B) and long-term (5 days) treatment (C) with PI3K and MEK inhibitors

However, *KRAS*(G13D)-mutated cells containing an additional loss of function mutation in *PTEN*, shows hyper activation of the PI3K/Akt pathway and PI3K-dependent phosphorylation of YB-1. Based on this observation, *PTEN* mutation appears to have a dominant role over *KRAS* mutation to phosphorylate YB-1 through PI3K as summarized in Fig. 4.1 B. The major role of the PI3K pathway in the phosphorylation of YB-1 in *PTEN/KRAS*(G13D)-mutated cells is also supported by the established prosurvival role of the PI3K pathway as the most altered signaling pathway in human cancers (Arcaro and Guerreiro, 2007, Courtney et al., 2010). YB-1 regulates the transcription of the *PIK3CA* gene, which codes for the p110alpha catalytic subunit of PI3K (Astanehe et al., 2009). Thus, a stimulatory loop exists between PI3K and YB-1 in which PI3K stimulates YB-1 by phosphorylation at S102. Stimulation of YB-1 enhances expression of PI3K according to Astaneh *et al.* (Astanehe et al., 2009). The described loop seems to operate in those tumor cells that are preferentially reliant on the PI3K pathway. Therefore, depending on the presence or absence of the additional mutation either the MAPK pathway or the PI3K pathway becomes dominant and regulates phosphorylation of YB-1 in *KRAS*(G13D)-mutated BCCs. This novel finding could be useful in deciphering therapeutic paradigms while targeting *KRAS* mutated tumors.

The *in vitro* data from this study showing the signaling pathways regulating YB-1 phosphorylation was further supported by the data obtained from tumor samples collected from breast cancer patients. All the tumor samples showed marked elevation of YB-1 phosphorylation along with enhanced phosphorylation of ERK1/2 and enhanced expression of EGFR. Unlike the tumor tissues, the corresponding normal tissue showed negligible levels of P-YB-1, P-ERK and EGFR expression (Fig. 3.19). Although the *KRAS* mutation status was not known in the tumor tissues, the hyperphosphorylation of YB-1 and ERK1/2 in association with EGFR expression in 5 out of 6 ductal carcinoma tissues is in line with the *in vitro* data. Interestingly, the patient number 3 (PT3) showed relatively lower level of P-YB-1 which was corresponded with the lower level of P-ERK1/2 and EGFR expression. This observation further strengthens the stated association. According to the histopathology data the two TNBC tumors (Tab. 1) also presented hyper activation of the ERK/YB-1 pathway in association with enhanced EGFR expression. This is in line with the *in vitro* data obtained from the two *KRAS*-mutated TNBC cell lines MDA-MB-231 and MDA-MB-453, the main cell lines investigated in the present study. The correlation between phosphorylation of YB-1 and the expression of EGFR in the TNBC patients and TNBC cell lines showed the clinical significance of the MAPK pathway in phosphorylation of YB-1. High level of



phosphorylation of ERK1/2 and YB-1 in non-TNBC tumors could be due to other alterations such as mutation in EGFR, RAS or RAF, which can also hyperactivate the MAPK pathway. Independent of the mechanism(s) involved in the activation of the ERK/YB-1 pathway in non-TNBC cells, this observation additionally highlights the importance of the present finding in targeting YB-1 signaling not only in TNBC but also in non-TNBC. Additionally, the low level of phosphorylated YB-1 in normal tissue obtained from patient number one (PT1) is in line with the data obtained from normal breast epithelial cell line MCF-10A (Fig.3.1) and the de novo transformed breast epithelial cell line HBL-100, showing negligible levels of YB-1 phosphorylation compared to KRAS-mutated cells. This observation and the lack of the inhibitory effect of PI3K and MEK inhibitors on the proliferation of HBL-100 cells after single- or dual-treatment suggest that the proposed targeting strategy seems to be very efficient and specifically target tumor tissues and might spare the normal tissue.

#### **4.2 Crosstalk between MAPK and PI3K pathways regulate YB-1 phosphorylation**

Irrespective of the central pathway regulating the phosphorylation of YB-1 in *KRAS* mutated BCC, dual targeting of MAPK and PI3K pathway strongly inhibits the phosphorylation of YB-1. The RAS-ERK and PI3K signaling pathways are the major pathways that regulate cellular growth, proliferation, differentiation, metabolism, and motility. Initially RAS-ERK and PI3K were considered to act as linear signaling pathways activated by different stimuli, but recent studies showed that these two pathways intersect to regulate each other and co-regulate downstream functions. Such cross-inhibition has been well reported, in which inhibition of one pathway leads to the activation of other pathway (Mendoza et al., 2011, Zhou et al., 2015, Pitts et al., 2014). A cross-inhibition exist within the two pathways between Akt and Raf (Manning and Toker, 2017). Thus, according to the possible crosstalk between PI3K/Akt and MAPK/ERK pathway, it is expected that inhibition of one pathway leads to the activation of YB-1 through the alternative pathway. Thus as summarized in Fig. 4.1 C, dual targeting of both the pathways is an efficient approach to block YB-1 phosphorylation. There are reports, which suggest the importance of dual targeting of MAPK and PI3K pathways (Hoeflich et al., 2012, Grant, 2008), through a synthetic lethal interaction between the two pathways (Guenther et al., 2013). So far, the role of the described interaction between the two pathways on YB-1 activity in *KRAS*-mutated cells has not been reported.

Clement et al, 2018 showed that long-term inhibition of PI3K pathway results in PI3K independent reactivation of Akt through E3 ubiquitin ligase Skp2, IGF-1R, PDK-1 and mTORC2 (Clement et al., 2018). In line with this report, the present study shows that short-term inhibition of PI3K pathway leads to complete inhibition of Akt activity and slight inhibition of YB-1 phosphorylation, but long-term inhibition of PI3K (as observed in proliferation assay) leads to reactivation of Akt and resistance towards PI3K inhibitor. Furthermore, knockdown of ERK2 or KRAS or short-term inhibition of MEK in *KRAS(G13D)*-mutated cells resulted into subsequent stimulation of Akt through PI3K. Thus, inhibition of MAPK pathway act similar to *PTEN* mutation by activation of PI3K activity in *PTEN* wild-type BCC. Interestingly knocking down of KRAS in *KRAS/PTEN* double mutated BCC showed no stimulatory effect on Akt whereas short-term inhibition of MEK leads to activation of Akt in these cells. The possible reason could be that MAPK pathway functions independent of KRAS in cells with additional *PTEN* mutations. Collectively, it is proposed that the MEK inhibition results in the simultaneous stimulation of PI3K activity which diminishes the efficacy of MEK inhibitor in targeting YB-1 phosphorylation. This leads to acquired resistance to MEK inhibition. Consequently, simultaneous blockage of PI3K and MEK leads to the stronger inhibition of YB-1 phosphorylation compared to single targeting approaches. Interestingly long-term inhibition of PI3K strongly suppresses the expression of YB-1, especially in *PTEN*-mutated cells. This observation is in line with the study from Lyabin et al, who have shown that inhibition of the mTOR kinase results in negative regulation of YB-1 synthesis (Lyabin and Ovchinnikov, 2016). PI3K is upstream of mTOR therefore long-term inhibition of PI3K results in down regulation of mTOR and subsequent suppression of YB-1 synthesis (Lyabin et al., 2012).

The Akt family includes three isoforms; Akt1, Akt2 and Akt3 with slight varying functions. Akt is one of the major downstream target of PI3K. In the present study, short-term inhibition of PI3K completely blocked Akt phosphorylation and slightly inhibited YB-1 phosphorylation in *KRAS(G13D)*-mutated cells and strongly inhibited YB-1 phosphorylation in *KRAS/PTEN* double mutated cells. The long-term inhibition of PI3K lead to the reactivation of Akt but the levels of P-YB-1 remains inhibited (see Fig. 3.21 & Fig. 30). Furthermore, unlike PI3K, inhibition of Akt showed no inhibitory effect on the phosphorylation of YB-1. These data and the data obtained from genetic approaches (Fig. 3B-C) indicate that inhibition of YB-1 phosphorylation by PI3K targeting is independent of Akt in *KRAS(G13D)*-mutated cells. This data is in line with the recent studies showing Akt-independent signaling of PI3K in cancer

(Lien et al., 2017, Bruhn et al., 2013). Gagliardi et al showed that the overexpression of activated Akt is not enough to restore malignant phenotypes following knockdown of PDK1, an immediate downstream effector of PI3K (Fig. 2, Introduction section), suggesting a subset of tumors that are PI3K/PDK1-dependent but Akt independent (Gagliardi et al., 2012). There are reports suggesting Akt as the downstream target of PI3K in phosphorylation of YB-1. Sutherland *et al.* (Sutherland et al., 2005) demonstrated that YB-1 forms a complex with activated Akt1 after stimulation of cells with IGF-1 in MDA-MB-231 cells. Since the status of YB-1 phosphorylation has not been shown by Sutherland *et al.* (Sutherland et al., 2005), conclusions cannot be made regarding whether IGF1-induced Akt1/YB-1 complex formation depends on YB-1 phosphorylation. Although the authors showed that activated Akt induces YB-1 phosphorylation at Ser-102 in a test-tube radioactive assay, from an *in vitro* assay, it cannot be concluded that a similar event occurs under physiological conditions. Therefore, present study proposes Akt independent mode of PI3K mediated YB-1 phosphorylation in KRAS(G13D)-mutated BCC.

#### **4.3 YB-1 regulates proliferation of KRAS(G13D)-mutated BCC**

Transgenic expression of YB-1 causes the development of breast carcinomas with various histological types, indicating that YB-1 is an oncogene (Davies et al., 2014). YB-1 knockdown is reported to inhibit cell proliferation of human BCC, prostate cancer cells and multiple myeloma cells in culture (Basaki et al., 2010, Liu et al., 2015, Chatterjee et al., 2008). YB-1 knockdown also suppresses the expression of various cell cycle, DNA replication as well as growth factor genes (Wu et al., 2007, Davies et al., 2011). Overexpression of YB-1 induces EGF/TGF $\alpha$ -independent cell growth and constitutive EGFR activation in human mammary cell lines (Berquin et al., 2005). YB-1 knockout mice exhibit a marked decrease in cell proliferation rates and are embryonic lethal (Lu et al., 2005, Uchiumi et al., 2006). In the present study YB-1 is shown to strongly regulate proliferation of KRAS mutated BCC. YB-1 knockout clones showed about 75% reduction in cell proliferation when compared to the parental cells. The further inhibition of the prosurvival pathways like MAPK and PI3K showed no further inhibition. This specifies that the entire proliferative effect of these pathways is operating through YB-1. Recent studies also pointed out that YB-1 is involved in cell proliferation by regulating the expression of key proteins of cell cycle progression like cyclin A and cyclin B1 (Jurchott et al., 2003) as well as replication (En-Nia

et al., 2005, Gu et al., 2001). The cell cycle control is predominantly regulated at the G1/S transition, the induction of positive factors or deregulation of negative factors that regulate cell cycle progression may cause an imbalance in this transition, leading to malignant transformation (Weinberg, 1989). Nuclear YB-1 expression is enhanced during the G1-S transition of the cell cycle and this nuclear accumulation of YB-1 is shown to be associated with enhanced cyclin A and cyclin B1 mRNA as well as protein expression (Jurchott et al., 2003). Furthermore, alterations in the levels of nuclear YB-1 in G1/S transition have been identified in different types of tumours, including osteosarcoma (Benassi et al, 1997), suggesting that YB-1 is involved in the G1/S transition and proliferation of osteosarcoma cells. Furthermore, previous studies on human prostate, breast and multiple myeloma cell lines suggest a role of YB-1 in proliferation (Basaki et al., 2010, Liu et al., 2015, Chatterjee et al., 2008). The present study shows a marked inhibition of cell proliferation in *KRAS(G13D)*-mutated BCC tested by knockdown and knockout of YB-1. Thus, YB-1 is a potent mitogenic biomarker of growth in cancer cells. Furthermore, cyclin D1 is specifically down-regulated by YB-1 knockdown in human multiple myeloma cells, resulting in a marked decrease of viable cells, suggesting that YB-1 knockdown-induced cell growth arrest is due to decreased expression of cyclin D1 (Harada et al., 2014). In the current study, it is partially confirmed that inhibition of YB-1 dependent cell proliferation after applying PI3K and MEK inhibitors is a cytostatic rather than a cytotoxic effect.

The present study highlighted the importance of phosphorylation of YB-1 in cell proliferation depending on the status of KRAS. Inhibiting the MAPK or PI3K pathway slightly inhibits the YB-1 phosphorylation and cell proliferation. Targeting MAPK and PI3K pathways simultaneously results in a strong inhibition of YB-1 phosphorylation and consequently significant inhibition of cell proliferation in *KRAS(G13D)*-mutated BCC. This highlights the importance of YB-1 phosphorylation in cells proliferation. Re-growing of cells after supplying inhibitors-free medium indicates a cytostatic effect rather than a cytotoxic effect of P-YB-1. Although this conclusion needs further investigation. In *KRAS* wild-type SKBR3 cells, inhibition of MAPK or PI3K simultaneously or alone showed similar level of antiproliferative activity. This data suggest that YB-1 might not be the major regulator of cell proliferation in *KRAS* wild-type BCC. In HBL-100 cell lines there was no effect on inhibition of cell proliferation after either targeting MAPK or PI3K pathway alone or in combination. This data further correlates with the pattern of YB-1 phosphorylation after indicated

treatments. Since HBL-100 are not the real BCC, it can be argued that the activity of YB-1 is highly specific to cancer cells.

#### **4.4 YB-1 regulates DNA DSB repair by HR and A-NHEJ pathways through Kap-1 mediated end resection**

YB-1 regulates activity of several DNA repair proteins involved in single strand break repair pathways including base excision repair, nucleotide excision repair, and mismatch repair (MMR) pathways (de Souza-Pinto et al., 2009, Das et al., 2007, Alemasova et al., 2016, Fomina et al., 2015). YB-1 is also known to stimulate repair of DNA DSB after exposure to ionizing radiation (Toulany et al., 2011). However, specific DNA DSB repair pathways regulated by YB-1 and the underlying mechanism is not known. In the present study it was discovered that YB-1 regulates DSB through HR and A-NHEJ pathways through Kap-1 mediated end resection.

The role of YB-1 in DSB was verified by strong radiosensitization of YB-1 knockout MDA-MB-231 cells. In the consequent rescue experiments where wild-type YB-1 was expressed in the YB-1 knockout clones, the cells became radioresistance to the level similar to the parental cells. Phosphorylation of YB-1 at Serine 102 (Ser-102) is essential for YB-1 activity. Role of this YB-1 phosphorylation on DSB repair has not been described before. In line with that, the data from present study shows that phosphorylation of YB-1 is essential for stimulating DSB repair and radioresistance. This could be confirmed by the rescue experiment in which wild-type YB-1 and YB-1(S102A) were overexpressed in YB-1 knockout clones.

The underlying pathways involved in stimulation of DSB by YB-1 is not known. In this study, by applying several approaches it could be demonstrated that YB-1 has a significant role in the repair of DNA DSBs through the HR and A-NHEJ. The effect of YB-1 in DSB repair was more pronounced in sub-confluent cells (in active log phase), which indicates that YB-1 probably regulate the DSB repair pathway mainly in S-G2 phase of cell cycle. Thus, stimulation of DSB repair by YB-1 in growing cells may propose YB-1 as an appropriate target in combination with radiotherapy in highly proliferating tumor cells. Function of YB-1 in HR and A-NHEJ was approved by using Rad51 inhibitor B02 and PARP inhibitor Talazoparib, respectively.

Since PARP inhibitors have entered in clinical trials (Kurnit et al., 2018, O'Sullivan Coyne et al., 2015), findings from present study further emphasizes potential applicability of these inhibitors in combination with radiotherapy in tumors overexpressing YB-1.

The data obtained from proteomic study reveals that YB-1 regulates the expression of many proteins that directly or indirectly are involved in DNA repair. KRAB-associated protein 1 (KAP-1), which is involved in DSB repair (Tubbs et al., 2014) was significantly downregulated in YB-1 knockout cells. KAP-1 also known as TRIM28, TIF1 $\beta$ , or KRIP-1 has been reported to promote DNA end resection in murine G<sub>1</sub>-phase lymphocytes when these DNA ends are not protected by H2AX and 53BP1. A single-amino-acid change that reflects a KAP-1 polymorphism between primates and other mammalian species disrupts its ability to promote DNA end resection in murine cells (Tubbs et al., 2014). To be repaired by HR or A-NHEJ pathways, DSB ends must first be degraded to generate long 3'- single strand DNA (ssDNA) tails, a process known as 5'-3' end resection. As a result of this process, stretches of ssDNA are formed and rapidly coated by replication protein A (RPA), a heterotrimeric ssDNA-binding protein. RPA protects the ssDNA from degradation by nucleases and serves as a platform to activate cell cycle checkpoints. RPA is replaced later by Rad51 protein molecules, which initiate the homology search during the S-G2 phase of the cell cycle in HR repair pathway. In A-NHEJ repair pathway, RPA protein is sequentially replaced by XRCC1, ligase 2 and ligase 3 to ligate the strands. Thus, in YB-1 knockout cells, it is expected that downregulation of KAP-1 diminishes RPA foci after irradiation.

Ku70/Ku80 hetero-dimer initiates the repair of DSB by NHEJ. It rapidly and stably binds to DSB, prevents end degradation by the HR and end resection machinery. It also serves as the platform for the assembly of the other NHEJ factors, including end processing factors in a multiprotein complex. A-NHEJ pathway is distinct from NHEJ as it is Ku-independent, it requires component of HR end resection machinery and frequently involves longer tracts of microhomology. The competition between Ku and the end resection machinery for a DSB end determines whether the DNA damage will be repaired by NHEJ or channelled into the HR or occasionally into the A-NHEJ pathway. Overexpression of YB-1 can enhance the KAP-1 mediated end resection, which results into predominating HR and A-NHEJ.

Given the role of end resection in A-NHEJ, it was generally assumed that DSB repair by A-NHEJ pathway occurs predominantly in S and G2 phase cells when the end resection machineries are active. Despite the negative regulation of end resection in G1 cells, it is evident that the repair of DSB by A-NHEJ also occurs in this phase of the cell cycle. Both CtIP and MRN appear to be responsible for the end resection in G1 cells. Furthermore, since inactivation of NHEJ results in increased repair of DSB by A-NHEJ in G1 cells, it seems that NHEJ suppresses DSB repair by A-NHEJ in G1 cells. While phosphorylation of CtIP by cyclin-dependent protein kinases is critical for its role in initiating resection for HR in G2 cells, CtIP is phosphorylated in a DNA damage-inducible manner by Polo-like kinase 3 to activate CtIP/MRN-dependent resection in G1 cells. This leads to the conclusion that cancer cells with high level of YB-1 predominantly regulates DSB by HR in G2 and M phase and by A-NHEJ in all the phases of cell cycle.

The data from repair assay shows that there is no significant role of YB-1 in the repair of DNA DSB through the classical NHEJ pathway (Fig.3.33). This observation is further validated by the data from  $\gamma$ H2AX assay, where Parental and YB-1 knockout cells showed enhanced DNA damage when treated with Nu7441 (inhibitor of DNA-PKcs). Interestingly in these experiments the YB-1 knockout cells showed significant increase in DNA DSB as compared to the parental cells. The possible interpretation for this observation could be that in the presence of YB-1, there is enhanced expression of KAP-1 protein, which influenced the cells to predominantly perform the DNA DSB repair through HR or A-NHEJ pathway (Fig. 4.2). Whereas in the absence of YB-1 there is strong inhibition of HR and A-NHEJ pathways which might result in the activation of C-NHEJ pathway, possibly through a cross-talk between HR and C-NHEJ pathway as described before in literature (Sunada et al., 2018, Her and Bunting, 2018). This is depicted in detail in the Fig. 4.2. Hence, the presence of elevated levels of P-YB-1 in *KRAS*(G13D)-mutated BCC, induces HR and A-NHEJ dependent DSB repair and consequently provides radio-resistance. Therefore targeting YB-1 in combination with radiotherapy can be an efficient approach to treat *KRAS* mutated cancers.

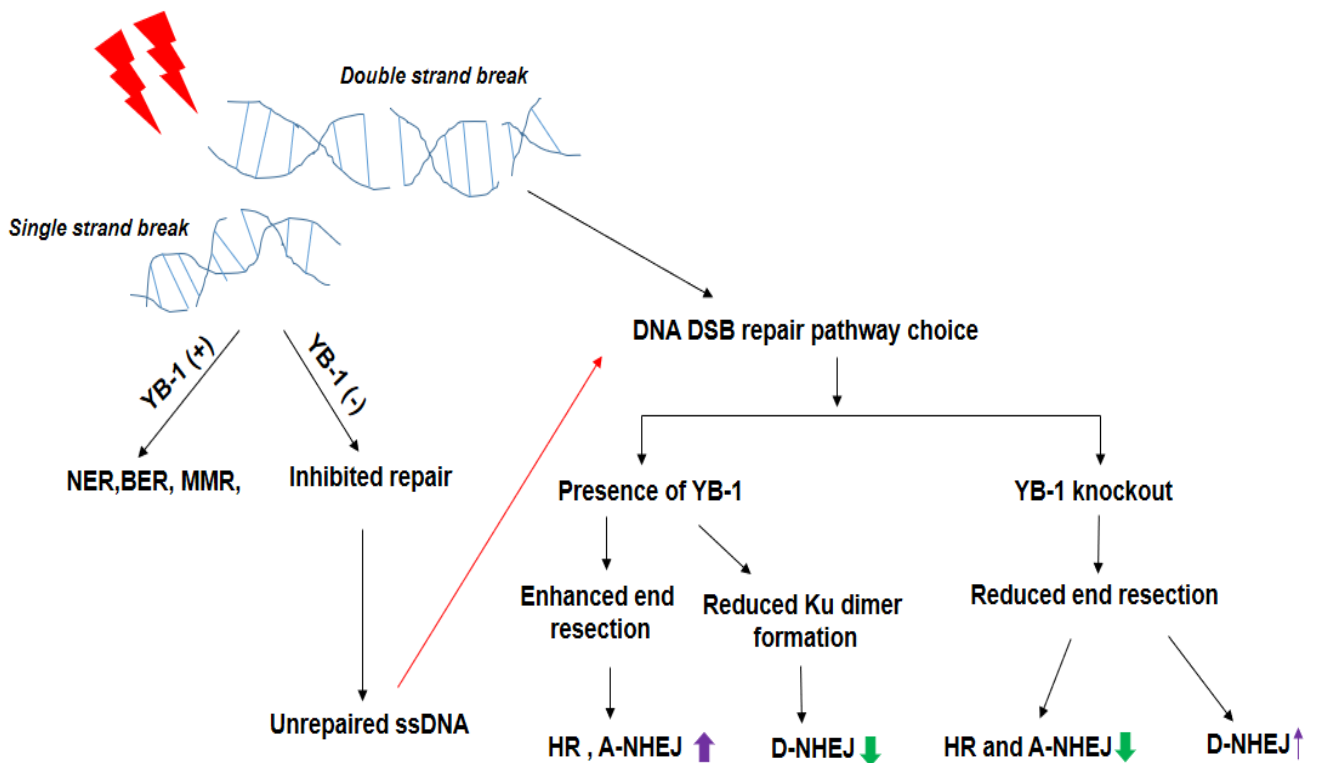


Fig. 4.2 Schematic representation of role of YB-1 in DNA DSB repair choice (self-compilation).

## CONCLUSION

The present study highlights three major novel findings, which could be imperative in therapeutic targeting of KRAS mutated BCC:

1) The data revealed the underlying signaling pathways, i.e. the MAPK/ERK and PI3K/Akt pathways involved in phosphorylation of YB-1 in KRAS mutated BCC. The presented mechanistic study also provides a rationale for dual targeting of MEK and PI3K as an efficient approach to target YB-1 phosphorylation at Ser-102. The data obtained from patient tumor tissues supports the *in vitro* results. Thus, the provided knowledge is of particular importance in designing the therapeutic paradigms for targeting KRAS mutated breast cancer and other tumor entities with higher rates of KRAS mutation, e.g., pancreatic cancer and colorectal cancer.



2) The data from YB-1 knockout cells divulge the strong role of YB-1 in proliferation of KRAS mutated BCC. The major cell lines investigated in the present study were TNBC cells, which is the highly aggressive and therapy resistant sub-type of breast cancer. Thus, YB-1 might be an appropriate target for therapy of KRAS(G13D)-mutated breast cancer including TNBC. The tumor samples from breast cancer patients investigated in the present study also revealed the activation of YB-1 and the components of its upstream signaling cascade, which emphasize the clinical significance of the present study.

3) This study uncovered the novel mechanism by which YB-1 regulates DNA DSB repair through HR and A-NHEJ pathway and mediates radioresistance. This mechanistic study implies KAP-1 as the crucial factor between DNA end resection dependent or independent mode of DSB repair through YB-1. Thus, YB-1 targeting approach may be an efficient strategy to overcome radiotherapy resistance of solid tumors. Along with the clinical significance, this finding is also very important for the field of DNA repair.

## REFERENCES

- ALEMASOVA, E. E., MOOR, N. A., NAUMENKO, K. N., KUTUZOV, M. M., SUKHANOVA, M. V., PESTRYAKOV, P. E. & LAVRIK, O. I. 2016. Y-box-binding protein 1 as a non-canonical factor of base excision repair. *Biochim Biophys Acta*, 1864, 1631-1640.
- ALESSI, D. R., JAMES, S. R., DOWNES, C. P., HOLMES, A. B., GAFFNEY, P. R., REESE, C. B. & COHEN, P. 1997. Characterization of a 3-phosphoinositide-dependent protein kinase which phosphorylates and activates protein kinase Balpha. *Curr Biol*, 7, 261-9.
- ARCARO, A. & GUERREIRO, A. S. 2007. The phosphoinositide 3-kinase pathway in human cancer: genetic alterations and therapeutic implications. *Curr Genomics*, 8, 271-306.
- ASTANEHE, A., FINKBEINER, M. R., HOJABRPOUR, P., TO, K., FOTOVATI, A., SHADEO, A., STRATFORD, A. L., LAM, W. L., BERQUIN, I. M., DURONIO, V. & DUNN, S. E. 2009. The transcriptional induction of PIK3CA in tumor cells is dependent on the oncoprotein Y-box binding protein-1. *Oncogene*, 28, 2406-18.
- BARGOU, R. C., JURCHOTT, K., WAGENER, C., BERGMANN, S., METZNER, S., BOMMERT, K., MAPARA, M. Y., WINZER, K. J., DIETEL, M., DORKEN, B. & ROYER, H. D. 1997. Nuclear localization and increased levels of transcription factor YB-1 in primary human breast cancers are associated with intrinsic MDR1 gene expression. *Nat Med*, 3, 447-50.
- BASAKI, Y., TAGUCHI, K., IZUMI, H., MURAKAMI, Y., KUBO, T., HOSOI, F., WATARI, K., NAKANO, K., KAWAGUCHI, H., OHNO, S., KOHNO, K., ONO, M. & KUWANO, M. 2010. Y-box binding protein-1 (YB-1) promotes cell cycle progression through CDC6-dependent pathway in human cancer cells. *Eur J Cancer*, 46, 954-65.
- BEAGLE, B. & FRUMAN, D. A. 2011. A lipid kinase cousin cooperates to promote cancer. *Cancer Cell*, 19, 693-5.

- BERQUIN, I. M., PANG, B., DZIUBINSKI, M. L., SCOTT, L. M., CHEN, Y. Q., NOLAN, G. P. & ETHIER, S. P. 2005. Y-box-binding protein 1 confers EGF independence to human mammary epithelial cells. *Oncogene*, 24, 3177-86.
- BIANCHINI, G., BALKO, J. M., MAYER, I. A., SANDERS, M. E. & GIANNI, L. 2016. Triple-negative breast cancer: challenges and opportunities of a heterogeneous disease. *Nat Rev Clin Oncol*, 13, 674-690.
- BIEMAR, F. & FOTI, M. 2013. Global progress against cancer-challenges and opportunities. *Cancer Biol Med*, 10, 183-6.
- BOMMERT, K. S., EFFENBERGER, M., LEICH, E., KUSPERT, M., MURPHY, D., LANGER, C., MOLL, R., JANZ, S., MOTTOK, A., WEISSBACH, S., ROSENWALD, A., BARGOU, R. & BOMMERT, K. 2013. The feed-forward loop between YB-1 and MYC is essential for multiple myeloma cell survival. *Leukemia*, 27, 441-50.
- BRANDSMA, I. & GENT, D. C. 2012. Pathway choice in DNA double strand break repair: observations of a balancing act. *Genome Integr*, 3, 9.
- BRUHN, M. A., PEARSON, R. B., HANNAN, R. D. & SHEPPARD, K. E. 2013. AKT-independent PI3-K signaling in cancer - emerging role for SGK3. *Cancer Manag Res*, 5, 281-92.
- BUROTTO, M., CHIOU, V. L., LEE, J. M. & KOHN, E. C. 2014. The MAPK pathway across different malignancies: a new perspective. *Cancer*, 120, 3446-56.
- CASTELLANO, E. & DOWNWARD, J. 2011. RAS Interaction with PI3K: More Than Just Another Effector Pathway. *Genes Cancer*, 2, 261-74.
- CHATTERJEE, M., RANCSO, C., STUHMER, T., ECKSTEIN, N., ANDRULIS, M., GERECKE, C., LORENTZ, H., ROYER, H. D. & BARGOU, R. C. 2008. The Y-box binding protein YB-1 is associated with progressive disease and mediates survival and drug resistance in multiple myeloma. *Blood*, 111, 3714-22.
- CHATTERJEE, N. & WALKER, G. C. 2017. Mechanisms of DNA damage, repair, and mutagenesis. *Environ Mol Mutagen*, 58, 235-263.
- CHATTOPADHYAY, R., DAS, S., MAITI, A. K., BOLDOGH, I., XIE, J., HAZRA, T. K., KOHNO, K., MITRA, S. & BHAKAT, K. K. 2008. Regulatory role of human AP-endonuclease (APE1/Ref-1) in YB-1-mediated activation of the multidrug resistance gene MDR1. *Mol Cell Biol*, 28, 7066-80.
- CHEN, H., ZHU, G., LI, Y., PADIA, R. N., DONG, Z., PAN, Z. K., LIU, K. & HUANG, S. 2009. Extracellular signal-regulated kinase signaling pathway regulates breast cancer cell migration by maintaining slug expression. *Cancer Res*, 69, 9228-35.
- CLEMENT, E., INUZUKA, H., NIHIRA, N. T., WEI, W. & TOKER, A. 2018. Skp2-dependent reactivation of AKT drives resistance to PI3K inhibitors. *Sci Signal*, 11.
- COURTNEY, K. D., CORCORAN, R. B. & ENGELMAN, J. A. 2010. The PI3K pathway as drug target in human cancer. *J Clin Oncol*, 28, 1075-83.
- DAHL, E., EN-NIA, A., WIESMANN, F., KRINGS, R., DJUDJAJ, S., BREUER, E., FUCHS, T., WILD, P. J., HARTMANN, A., DUNN, S. E. & MERTENS, P. R. 2009. Nuclear detection of Y-box protein-1 (YB-1) closely associates with progesterone receptor negativity and is a strong adverse survival factor in human breast cancer. *BMC Cancer*, 9, 410.
- DAS, S., CHATTOPADHYAY, R., BHAKAT, K. K., BOLDOGH, I., KOHNO, K., PRASAD, R., WILSON, S. H. & HAZRA, T. K. 2007. Stimulation of NEIL2-mediated oxidized base excision repair via YB-1 interaction during oxidative stress. *J Biol Chem*, 282, 28474-84.
- DAVIES, A. H., BARRETT, I., PAMBID, M. R., HU, K., STRATFORD, A. L., FREEMAN, S., BERQUIN, I. M., PELECH, S., HIETER, P., MAXWELL, C. & DUNN, S. E. 2011. YB-1 evokes susceptibility to cancer through cytokinesis failure, mitotic dysfunction and HER2 amplification. *Oncogene*, 30, 3649-60.
- DAVIES, A. H., REIPAS, K. M., PAMBID, M. R., BERNS, R., STRATFORD, A. L., FOTOVATI, A., FIRMINO, N., ASTANEHE, A., HU, K., MAXWELL, C., MILLS, G. B. & DUNN, S. E. 2014. YB-1 transforms human mammary epithelial cells through chromatin remodeling leading to the development of basal-like breast cancer. *Stem Cells*, 32, 1437-50.

- DAVIS, A. J. & CHEN, D. J. 2013. DNA double strand break repair via non-homologous end-joining. *Transl Cancer Res*, 2, 130-143.
- DE LANGEN, A. J. & SMIT, E. F. 2017. Therapeutic approach to treating patients with BRAF-mutant lung cancer: latest evidence and clinical implications. *Ther Adv Med Oncol*, 9, 46-58.
- DE SOUZA-PINTO, N. C., MASON, P. A., HASHIGUCHI, K., WEISSMAN, L., TIAN, J., GUAY, D., LEBEL, M., STEVNSNER, T. V., RASMUSSEN, L. J. & BOHR, V. A. 2009. Novel DNA mismatch-repair activity involving YB-1 in human mitochondria. *DNA Repair (Amst)*, 8, 704-19.
- DE ZIO, D., CIANFANELLI, V. & CECCONI, F. 2013. New insights into the link between DNA damage and apoptosis. *Antioxid Redox Signal*, 19, 559-71.
- DHILLON, A. S., VON KRIEGSHEIM, A., GRINDLAY, J. & KOLCH, W. 2007. Phosphatase and feedback regulation of Raf-1 signaling. *Cell Cycle*, 6, 3-7.
- DIANA, A., FRANZESE, E., CENTONZE, S., CARLINO, F., DELLA CORTE, C. M., VENTRIGLIA, J., PETRILLO, A., DE VITA, F., ALFANO, R., CIARDIELLO, F. & ORDITURA, M. 2018. Triple-Negative Breast Cancers: Systematic Review of the Literature on Molecular and Clinical Features with a Focus on Treatment with Innovative Drugs. *Curr Oncol Rep*, 20, 76.
- DONAUBAUER, E. M. & HUNZICKER-DUNN, M. E. 2016. Extracellular Signal-regulated Kinase (ERK)-dependent Phosphorylation of Y-Box-binding Protein 1 (YB-1) Enhances Gene Expression in Granulosa Cells in Response to Follicle-stimulating Hormone (FSH). *J Biol Chem*, 291, 12145-60.
- ELISEEVA, I. A., KIM, E. R., GURYANOV, S. G., OVCHINNIKOV, L. P. & LYABIN, D. N. 2011. Y-box-binding protein 1 (YB-1) and its functions. *Biochemistry (Mosc)*, 76, 1402-33.
- EN-NIA, A., YILMAZ, E., KLINGE, U., LOVETT, D. H., STEFANIDIS, I. & MERTENS, P. R. 2005. Transcription factor YB-1 mediates DNA polymerase alpha gene expression. *J Biol Chem*, 280, 7702-11.
- EVDOKIMOVA, V., TOGNON, C., NG, T., RUZANOV, P., MELNYK, N., FINK, D., SOROKIN, A., OVCHINNIKOV, L. P., DAVICIONI, E., TRICHE, T. J. & SORENSEN, P. H. 2009. Translational activation of snail1 and other developmentally regulated transcription factors by YB-1 promotes an epithelial-mesenchymal transition. *Cancer Cell*, 15, 402-15.
- FOMINA, E. E., PESTRYAKOV, P. E., MALTSEVA, E. A., PETRUSEVA, I. O., KRETOV, D. A., OVCHINNIKOV, L. P. & LAVRIK, O. I. 2015. Y-box binding protein 1 (YB-1) promotes detection of DNA bulky lesions by XPC-HR23B factor. *Biochemistry (Mosc)*, 80, 219-27.
- FRANKE, T. F., YANG, S. I., CHAN, T. O., DATTA, K., KAZLAUSKAS, A., MORRISON, D. K., KAPLAN, D. R. & TSICHLIS, P. N. 1995. The protein kinase encoded by the Akt proto-oncogene is a target of the PDGF-activated phosphatidylinositol 3-kinase. *Cell*, 81, 727-36.
- FUKADA, T. & TONKS, N. K. 2003. Identification of YB-1 as a regulator of PTP1B expression: implications for regulation of insulin and cytokine signaling. *EMBO J*, 22, 479-93.
- GAGLIARDI, P. A., DI BLASIO, L., ORSO, F., SEANO, G., SESSA, R., TAVERNA, D., BUSSOLINO, F. & PRIMO, L. 2012. 3-phosphoinositide-dependent kinase 1 controls breast tumor growth in a kinase-dependent but Akt-independent manner. *Neoplasia*, 14, 719-31.
- GAUDREULT, I., GUAY, D. & LEBEL, M. 2004. YB-1 promotes strand separation in vitro of duplex DNA containing either mispaired bases or cisplatin modifications, exhibits endonucleolytic activities and binds several DNA repair proteins. *Nucleic Acids Res*, 32, 316-27.
- GHONCHEH, M., POURNAMDAR, Z. & SALEHINIYA, H. 2016. Incidence and Mortality and Epidemiology of Breast Cancer in the World. *Asian Pac J Cancer Prev*, 17, 43-6.
- GILTNAME, J. M. & BALKO, J. M. 2014. Rationale for targeting the Ras/MAPK pathway in triple-negative breast cancer. *Discov Med*, 17, 275-83.
- GLOBAL BURDEN OF DISEASE CANCER, C., FITZMAURICE, C., ALLEN, C., BARBER, R. M., BARREGARD, L., BHUTTA, Z. A., BRENNER, H., DICKER, D. J., CHIMED-ORCHIR, O., DANDONA, R., DANDONA, L., FLEMING, T., FOROUZANFAR, M. H., HANCOCK, J., HAY, R. J., HUNTER-MERRILL, R., HUYNH, C., HOSGOOD, H. D., JOHNSON, C. O., JONAS, J. B., KHUBCHANDANI, J., KUMAR, G. A., KUTZ, M., LAN, Q., LARSON, H. J., LIANG, X., LIM, S. S., LOPEZ, A. D., MACINTYRE, M. F., MARCZAK, L., MARQUEZ, N., MOKDAD, A. H., PINHO, C., POURMALEK, F., SALOMON, J. A.,

- SANABRIA, J. R., SANDAR, L., SARTORIUS, B., SCHWARTZ, S. M., SHACKELFORD, K. A., SHIBUYA, K., STANAWAY, J., STEINER, C., SUN, J., TAKAHASHI, K., VOLLSET, S. E., VOS, T., WAGNER, J. A., WANG, H., WESTERMAN, R., ZEEB, H., ZOECKLER, L., ABD-ALLAH, F., AHMED, M. B., ALABED, S., ALAM, N. K., ALDHAHRI, S. F., ALEM, G., ALEMAYOHU, M. A., ALI, R., AL-RADDADI, R., AMARE, A., AMOAKO, Y., ARTAMAN, A., ASAYESH, H., ATNAFU, N., AWASTHI, A., SALEEM, H. B., BARAC, A., BEDI, N., BENSENOR, I., BERHANE, A., BERNABE, E., BETSU, B., BINAGWAHO, A., BONEYA, D., CAMPOS-NONATO, I., CASTANEDA-ORJUELA, C., CATALA-LOPEZ, F., CHIANG, P., CHIBUEZE, C., CHITHEER, A., CHOI, J. Y., COWIE, B., DAMTEW, S., DAS NEVES, J., DEY, S., DHARMARATNE, S., DHILLON, P., DING, E., DRISCOLL, T., EKWUEME, D., ENDRIES, A. Y., FARVID, M., FARZADFAR, F., FERNANDES, J., FISCHER, F., TT, G. H., GEBRU, A., GOPALANI, S., et al. 2017. Global, Regional, and National Cancer Incidence, Mortality, Years of Life Lost, Years Lived With Disability, and Disability-Adjusted Life-years for 32 Cancer Groups, 1990 to 2015: A Systematic Analysis for the Global Burden of Disease Study. *JAMA Oncol*, 3, 524-548.
- GONCALVES, H., JR., GUERRA, M. R., DUARTE CINTRA, J. R., FAYER, V. A., BRUM, I. V. & BUSTAMANTE TEIXEIRA, M. T. 2018. Survival Study of Triple-Negative and Non-Triple-Negative Breast Cancer in a Brazilian Cohort. *Clin Med Insights Oncol*, 12, 1179554918790563.
- GOPAL, S. K., GREENING, D. W., MATHIAS, R. A., JI, H., RAI, A., CHEN, M., ZHU, H. J. & SIMPSON, R. J. 2015. YBX1/YB-1 induces partial EMT and tumorigenicity through secretion of angiogenic factors into the extracellular microenvironment. *Oncotarget*, 6, 13718-30.
- GRANT, S. 2008. Cotargeting survival signaling pathways in cancer. *J Clin Invest*, 118, 3003-6.
- GU, C., OYAMA, T., OSAKI, T., KOHNO, K. & YASUMOTO, K. 2001. Expression of Y box-binding protein-1 correlates with DNA topoisomerase IIalpha and proliferating cell nuclear antigen expression in lung cancer. *Anticancer Res*, 21, 2357-62.
- GUARINO, A. M., TROIANO, A., PIZZO, E., BOSSO, A., VIVO, M., PINTO, G., AMORESANO, A., POLLICE, A., LA MANTIA, G. & CALABRO, V. 2018. Oxidative Stress Causes Enhanced Secretion of YB-1 Protein that Restrains Proliferation of Receiving Cells. *Genes (Basel)*, 9.
- GUENTHER, M. K., GRAAB, U. & FULDA, S. 2013. Synthetic lethal interaction between PI3K/Akt/mTOR and Ras/MEK/ERK pathway inhibition in rhabdomyosarcoma. *Cancer Lett*, 337, 200-9.
- GUNN, A. & STARK, J. M. 2012. I-SceI-based assays to examine distinct repair outcomes of mammalian chromosomal double strand breaks. *Methods Mol Biol*, 920, 379-91.
- GUO, T., ZHAO, S., WANG, P., XUE, X., ZHANG, Y., YANG, M., LI, N., LI, Z., XU, L., JIANG, L., ZHAO, L., MA, P. C., ROSELL, R., LI, J. & GU, C. 2017. YB-1 regulates tumor growth by promoting MACC1/c-Met pathway in human lung adenocarcinoma. *Oncotarget*, 8, 48110-48125.
- HANAHAN, D. & WEINBERG, R. A. 2011. Hallmarks of cancer: the next generation. *Cell*, 144, 646-74.
- HARADA, M., KOTAKE, Y., OHHATA, T., KITAGAWA, K., NIIDA, H., MATSUURA, S., FUNAI, K., SUGIMURA, H., SUDA, T. & KITAGAWA, M. 2014. YB-1 promotes transcription of cyclin D1 in human non-small-cell lung cancers. *Genes Cells*, 19, 504-16.
- HARTLERODE, A. J. & SCULLY, R. 2009. Mechanisms of double-strand break repair in somatic mammalian cells. *Biochem J*, 423, 157-68.
- HASEGAWA, S. L., DOETSCH, P. W., HAMILTON, K. K., MARTIN, A. M., OKENQUIST, S. A., LENZ, J. & BOSS, J. M. 1991. DNA binding properties of YB-1 and dbpA: binding to double-stranded, single-stranded, and abasic site containing DNAs. *Nucleic Acids Res*, 19, 4915-20.
- HER, J. & BUNTING, S. F. 2018. How cells ensure correct repair of DNA double-strand breaks. *J Biol Chem*, 293, 10502-10511.
- HIRSCH, E., CIRAOLO, E., FRANCO, I., GHIGO, A. & MARTINI, M. 2014. PI3K in cancer-stroma interactions: bad in seed and ugly in soil. *Oncogene*, 33, 3083-90.
- HOBBS, G. A., DER, C. J. & ROSSMAN, K. L. 2016. RAS isoforms and mutations in cancer at a glance. *J Cell Sci*, 129, 1287-92.
- HOEFLICH, K. P., MERCHANT, M., ORR, C., CHAN, J., DEN OTTER, D., BERRY, L., KASMAN, I., KOEPPEN, H., RICE, K., YANG, N. Y., ENGST, S., JOHNSTON, S., FRIEDMAN, L. S. & BELVIN, M. 2012.

- Intermittent administration of MEK inhibitor GDC-0973 plus PI3K inhibitor GDC-0941 triggers robust apoptosis and tumor growth inhibition. *Cancer Res*, 72, 210-9.
- HOPKINS, B. D., HODAKOSKI, C., BARROWS, D., MENSE, S. M. & PARSONS, R. E. 2014. PTEN function: the long and the short of it. *Trends Biochem Sci*, 39, 183-90.
- INOUE, I., MATSUMOTO, K., YU, Y. & BAY, B. H. 2012. Surmounting chemoresistance by targeting the Y-box binding protein-1. *Anat Rec (Hoboken)*, 295, 215-22.
- IRIE, H. Y., PEARLINE, R. V., GRUENEBERG, D., HSIA, M., RAVICHANDRAN, P., KOTHARI, N., NATESAN, S. & BRUGGE, J. S. 2005. Distinct roles of Akt1 and Akt2 in regulating cell migration and epithelial-mesenchymal transition. *J Cell Biol*, 171, 1023-34.
- ISE, T., NAGATANI, G., IMAMURA, T., KATO, K., TAKANO, H., NOMOTO, M., IZUMI, H., OHMORI, H., OKAMOTO, T., OHGA, T., UCHIUMI, T., KUWANO, M. & KOHNO, K. 1999. Transcription factor Y-box binding protein 1 binds preferentially to cisplatin-modified DNA and interacts with proliferating cell nuclear antigen. *Cancer Res*, 59, 342-6.
- IZUMI, H., IMAMURA, T., NAGATANI, G., ISE, T., MURAKAMI, T., URAMOTO, H., TORIGOE, T., ISHIGUCHI, H., YOSHIDA, Y., NOMOTO, M., OKAMOTO, T., UCHIUMI, T., KUWANO, M., FUNA, K. & KOHNO, K. 2001. Y box-binding protein-1 binds preferentially to single-stranded nucleic acids and exhibits 3'→5' exonuclease activity. *Nucleic Acids Res*, 29, 1200-7.
- JIANG, B. B., YAN, K., ZHANG, Z. Y., YANG, W., WU, W., YIN, S. S. & CHEN, M. H. 2019. The value of KRAS gene status in predicting local tumor progression of colorectal liver metastases following radiofrequency ablation. *Int J Hyperthermia*, 36, 211-219.
- JIANG, L., YUAN, G. L., LIANG, Q. L., ZHANG, H. J., HUANG, J., CHENG, S. A. & PENG, X. X. 2017. Positive expression of Y-box binding protein 1 and prognosis in non-small cell lung cancer: a meta-analysis. *Oncotarget*.
- JURCHOTT, K., BERGMANN, S., STEIN, U., WALTHER, W., JANZ, M., MANNI, I., PIAGGIO, G., FIETZE, E., DIETEL, M. & ROYER, H. D. 2003. YB-1 as a cell cycle-regulated transcription factor facilitating cyclin A and cyclin B1 gene expression. *J Biol Chem*, 278, 27988-96.
- JURCHOTT, K., KUBAN, R. J., KRECH, T., BLUTHGEN, N., STEIN, U., WALTHER, W., FRIESE, C., KIELBASA, S. M., UNGETHUM, U., LUND, P., KNOSEL, T., KEMMNER, W., MORKEL, M., FRITZMANN, J., SCHLAG, P. M., BIRCHMEIER, W., KRUEGER, T., SPERLING, S., SERS, C., ROYER, H. D., HERZEL, H. & SCHAFFER, R. 2010. Identification of Y-box binding protein 1 as a core regulator of MEK/ERK pathway-dependent gene signatures in colorectal cancer cells. *PLoS Genet*, 6, e1001231.
- KATZ, M., AMIT, I. & YARDEN, Y. 2007. Regulation of MAPKs by growth factors and receptor tyrosine kinases. *Biochim Biophys Acta*, 1773, 1161-76.
- KECHAGIOGLOU, P., PAPI, R. M., PROVATOPOULOU, X., KALOGERA, E., PAPADIMITRIOU, E., GRIGOROPOULOS, P., NONNI, A., ZOGRAFOS, G., KYRIAKIDIS, D. A. & GOUNARIS, A. 2014. Tumor suppressor PTEN in breast cancer: heterozygosity, mutations and protein expression. *Anticancer Res*, 34, 1387-400.
- KHAN, M. I., ADHAMI, V. M., LALL, R. K., SECHI, M., JOSHI, D. C., HAIDAR, O. M., SYED, D. N., SIDDIQUI, I. A., CHIU, S. Y. & MUKHTAR, H. 2014. YB-1 expression promotes epithelial-to-mesenchymal transition in prostate cancer that is inhibited by a small molecule fisetin. *Oncotarget*, 5, 2462-74.
- KHANDELWAL, P., PADALA, M. K., COX, J. & GUNTAKA, R. V. 2009. The N-terminal domain of y-box binding protein-1 induces cell cycle arrest in g2/m phase by binding to cyclin d1. *Int J Cell Biol*, 2009, 243532.
- KIM, E. R., SELYUTINA, A. A., BULDAKOV, I. A., EVDOKIMOVA, V., OVCHINNIKOV, L. P. & SOROKIN, A. V. 2013. The proteolytic YB-1 fragment interacts with DNA repair machinery and enhances survival during DNA damaging stress. *Cell Cycle*, 12, 3791-803.
- KNICKELBEIN, K. & ZHANG, L. 2015. Mutant KRAS as a critical determinant of the therapeutic response of colorectal cancer. *Genes Dis*, 2, 4-12.
- KOIKE, K., UCHIUMI, T., OHGA, T., TOH, S., WADA, M., KOHNO, K. & KUWANO, M. 1997. Nuclear translocation of the Y-box binding protein by ultraviolet irradiation. *FEBS Lett*, 417, 390-4.

- KOSNOPFEL, C., SINNBERG, T., SAUER, B., BUSCH, C., NIESSNER, H., SCHMITT, A., FORCHHAMMER, S., GRIMMEL, C., MERTENS, P. R., HAILFINGER, S., DUNN, S. E., GARBE, C. & SCHITTEK, B. 2018. YB-1 Expression and Phosphorylation Regulate Tumorigenicity and Invasiveness in Melanoma by Influencing EMT. *Mol Cancer Res*, 16, 1149-1160.
- KOSNOPFEL, C., SINNBERG, T., SAUER, B., NIESSNER, H., SCHMITT, A., MAKINO, E., FORSCHNER, A., HAILFINGER, S., GARBE, C. & SCHITTEK, B. 2017. Human melanoma cells resistant to MAPK inhibitors can be effectively targeted by inhibition of the p90 ribosomal S6 kinase. *Oncotarget*, 8, 35761-35775.
- KRETOV, D. A., CURMI, P. A., HAMON, L., ABRAKHI, S., DESFORGES, B., OVCHINNIKOV, L. P. & PASTRE, D. 2015. mRNA and DNA selection via protein multimerization: YB-1 as a case study. *Nucleic Acids Res*, 43, 9457-73.
- KROHN, R., RAFFETSEDER, U., BOT, I., ZERNECKE, A., SHAGDARSUREN, E., LIEHN, E. A., VAN SANTBRINK, P. J., NELSON, P. J., BIESSSEN, E. A., MERTENS, P. R. & WEBER, C. 2007. Y-box binding protein-1 controls CC chemokine ligand-5 (CCL5) expression in smooth muscle cells and contributes to neointima formation in atherosclerosis-prone mice. *Circulation*, 116, 1812-20.
- KURNIT, K. C., COLEMAN, R. L. & WESTIN, S. N. 2018. Using PARP Inhibitors in the Treatment of Patients With Ovarian Cancer. *Curr Treat Options Oncol*, 19, 1.
- KUWANO, M., ODA, Y., IZUMI, H., YANG, S. J., UCHIUMI, T., IWAMOTO, Y., TOI, M., FUJII, T., YAMANA, H., KINOSHITA, H., KAMURA, T., TSUNEYOSHI, M., YASUMOTO, K. & KOHNO, K. 2004. The role of nuclear Y-box binding protein 1 as a global marker in drug resistance. *Mol Cancer Ther*, 3, 1485-92.
- LASHAM, A., LINDRIDGE, E., RUDERT, F., ONRUST, R. & WATSON, J. 2000. Regulation of the human fas promoter by YB-1, Puralpha and AP-1 transcription factors. *Gene*, 252, 1-13.
- LASHAM, A., PRINT, C. G., WOOLLEY, A. G., DUNN, S. E. & BRAITHWAITE, A. W. 2013. YB-1: oncoprotein, prognostic marker and therapeutic target? *Biochem J*, 449, 11-23.
- LASHAM, A., SAMUEL, W., CAO, H., PATEL, R., MEHTA, R., STERN, J. L., REID, G., WOOLLEY, A. G., MILLER, L. D., BLACK, M. A., SHELLING, A. N., PRINT, C. G. & BRAITHWAITE, A. W. 2012. YB-1, the E2F pathway, and regulation of tumor cell growth. *J Natl Cancer Inst*, 104, 133-46.
- LEE, A., WOO, J., PARK, H., SUNG, S. H., SEOH, J. Y., LIM, W. & MOON, B. I. 2016. The value of cytoplasmic Y-box-binding protein 1 as a prognostic marker for breast cancer in Korean. *Breast Cancer*, 23, 685-91.
- LEFLOCH, R., POUYSSEGUR, J. & LENORMAND, P. 2009. Total ERK1/2 activity regulates cell proliferation. *Cell Cycle*, 8, 705-11.
- LEUNG, G. P., FENG, T., SIGOILLOT, F. D., GEYER, F. C., SHIRLEY, M. D., RUDDY, D. A., RAKIEC, D. P., FREEMAN, A. K., ENGELMAN, J. A., JASKELIOFF, M. & STUART, D. D. 2019. Hyperactivation of MAPK Signaling Is Deleterious to RAS/RAF-mutant Melanoma. *Mol Cancer Res*, 17, 199-211.
- LEVIDOU, G., SAETTA, A. A., GIGELOU, F., KARLOU, M., PAPANASTASIOU, P., STAMATELLI, A., KAVANTZAS, N., MICHALOPOULOS, N. V., AGROGIANNIS, G., PATSOURIS, E. & KORKOLOPOULOU, P. 2012. ERK/pERK expression and B-raf mutations in colon adenocarcinomas: correlation with clinicopathological characteristics. *World J Surg Oncol*, 10, 47.
- LI, L., ZHAO, G. D., SHI, Z., QI, L. L., ZHOU, L. Y. & FU, Z. X. 2016a. The Ras/Raf/MEK/ERK signaling pathway and its role in the occurrence and development of HCC. *Oncol Lett*, 12, 3045-3050.
- LI, Z., PEARLMAN, A. H. & HSIEH, P. 2016b. DNA mismatch repair and the DNA damage response. *DNA Repair (Amst)*, 38, 94-101.
- LIEN, E. C., DIBBLE, C. C. & TOKER, A. 2017. PI3K signaling in cancer: beyond AKT. *Curr Opin Cell Biol*, 45, 62-71.
- LINDQUIST, J. A. & MERTENS, P. R. 2018. Cold shock proteins: from cellular mechanisms to pathophysiology and disease. *Cell Commun Signal*, 16, 63.

- LIU, T. T., ARANGO-ARGOTY, G., LI, Z., LIN, Y., KIM, S. W., DUECK, A., OZSOLAK, F., MONAGHAN, A. P., MEISTER, G., DEFRANCO, D. B. & JOHN, B. 2015. Noncoding RNAs that associate with YB-1 alter proliferation in prostate cancer cells. *RNA*, 21, 1159-72.
- LU, Z. H., BOOKS, J. T. & LEY, T. J. 2005. YB-1 is important for late-stage embryonic development, optimal cellular stress responses, and the prevention of premature senescence. *Mol Cell Biol*, 25, 4625-37.
- LYABIN, D. N., ELISEEVA, I. A. & OVCHINNIKOV, L. P. 2012. YB-1 synthesis is regulated by mTOR signaling pathway. *PLoS One*, 7, e52527.
- LYABIN, D. N. & OVCHINNIKOV, L. P. 2016. Selective regulation of YB-1 mRNA translation by the mTOR signaling pathway is not mediated by 4E-binding protein. *Sci Rep*, 6, 22502.
- LYONS, S. M., ACHORN, C., KEDERSHA, N. L., ANDERSON, P. J. & IVANOV, P. 2016. YB-1 regulates tRNA-induced Stress Granule formation but not translational repression. *Nucleic Acids Res*, 44, 6949-60.
- MAEHAMA, T. & DIXON, J. E. 1998. The tumor suppressor, PTEN/MMAC1, dephosphorylates the lipid second messenger, phosphatidylinositol 3,4,5-trisphosphate. *J Biol Chem*, 273, 13375-8.
- MALUMBRES, M. & BARBACID, M. 2003. RAS oncogenes: the first 30 years. *Nat Rev Cancer*, 3, 459-65.
- MANNING, B. D. & CANTLEY, L. C. 2007. AKT/PKB signaling: navigating downstream. *Cell*, 129, 1261-74.
- MANNING, B. D. & TOKER, A. 2017. AKT/PKB Signaling: Navigating the Network. *Cell*, 169, 381-405.
- MAROULAKOU, I. G., OEMLER, W., NABER, S. P. & TSICHLIS, P. N. 2007. Akt1 ablation inhibits, whereas Akt2 ablation accelerates, the development of mammary adenocarcinomas in mouse mammary tumor virus (MMTV)-ErbB2/neu and MMTV-polyoma middle T transgenic mice. *Cancer Res*, 67, 167-77.
- MAURYA, P. K., MISHRA, A., YADAV, B. S., SINGH, S., KUMAR, P., CHAUDHARY, A., SRIVASTAVA, S., MURUGESAN, S. N. & MANI, A. 2017. Role of Y Box Protein-1 in cancer: As potential biomarker and novel therapeutic target. *J Cancer*, 8, 1900-1907.
- MCCAIN, J. 2013. The MAPK (ERK) Pathway: Investigational Combinations for the Treatment Of BRAF-Mutated Metastatic Melanoma. *P T*, 38, 96-108.
- MCCUBREY, J. A., STEELMAN, L. S., CHAPPELL, W. H., ABRAMS, S. L., WONG, E. W., CHANG, F., LEHMANN, B., TERRIAN, D. M., MILELLA, M., TAFURI, A., STIVALA, F., LIBRA, M., BASECKE, J., EVANGELISTI, C., MARTELLI, A. M. & FRANKLIN, R. A. 2007. Roles of the Raf/MEK/ERK pathway in cell growth, malignant transformation and drug resistance. *Biochim Biophys Acta*, 1773, 1263-84.
- MENDOZA, M. C., ER, E. E. & BLENIS, J. 2011. The Ras-ERK and PI3K-mTOR pathways: cross-talk and compensation. *Trends Biochem Sci*, 36, 320-8.
- MENEGAKIS, A., DE COLLE, C., YAROMINA, A., HENNENLOTTER, J., STENZL, A., SCHARPF, M., FEND, F., NOELL, S., TATAGIBA, M., BRUCKER, S., WALLWIENER, D., BOEKE, S., RICARDI, U., BAUMANN, M. & ZIPS, D. 2015a. Residual gammaH2AX foci after ex vivo irradiation of patient samples with known tumour-type specific differences in radio-responsiveness. *Radiother Oncol*, 116, 480-5.
- MENEGAKIS, A., VON NEUBECK, C., YAROMINA, A., THAMES, H., HERING, S., HENNENLOTTER, J., SCHARPF, M., NOELL, S., KRAUSE, M., ZIPS, D. & BAUMANN, M. 2015b. gammaH2AX assay in ex vivo irradiated tumour specimens: A novel method to determine tumour radiation sensitivity in patient-derived material. *Radiother Oncol*, 116, 473-9.
- MERTENS, P. R., ALFONSO-JAUME, M. A., STEINMANN, K. & LOVETT, D. H. 1999. YB-1 regulation of the human and rat gelatinase A genes via similar enhancer elements. *J Am Soc Nephrol*, 10, 2480-7.
- MINJGEE, M., TOULANY, M., KEHLBACH, R., GIEHL, K. & RODEMANN, H. P. 2011. K-RAS(V12) induces autocrine production of EGFR ligands and mediates radioresistance through EGFR-dependent Akt signaling and activation of DNA-PKcs. *Int J Radiat Oncol Biol Phys*, 81, 1506-14.

- MLADENOV, E., MAGIN, S., SONI, A. & ILIAKIS, G. 2013. DNA double-strand break repair as determinant of cellular radiosensitivity to killing and target in radiation therapy. *Front Oncol*, 3, 113.
- MONTAGUT, C. & SETTLEMAN, J. 2009. Targeting the RAF-MEK-ERK pathway in cancer therapy. *Cancer Lett*, 283, 125-34.
- MURRAY, M. T. 1994. Nucleic acid-binding properties of the *Xenopus* oocyte Y box protein mRNP3+4. *Biochemistry*, 33, 13910-7.
- MURUGESAN, S. N., YADAV, B. S., MAURYA, P. K., CHAUDHARY, A., SINGH, S. & MANI, A. 2018. Expression and network analysis of YBX1 interactors for identification of new drug targets in lung adenocarcinoma. *J Genomics*, 6, 103-112.
- MYLONA, E., MELISSARIS, S., GIANNOPOULOU, I., THEOHARI, I., PAPADIMITRIOU, C., KERAMOPOULOS, A. & NAKOPOULOU, L. 2014. Y-box-binding protein 1 (YB1) in breast carcinomas: relation to aggressive tumor phenotype and identification of patients at high risk for relapse. *Eur J Surg Oncol*, 40, 289-96.
- NANDAN, M. O. & YANG, V. W. 2011. An Update on the Biology of RAS/RAF Mutations in Colorectal Cancer. *Curr Colorectal Cancer Rep*, 7, 113-120.
- NORMAN, J. T., LINDAHL, G. E., SHAKIB, K., EN-NIA, A., YILMAZ, E. & MERTENS, P. R. 2001. The Y-box binding protein YB-1 suppresses collagen alpha 1(I) gene transcription via an evolutionarily conserved regulatory element in the proximal promoter. *J Biol Chem*, 276, 29880-90.
- NOWSHEEN, S. & YANG, E. S. 2012. The intersection between DNA damage response and cell death pathways. *Exp Oncol*, 34, 243-54.
- O'SULLIVAN COYNE, G., CHEN, A. & KUMMAR, S. 2015. Delivering on the promise: poly ADP ribose polymerase inhibition as targeted anticancer therapy. *Curr Opin Oncol*, 27, 475-81.
- OKAMOTO, T., IZUMI, H., IMAMURA, T., TAKANO, H., ISE, T., UCHIUMI, T., KUWANO, M. & KOHNO, K. 2000. Direct interaction of p53 with the Y-box binding protein, YB-1: a mechanism for regulation of human gene expression. *Oncogene*, 19, 6194-202.
- PAGANO, C., DI MARTINO, O., RUGGIERO, G., MARIA GUARINO, A., MUELLER, N., SIAUCIUNAITE, R., REISCHL, M., SIMON FOULKES, N., VALLONE, D. & CALABRO, V. 2017. The tumor-associated YB-1 protein: new player in the circadian control of cell proliferation. *Oncotarget*, 8, 6193-6205.
- PENG, Q., DENG, Z., PAN, H., GU, L., LIU, O. & TANG, Z. 2018. Mitogen-activated protein kinase signaling pathway in oral cancer. *Oncol Lett*, 15, 1379-1388.
- PESTRYAKOV, P., ZHARKOV, D. O., GRIN, I., FOMINA, E. E., KIM, E. R., HAMON, L., ELISEEVA, I. A., PETRUSEVA, I. O., CURMI, P. A., OVCHINNIKOV, L. P. & LAVRIK, O. I. 2012. Effect of the multifunctional proteins RPA, YB-1, and XPC repair factor on AP site cleavage by DNA glycosylase NEIL1. *J Mol Recognit*, 25, 224-33.
- PFEIFFER, P., GOEDECKE, W. & OBE, G. 2000. Mechanisms of DNA double-strand break repair and their potential to induce chromosomal aberrations. *Mutagenesis*, 15, 289-302.
- PITTS, T. M., NEWTON, T. P., BRADSHAW-PIERCE, E. L., ADDISON, R., ARCAROLI, J. J., KLAUCK, P. J., BAGBY, S. M., HYATT, S. L., PURKEY, A., TENTLER, J. J., TAN, A. C., MESSERSMITH, W. A., ECKHARDT, S. G. & LEONG, S. 2014. Dual pharmacological targeting of the MAP kinase and PI3K/mTOR pathway in preclinical models of colorectal cancer. *PLoS One*, 9, e113037.
- RACHAGANI, S., SENAPATI, S., CHAKRABORTY, S., PONNUSAMY, M. P., KUMAR, S., SMITH, L. M., JAIN, M. & BATRA, S. K. 2011. Activated KrasG(1)(2)D is associated with invasion and metastasis of pancreatic cancer cells through inhibition of E-cadherin. *Br J Cancer*, 104, 1038-48.
- RODRIGUEZ-ROCHA, H., GARCIA-GARCIA, A., PANAYIOTIDIS, M. I. & FRANCO, R. 2011. DNA damage and autophagy. *Mutat Res*, 711, 158-66.
- ROGAKOU, E. P., PILCH, D. R., ORR, A. H., IVANOVA, V. S. & BONNER, W. M. 1998. DNA double-stranded breaks induce histone H2AX phosphorylation on serine 139. *J Biol Chem*, 273, 5858-68.
- ROTHKAMM, K., KRUGER, I., THOMPSON, L. H. & LOBRICH, M. 2003. Pathways of DNA double-strand break repair during the mammalian cell cycle. *Mol Cell Biol*, 23, 5706-15.



- RUFF, P., DONNIANNI, R. A., GLANCY, E., OH, J. & SYMINGTON, L. S. 2016. RPA Stabilization of Single-Stranded DNA Is Critical for Break-Induced Replication. *Cell Rep*, 17, 3359-3368.
- RUZANOV, P. V., EVDOKIMOVA, V. M., KORNEEVA, N. L., HERSHEY, J. W. & OVCHINNIKOV, L. P. 1999. Interaction of the universal mRNA-binding protein, p50, with actin: a possible link between mRNA and microfilaments. *J Cell Sci*, 112 ( Pt 20), 3487-96.
- SARBASSOV, D. D., GUERTIN, D. A., ALI, S. M. & SABATINI, D. M. 2005. Phosphorylation and regulation of Akt/PKB by the rictor-mTOR complex. *Science*, 307, 1098-101.
- SCHIPLER, A. & ILIAKIS, G. 2013. DNA double-strand-break complexity levels and their possible contributions to the probability for error-prone processing and repair pathway choice. *Nucleic Acids Res*, 41, 7589-605.
- SCHITTEK, B., PSENNER, K., SAUER, B., MEIER, F., IFTNER, T. & GARBE, C. 2007. The increased expression of Y box-binding protein 1 in melanoma stimulates proliferation and tumor invasion, antagonizes apoptosis and enhances chemoresistance. *Int J Cancer*, 120, 2110-8.
- SHAO, F., SUN, H. & DENG, C. X. 2017. Potential therapeutic targets of triple-negative breast cancer based on its intrinsic subtype. *Oncotarget*, 8, 73329-73344.
- SHAO, G. L., WANG, M. C., FAN, X. L., ZHONG, L., JI, S. F., SANG, G. & WANG, S. 2018. Correlation Between Raf/MEK/ERK Signaling Pathway and Clinicopathological Features and Prognosis for Patients With Breast Cancer Having Axillary Lymph Node Metastasis. *Technol Cancer Res Treat*, 17, 1533034617754024.
- SINNBERG, T., SAUER, B., HOLM, P., SPANGLER, B., KUPHAL, S., BOSSERHOFF, A. & SCHITTEK, B. 2012. MAPK and PI3K/AKT mediated YB-1 activation promotes melanoma cell proliferation which is counteracted by an autoregulatory loop. *Exp Dermatol*, 21, 265-70.
- SMITH, E. R., SMEDBERG, J. L., RULA, M. E. & XU, X. X. 2004. Regulation of Ras-MAPK pathway mitogenic activity by restricting nuclear entry of activated MAPK in endoderm differentiation of embryonic carcinoma and stem cells. *J Cell Biol*, 164, 689-99.
- SONODA, E., SASAKI, M. S., MORRISON, C., YAMAGUCHI-IWAI, Y., TAKATA, M. & TAKEDA, S. 1999. Sister chromatid exchanges are mediated by homologous recombination in vertebrate cells. *Mol Cell Biol*, 19, 5166-9.
- STEELMAN, L. S., ABRAMS, S. L., SHELTON, J. G., CHAPPELL, W. H., BASECKE, J., STIVALA, F., DONIA, M., NICOLETTI, F., LIBRA, M., MARTELLI, A. M. & MCCUBREY, J. A. 2010. Dominant roles of the Raf/MEK/ERK pathway in cell cycle progression, prevention of apoptosis and sensitivity to chemotherapeutic drugs. *Cell Cycle*, 9, 1629-38.
- STOKOE, D., STEPHENS, L. R., COPELAND, T., GAFFNEY, P. R., REESE, C. B., PAINTER, G. F., HOLMES, A. B., MCCORMICK, F. & HAWKINS, P. T. 1997. Dual role of phosphatidylinositol-3,4,5-trisphosphate in the activation of protein kinase B. *Science*, 277, 567-70.
- STRATFORD, A. L., FRY, C. J., DESILETS, C., DAVIES, A. H., CHO, Y. Y., LI, Y., DONG, Z., BERQUIN, I. M., ROUX, P. P. & DUNN, S. E. 2008. Y-box binding protein-1 serine 102 is a downstream target of p90 ribosomal S6 kinase in basal-like breast cancer cells. *Breast Cancer Res*, 10, R99.
- STRATFORD, A. L., HABIBI, G., ASTANEHE, A., JIANG, H., HU, K., PARK, E., SHADEO, A., BUYS, T. P., LAM, W., PUGH, T., MARRA, M., NIELSEN, T. O., KLINGE, U., MERTENS, P. R., APARICIO, S. & DUNN, S. E. 2007. Epidermal growth factor receptor (EGFR) is transcriptionally induced by the Y-box binding protein-1 (YB-1) and can be inhibited with Iressa in basal-like breast cancer, providing a potential target for therapy. *Breast Cancer Res*, 9, R61.
- SUNADA, S., NAKANISHI, A. & MIKI, Y. 2018. Crosstalk of DNA double-strand break repair pathways in poly(ADP-ribose) polymerase inhibitor treatment of breast cancer susceptibility gene 1/2-mutated cancer. *Cancer Sci*, 109, 893-899.
- SUTHERLAND, B. W., KUCAB, J., WU, J., LEE, C., CHEANG, M. C., YORIDA, E., TURBIN, D., DEDHAR, S., NELSON, C., POLLAK, M., LEIGHTON GRIMES, H., MILLER, K., BADVE, S., HUNTSMAN, D., BLAKE-GILKS, C., CHEN, M., PALLAN, C. J. & DUNN, S. E. 2005. Akt phosphorylates the Y-box binding protein 1 at Ser102 located in the cold shock domain and affects the anchorage-independent growth of breast cancer cells. *Oncogene*, 24, 4281-92.

- SYMINGTON, L. S. 2014. End resection at double-strand breaks: mechanism and regulation. *Cold Spring Harb Perspect Biol*, 6.
- TAFURI, S. R. & WOLFFE, A. P. 1992. DNA binding, multimerization, and transcription stimulation by the *Xenopus* Y box proteins in vitro. *New Biol*, 4, 349-59.
- TIWARI, A., REBHOLZ, S., MAIER, E., DEGHAN HARATI, M., ZIPS, D., SERS, C., RODEMANN, H. P. & TOULANY, M. 2018. Stress-Induced Phosphorylation of Nuclear YB-1 Depends on Nuclear Trafficking of p90 Ribosomal S6 Kinase. *Int J Mol Sci*, 19.
- TONG, H., ZHAO, K., ZHANG, J., ZHU, J. & XIAO, J. 2019. YB-1 modulates the drug resistance of glioma cells by activation of MDM2/p53 pathway. *Drug Des Devel Ther*, 13, 317-326.
- TOULANY, M., IIDA, M., KEINATH, S., IYI, F. F., MUECK, K., FEHRENBACHER, B., MANSOUR, W. Y., SCHALLER, M., WHEELER, D. L. & RODEMANN, H. P. 2016. Dual targeting of PI3K and MEK enhances the radiation response of K-RAS mutated non-small cell lung cancer. *Oncotarget*, 7, 43746-43761.
- TOULANY, M., MINJGEE, M., SAKI, M., HOLLER, M., MEIER, F., EICHELER, W. & RODEMANN, H. P. 2014. ERK2-dependent reactivation of Akt mediates the limited response of tumor cells with constitutive K-RAS activity to PI3K inhibition. *Cancer Biol Ther*, 15, 317-28.
- TOULANY, M., SCHICKFLUSS, T. A., EICHELER, W., KEHLBACH, R., SCHITTEK, B. & RODEMANN, H. P. 2011. Impact of oncogenic K-RAS on YB-1 phosphorylation induced by ionizing radiation. *Breast Cancer Res*, 13, R28.
- TUBBS, A. & NUSSENZWEIG, A. 2017. Endogenous DNA Damage as a Source of Genomic Instability in Cancer. *Cell*, 168, 644-656.
- TUBBS, A. T., DORSETT, Y., CHAN, E., HELMINK, B., LEE, B. S., HUNG, P., GEORGE, R., BREDEMEYER, A. L., MITTAL, A., PAPPU, R. V., CHOWDHURY, D., MOSAMMAPARAST, N., KRANGEL, M. S. & SLECKMAN, B. P. 2014. KAP-1 promotes resection of broken DNA ends not protected by gamma-H2AX and 53BP1 in G(1)-phase lymphocytes. *Mol Cell Biol*, 34, 2811-21.
- UCHIUMI, T., FOTOVATI, A., SASAGURI, T., SHIBAHARA, K., SHIMADA, T., FUKUDA, T., NAKAMURA, T., IZUMI, H., TSUZUKI, T., KUWANO, M. & KOHNO, K. 2006. YB-1 is important for an early stage embryonic development: neural tube formation and cell proliferation. *J Biol Chem*, 281, 40440-9.
- VAIMAN, A. V., STROMSKAYA, T. P., RYBALKINA, E. Y., SOROKIN, A. V., GURYANOV, S. G., ZABOTINA, T. N., MECHETNER, E. B., OVCHINNIKOV, L. P. & STAVROVSKAYA, A. A. 2006. Intracellular localization and content of YB-1 protein in multidrug resistant tumor cells. *Biochemistry (Mosc)*, 71, 146-54.
- VANHAESEBROECK, B., GUILLERMET-GUIBERT, J., GRAUPERA, M. & BILANGES, B. 2010. The emerging mechanisms of isoform-specific PI3K signalling. *Nat Rev Mol Cell Biol*, 11, 329-41.
- VICENT, S., LOPEZ-PICAZO, J. M., TOLEDO, G., LOZANO, M. D., TORRE, W., GARCIA-CORCHON, C., QUERO, C., SORIA, J. C., MARTIN-ALGARRA, S., MANZANO, R. G. & MONTUENGA, L. M. 2004. ERK1/2 is activated in non-small-cell lung cancer and associated with advanced tumours. *Br J Cancer*, 90, 1047-52.
- VIGNARD, J., MIREY, G. & SALLES, B. 2013. Ionizing-radiation induced DNA double-strand breaks: a direct and indirect lighting up. *Radiother Oncol*, 108, 362-9.
- VIKIS, H. & GUAN, K. L. 2002. Regulation of the Ras-MAPK pathway at the level of Ras and Raf. *Genet Eng (N Y)*, 24, 49-66.
- VOLINSKY, N. & KHOLODENKO, B. N. 2013. Complexity of receptor tyrosine kinase signal processing. *Cold Spring Harb Perspect Biol*, 5, a009043.
- WANG, M., HAN, J., MARCAR, L., BLACK, J., LIU, Q., LI, X., NAGULAPALLI, K., SEQUIST, L. V., MAK, R. H., BENES, C. H., HONG, T. S., GURTNER, K., KRAUSE, M., BAUMANN, M., KANG, J. X., WHETSTINE, J. R. & WILLERS, H. 2017. Radiation Resistance in KRAS-Mutated Lung Cancer Is Enabled by Stem-like Properties Mediated by an Osteopontin-EGFR Pathway. *Cancer Res*, 77, 2018-2028.

- WANG, X., GUO, X. B., SHEN, X. C., ZHOU, H., WAN, D. W., XUE, X. F., HAN, Y., YUAN, B., ZHOU, J., ZHAO, H., ZHI, Q. M. & KUANG, Y. T. 2015. Prognostic role of YB-1 expression in breast cancer: a meta-analysis. *Int J Clin Exp Med*, 8, 1780-91.
- WEI, W. J., MU, S. R., HEINER, M., FU, X., CAO, L. J., GONG, X. F., BINDEREIF, A. & HUI, J. 2012. YB-1 binds to CAUC motifs and stimulates exon inclusion by enhancing the recruitment of U2AF to weak polypyrimidine tracts. *Nucleic Acids Res*, 40, 8622-36.
- WEINBERG, R. A. 1989. Oncogenes, antioncogenes, and the molecular bases of multistep carcinogenesis. *Cancer Res*, 49, 3713-21.
- WELLBROCK, C. & AROZARENA, I. 2016. The Complexity of the ERK/MAP-Kinase Pathway and the Treatment of Melanoma Skin Cancer. *Front Cell Dev Biol*, 4, 33.
- WELSH, S. J. & CORRIE, P. G. 2015. Management of BRAF and MEK inhibitor toxicities in patients with metastatic melanoma. *Ther Adv Med Oncol*, 7, 122-36.
- WU, J., STRATFORD, A. L., ASTANEHE, A. & DUNN, S. E. 2007. YB-1 is a Transcription/Translation Factor that Orchestrates the Oncogenome by Hardwiring Signal Transduction to Gene Expression. *Transl Oncogenomics*, 2, 49-65.
- WU, S. L., FU, X., HUANG, J., JIA, T. T., ZONG, F. Y., MU, S. R., ZHU, H., YAN, Y., QIU, S., WU, Q., YAN, W., PENG, Y., CHEN, J. & HUI, J. 2015. Genome-wide analysis of YB-1-RNA interactions reveals a novel role of YB-1 in miRNA processing in glioblastoma multiforme. *Nucleic Acids Res*, 43, 8516-28.
- YANG, F., GAO, J. Y., CHEN, H., DU, Z. H., ZHANG, X. Q. & GAO, W. 2017. Targeted inhibition of the phosphoinositide 3-kinase impairs cell proliferation, survival, and invasion in colon cancer. *Onco Targets Ther*, 10, 4413-4422.
- YAO, H., HE, G., YAN, S., CHEN, C., SONG, L., ROSOL, T. J. & DENG, X. 2017. Triple-negative breast cancer: is there a treatment on the horizon? *Oncotarget*, 8, 1913-1924.
- YOSHIMATSU, T., URAMOTO, H., OYAMA, T., YASHIMA, Y., GU, C., MORITA, M., SUGIO, K., KOHNO, K. & YASUMOTO, K. 2005. Y-box-binding protein-1 expression is not correlated with p53 expression but with proliferating cell nuclear antigen expression in non-small cell lung cancer. *Anticancer Res*, 25, 3437-43.
- YU, Z., YE, S., HU, G., LV, M., TU, Z., ZHOU, K. & LI, Q. 2015. The RAF-MEK-ERK pathway: targeting ERK to overcome obstacles to effective cancer therapy. *Future Med Chem*, 7, 269-89.
- ZHAO, H. & XU, Y. H. 1999. Mad-overexpression down regulates the malignant growth and p53 mediated apoptosis in human hepatocellular carcinoma BEL-7404 cells. *Cell Res*, 9, 51-9.
- ZHOU, J., DU, T., LI, B., RONG, Y., VERKHRATSKY, A. & PENG, L. 2015. Crosstalk Between MAPK/ERK and PI3K/AKT Signal Pathways During Brain Ischemia/Reperfusion. *ASN Neuro*, 7.

## CURICULUM VITAE

### Aadhya Tiwari

#### Research Experience:

Time period	Position/study program	Supervisor	Research institute
April, 2016- March 2019	PhD student	Prof. Dr. Mahmoud Toulany	Division of Radiobiology, Dept. Radiation Oncology, University Tuebingen (Head: Prof. Dr. H. Peter Rodemann)
Sep. 2013- June, 2015	Research Scholar	Prof.Dr. Alireza Gharabaghi	Dept. Functional and Restorative Neurosurgery, University Tuebingen
Sep. 2011-Oct. 2012	Junior Research Scholar	Prof Dr. Madan Mohan Godbole	Dept. Endocrinology, Sanjay Gandhi Postgraduate Institute of Medical Sciences (SGPGIMS), Lucknow, India
Oct. 2009- July, 2011	Junior Research Fellow	Dr. Vidita Vaidya	Dept. of Neuroscience, Tata Institute of Fundamental Research (TIFR), Mumbai India
2006-2008	Master of Science in Biotechnology		Integral University, Lucknow, India
2003-2006	Bachelors in Life sciences		Lucknow University, India

#### Publications:

##### A) Published

1. **Tiwari A**, Rebholz S., Maier E, Dehghan-Harati M, Sers C, Rodemann HP, Toulany M; Stress-induced phosphorylation of nuclear YB-1 depends on nuclear trafficking of p90 ribosomal s6 kinase. **Int J Mol Sci.** 2018 Aug 18;19(8).
2. Maier E, Atenberger A, **Tiwari A**, Fehrenbacher B, Schaller M, Gani C, Toulany M. Dual targeting of YB-1 and Akt inhibits proliferation and enhances the chemosensitivity of colorectal cancer cells. **Cancers** 2019 May 19, 11(4)

- Stephenson DT, O'Neill SM, Shetty S, **Tiwari A**, Arnold E, Samaroo H, Fu DU, Ring R, Campbell B, Pletcher M, Vaidya V, Morton D : Histopathological characterization of the BTBR mouse model of autistic-like behaviour reveals selective changes in neurodevelopmental proteins. **Mol Autism. 2011 May 16;2(1):7.**

**B) Under submission**

- Tiwari A**, Iida M, Kosnopfel C, Abbariki M, Menegakis A, Fehrenbacher B, Maier J, Schaller M, Brucker SY, Wheeler D, Harari P, Rothbauer U, Schittek B, Zips D, Rodemann HP, Toulany M. Growth and proliferation of KRAS(G13D)-mutated breast cancers is regulated by YB-1 through the crosstalk between the PI3K and MAPK pathways. **under submission**

**C) In Preparation**

- Tiwari A**, Kosnopfel C, Soni A, Schittek B, Iliakis G, Toulany M. Y-box binding protein-1 strongly regulates repair of DNA double-strand breaks in KRAS mutated breast cancer cells. **In prep.**

**Scientific presentations:**

**A: Oral presentations**

**Conference presentations**

- Aadhya Tiwari**, Daniel Zips, H. Peter Rodemann, Mahmoud Toulany; Y-box binding protein-1 is the major regulator of tumor growth and radioresistance in triple-negative breast cancer; GBS, 17<sup>th</sup> to 19<sup>th</sup> September 2018, Frankfurt, Germany
- Aadhya Tiwari**, **Mahmoud Toulany**; YB-1 stimulates DNA repair leads to radioresistance of TNBC cells. Annual DNA Repair meeting, 9<sup>th</sup> – 12<sup>th</sup> September, 2018, Karlsruhe, Germany
- Aadhya Tiwari**, Apostolos Menegakis, Daniel Zips, H. Peter Rodemann, Mahmoud Toulany; Y-box binding protein-1 mediates radioresistance of K-RAS mutated breast cancer cells; 27. Symposium Experimentelle Strahlentherapie und Klinische Strahlenbiologie; 22<sup>nd</sup> to 24<sup>th</sup> March, 2018, Hamburg, Germany
- Aadhya Tiwari**, Rodemann HP, Toulany M; K-RAS(G13D) mutational status dictates YB-1 phosphorylation induced by ionizing radiation; 26. Symposium Experimentelle Strahlentherapie und Klinische Strahlenbiologie; 9<sup>th</sup>. to 11<sup>th</sup> February 2017, Tuebingen, Germany

- 5) **Aadhya Tiwari**, H. Peter Rodemann, Mahmoud Toulany; Y-box binding protein-1 stimulates repair of ionizing radiation-induced DNA double strand breaks in K-RAS(G13D)-mutated breast cancer cells; ERRS and GBS, 17<sup>th</sup> to 21<sup>st</sup> September, 2017, Essen, Germany

### **Departmental Presentation**

- 1) **Aadhya Tiwari**, Mahmoud Toulany; Y-box binding protein-1 mediates radioresistance of K-RAS mutated breast cancer cells. 14<sup>th</sup> June, 2018, Dept. Of Radiation Biology, University of Tuebingen, Germany

### **B: Poster presentations**

- 1) **Tiwari A**, Rodemann HP, Toulany M; K-RAS(G13D) mutation interferes with radiation induced activation of Y-box binding protein-1 in triple-negative breast cancer cells; 15<sup>th</sup> Intern. Wolfsberg Meeting on Molecular Radiation Biology/Oncology, 2017, Ermatingen, Switzerland
- 2) **Tiwari A**, Rodemann HP, Toulany M; Constitutive phosphorylation of YB-1 in K-RAS mutated cells is regulated by the crosstalk between the PI3K/Akt and MAPK/ERK pathways; GBS meeting, 2016, Erlangen, Germany
- 3) Das AK, **Tiwari A**, Duman RS, Vaidya V: Role of CREB in emotion and cognition during development and adulthood of Rodent brain presented during DBS Annual Talks 2010, TIFR, India.
- 4) Arnold E, O'Neill SM, Samaroo H, Hannah D, Shetty S, **Tiwari A**, Vaidya VA, Campbell B, Ring RH, Stephenson DT: Reduced BDNF gene expression and impaired neurogenesis in the hippocampus of the inbred mouse strain BTBR presented during the Society for Neuroscience (SFN) meeting 2010, San Diego, USA

### **Award/Scholarship**

- 1) Travel Award to participate in annual meeting of Gesellschaft für Biologische Strahlenforschung - GBS, 17<sup>th</sup> to 19<sup>th</sup> September 2018, Frankfurt, Germany with an oral presentation.
- 2) Scholarship from Centre for Integrative Neuroscience (CIN), University of Tuebingen, to support the research project focusing on 'Neurobiology of Stroke' in the lab of Prof. Alireza Gharabaghi, Functional and Restorative Surgery, University of Tuebingen, Germany. September 2013 to June 2014.